INVITED PAPER

Advanced Optical Modulation Formats

Choice of the right modulation format is key to building flexible and cost-effective high-capacity optically routed wavelength division multiplexed fiber networks.

By Peter J. Winzer, *Senior Member IEEE*, and René-Jean Essiambre, *Member IEEE*

ABSTRACT | Fiber-optic communication systems form the high-capacity transport infrastructure that enables global broadband data services and advanced Internet applications. The desire for higher per-fiber transport capacities and, at the same time, the drive for lower costs per end-to-end transmitted information bit has led to optically routed networks with high spectral efficiencies. Among other enabling technologies, advanced optical modulation formats have become key to the design of modern wavelength division multiplexed (WDM) fiber systems. In this paper, we review optical modulation formats in the broader context of optically routed WDM networks. We discuss the generation and detection of multigigabit/s intensity- and phase-modulated formats, and highlight their resilience to key impairments found in optical networking, such as optical amplifier noise, multipath interference, chromatic dispersion, polarization-mode dispersion, WDM crosstalk, concatenated optical filtering, and fiber nonlinearity.

KEYWORDS | Differential phase modulation; digital modulation; intensity modulation; optical communication; optical networks; wavelength division multiplexing (WDM)

LIST OF ACRONYMS

ACRZ	Alternate-chirp return-to-zero
AMI	Alternate-mark inversion
ASE	Amplified spontaneous emission
BER	Bit-error ratio
CD	Chromatic dispersion
C-NRZ	Chirped nonreturn-to-zero
CRZ	Chirped return-to-zero
CSRZ	Carrier-suppressed return-to-zero
DB	Duobinary
DCF	Dispersion-compensating fiber
DCS	Duobinary carrier suppressed
DFB	Distributed feedback laser
DGD	Differential group delay
DI	Delay interferometer
DM	Data modulation
DMF	Data modulation format
DML	Directly modulated laser
DPSK	Differential phase shift keying
DQPSK	Differential quadrature phase shift keying
DST	Dispersion-supported transmission
EAM	Electroabsorption modulator
EML	Electroabsorption modulated laser
EPD	Electronic predistortion
FEC	Forward error correction
FM	Frequency modulation
FWM	Four-wave mixing
GVD	Group velocity dispersion
IFWM	Intrachannel four-wave mixing
ISD	Information spectral density
ISI	Intersymbol interference
ITU	International telecommunication union
IXPM	Intrachannel cross-phase modulation
M-ASK	Multilevel amplitude shift keying
MI	Modulation instability
MLSE	Maximum-likelihood sequence estimator
MPI	Multipath interference
MZM	Mach–Zehnder modulator
NL	Nonlinearity
NRD	Net residual dispersion
NRZ	Nonreturn-to-zero
NZDF	Nonzero dispersion shifted fiber
OA	Optical amplifier
OADM	Optical add/drop multiplexer
OOK	On/off keying
OSNR	Optical signal-to-noise ratio
OXC	Optical crossconnect
PASS	Phased amplitude shift signaling

Manuscript received June 13, 2005; revised November 28, 2005.
The authors are with Bell Labs, Lucent Technologies, Holmdel, NJ 07733 USA (e-mail: peter.winzer@ieee.org).
Digital Object Identifier: 10.1109/JPROC.2006.873438

PMD	Polarization-mode dispersion
Pol-SK	Polarization shift keying
PSBT	Phase-shaped binary transmission
PSP	Principal state of polarization
RDPS	Residual dispersion per span
RF	Radiofrequency
ROADM	Reconfigurable OADM
RX	Receiver
RZ	Return-to-zero
SE	Spectral efficiency
SPM	Self-phase modulation
SSB	Single sideband
SSMF	Standard single-mode fiber
TX	Transmitter
VSB	Vestigial sideband
WDM	Wavelength division multiplexing
XPM	Cross-phase modulation

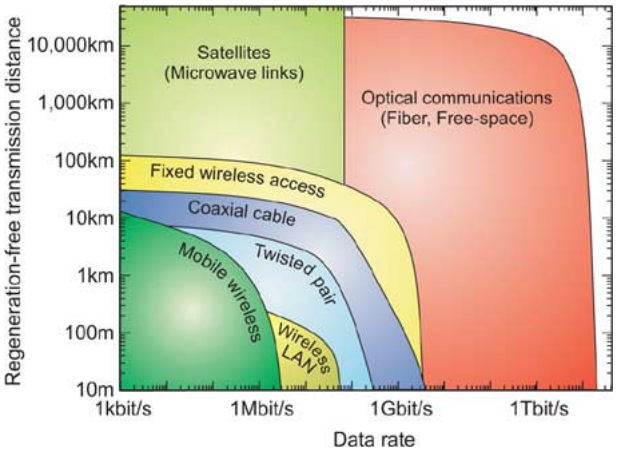

Fig. 1. ***Regeneration-free transmission distance versus data rate for various wireless and wireline communication technologies.***

I. INTRODUCTION

Today's information society relies to an unprecedented extent on broadband communication solutions, with applications such as high-speed Internet access, mobile voice and data services, multimedia broadcast systems, and high-capacity data networking for grid computing and remote storage. In order to most cost-effectively meet the widely differing bandwidth demands of various communication applications, several communication technologies are being used, each with their very own characteristics and advantages. One way of comparing these technologies is to look at the maximum data rates they support for a given, regeneration-free transmission distance. The regeneration-free transmission distance is defined as the distance that can be bridged without detecting and retransmitting the digital information anywhere along the propagation path. Fig. 1 compares the most widely used RF and optical communication technologies for wireline and wireless communications, based on this metric. The boundary lines represent approximate guides, which are constantly shifting out subject to technological improvements.

Fig. 1 clearly shows that *optical communication systems* can support Tb/s capacities over many thousand kilometers, which makes them the ideal technology base for high-capacity wireline networking. With unrivaled optical fiber attenuation coefficients below 0.2 dB/km across several THz of bandwidth, transmission distances exceeding 10 000 km, capacities of more than 10 Tb/s, and correspondingly high capacity × distance products of 36 Pb/s · km have been reported over a *single* optical fiber (125-μm diameter).[1] Table 1 shows a selection of record numbers

Table 1 Some Recent Record Fiber-Optic Transmission Results

Ref.	Capacity	Distance	Capacity×Distance
[3]	10.9 Tb/s (273 ch × 40 Gb/s)	117 km	1.3 Pb/s·km
[4]	10.2 Tb/s (256 ch × 42.7 Gb/s)	300 km	3.1 Pb/s·km
[5]	6.0 Tb/s (149 ch × 42.7 Gb/s)	6,100 km	36 Pb/s·km
[6]	2.6 Tb/s (64 ch × 42.7 Gb/s)	4,000 km	10 Pb/s·km
[7]	1.6 Tb/s (40 ch ×42.7 Gb/s)	10,000 km	16 Pb/s·km

achieved in research laboratories, with up to 256 WDM channels ("ch") at per-channel data rates of 40 Gb/s. The need for *system margins* to accommodate carrier-class quality of service in nonideal networks throughout the lifetime of aging system components typically lets commercial system capacities fall short of these record numbers by up to an order of magnitude [1], [2].

The driver behind the enormous interest in increasing system *reach* and aggregate WDM transport *capacity* is the steadily growing volume and bandwidth demand of data services and the desire to meet this demand by simultaneously reducing the *cost per transported information bit*. In WDM systems, this cost reduction is achieved by *sharing optical components* among many (or all) WDM channels; the most prominent examples for shared optical components are the optical fiber, used both for transport and dispersion management, and optical amplifiers, placed periodically along the transmission path to reamplify WDM channels. Since all shared optical components operate within limited wavelength windows, it is beneficial to space WDM channels as closely together as possible, with the ratio of net per-channel information data

[1]Record transmission results are typically reported in the postdeadline sessions of the annual Optical Fiber Communication Conference (OFC) and the annual European Conference on Optical Communication (ECOC).

rate to the WDM channel spacing being referred to as a system's *spectral efficiency* (b/s/Hz) [8], sometimes also called *information spectral density* [9]. For example, transmitting 40-Gb/s data information per WDM channel on the 100-GHz ITU frequency grid [10], one arrives at an SE of 0.4 b/s/Hz, irrespective of whether one directly transmits at 40.0 Gb/s, or, e.g., at 42.7 Gb/s to include a 7% overhead for FEC.

Another way of lowering the cost per information bit is to increase per-channel data rates. Once sufficiently mature optoelectronic technology at reasonable production volumes can be used, a fourfold[2] increase in per-channel data rate typically implies a 2.5-fold increase in transponder cost. Therefore, quadrupling per-channel data rates eventually leads to 40% transponder cost savings. These considerations, among others, have led to the development of technologies for 40-Gb/s per-channel data rates. Together with advances in narrowband optical filtering technology, now enabling wavelength multiplexing filters on a 50-GHz optical frequency grid, WDM systems with an SE of 0.8 b/s/Hz and beyond have been demonstrated.[3] Systems operating at 40 Gb/s are commercially available since early 2002 [2], [11].

In addition to increasing the point-to-point capabilities of optical transmission systems, and in order to further leverage broadband optical technologies, expanding *networking functionality* into the optical domain is yet another important aspect of reducing the cost per end-to-end transported information bit: (reconfigurable) optical add/drop multiplexers [(R)OADMs] allow adding and droping wavelength channels at nodes as needed, while OXCs allow switching wavelength channels between different optical fibers; both are becoming major building blocks of *optically routed networks* [12].

High-SE, high-capacity optically routed transport networks, which drive fiber-optic communications research today, are enabled by several key technologies.

- *Low-loss optical components* (including transmission fiber, dispersion-compensating devices, and optical switching/routing elements) minimize the need for optical amplification and reduce the associated amplification noise.
- *Low-noise optical amplifiers* (such as distributed Raman amplifiers) lower the noise accumulated along transmission lines.
- *Advanced optical fibers* reduce nonlinear signal distortions and enable higher signal launch powers.
- *FEC* allows for operation at poorer channel bit-error ratio (BER), which relaxes the requirements on the OSNR at the receiver.
- *Advanced modulation formats* are used to trade off noise resilience, fiber propagation characteristics, and resilience to narrowband optical filtering due to multiple passes through OADMs.

In this paper, we focus on how *advanced optical modulation formats* enable high-capacity optically routed transport networks. Being aware of the sophisticated modulation and detection schemes and algorithms employed in RF engineering, we first want to put the word "*advanced*" used in conjunction with optical modulation formats in proper context.

Designed for operation at multigigabit/s per-channel bitrates, optical communication transponders require *broadband* RF electronics and optoelectronics, spanning the entire baseband frequency spectrum from a few kHz to several tens of GHz. Up to a few years ago, technological difficulties in cost-effectively manufacturing devices suitable for such high speeds restricted their functionality to the most basic needs, i.e., performing binary modulation of the light emitted from a laser oscillator, and simple symbol-by-symbol fixed-threshold detection. As a result, lightwave systems deployed today almost exclusively use binary intensity modulation at the transmitter and square-law photodetection at the receiver; neither coherent demodulation, nor electronic equalization techniques, nor FEC is used in the majority of installed systems. At the turn of the millennium, however, this situation started to change significantly. Today, advances in high-speed electronics and optoelectronics are not only used to further push per-channel data rates, but also to increase the sophistication of transponder hardware. At 10-Gb/s data rates, *electronic signal processing* ranging from simple feed-forward equalizer (FFE) structures all the way to MLSEs is available today [13]–[15], and FEC has become a standard feature of 10-Gb/s and 40-Gb/s commercial optical communication systems [16]. Controlled *signal predistortion* at the transmitter is starting to become possible at 10 Gb/s [17], and *coherent detection*, allowing electronic signal processing to make use of the *optical phase* information, is experiencing renewed interest[4] [22], [23]. At the same time, systems start to no longer rely exclusively on phase-insensitive binary modulation of the optical intensity (OOK), but transition to other *modulation formats*, such as binary or multilevel phase modulation or partial response formats. In the optical communications community, all formats that go beyond OOK have therefore earned the qualifier *advanced*.

[2]Optical transport related standards such as the *synchronous optical network* (SONET) or the *synchronous digital hierarchy* (SDH) increase data rates by factors of four.

[3]Record transmission results are typically reported in the postdeadline sessions of the annual Optical Fiber Communication Conference (OFC) and the annual European Conference on Optical Communication (ECOC).

[4]Coherent detection using advanced optical modulation formats was widely discussed in the context of *unamplified* systems in the 1980s [18]–[20], where attenuation-limited single-span transmission required utmost receiver sensitivity. With the advent of efficient optical amplifiers, allowing for comparable direct-detection receiver sensitivities [20], [21], coherent systems research decayed in the early 1990s.

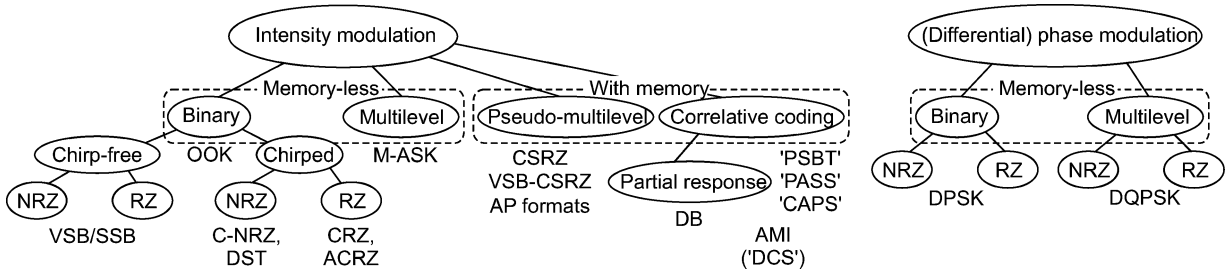

Fig. 2. ***Classification of the most important intensity and phase modulation formats discussed in optical communications today. (AP: alternate phase; CAPS: combined amplitude phase shift coding. All other acronyms are explained in the list of acronyms.)***

This paper is organized as follows. Section II presents a general classification of advanced optical modulation formats, describing the physical properties of a lightwave that can be used to convey digital information. Section III discusses modulator technologies used to imprint data information onto a laser carrier. Since the design of optical transmitters and receivers is intimately related to the capabilities of high-speed optoelectronic hardware, an understanding of modulator technologies is vital to the understanding of optical modulation formats. Section IV covers various intensity modulation formats, and Section V deals with phase modulation. Finally, Section VI puts modulation formats in a systems context, describing fiber-optic propagation impairments and how they impact different modulation formats.

Since advanced optical modulation formats have received considerable interest over the last few years, we want to point the reader to some additional reviews on the topic, supplementing the material presented here [9], [24]–[32]. A good overview of state-of-the-art optical communication systems and technologies can be found in [33], [34], supplementing more fundamental textbook material [35]–[37].

II. CLASSIFICATION OF MODULATION FORMATS

In this section, we classify optical modulation formats according to their key attributes. We look at the *physical quantity* used to convey digital information, and at the *number of symbols* used to represent the binary transmit data. Furthermore, we consider *auxiliary modulation features* such as pulsed modulation or chirp, which can be used, e.g., to improve a format's transmission properties. To better understand this classification, and to get a comprehensive overview of optical modulation formats, Fig. 2 shows how the most important optical modulation formats discussed today fall into the categories established here. The individual formats will be described in more detail in Sections IV and V.

A. Data Modulation Formats (DMFs)

In single-mode optical fibers, the optical field[5] has three physical attributes that can be used to carry information: *intensity*, *phase* (including *frequency*), and *polarization*. Depending on which of the three quantities is used for information transport, we distinguish between intensity, phase (or frequency), and polarization DMFs. Note that this classification does not require a phase-modulated optical field to be constant-envelope, nor an intensity-modulated field to have constant phase. It is the physical quantity used to convey data information that drives the classification. To give some examples: DPSK (Section V-A) is a phase-modulated format, regardless of whether it is transmitted constant-envelope or by means of phase-modulated optical pulses in the form of RZ-DPSK. On the other hand, CSRZ (Section IV-C) is an intensity-modulated format, regardless of the fact that the optical field's phase is additionally modulated in order to beneficially influence the spectrum.

While intensity and phase DMFs have been widely used in high-speed optical communications, encoding information onto the *polarization* of light (Pol-SK) has received comparatively little attention [20], [39], [40]. This can primarily be attributed to the need for active polarization management at the receiver, necessitated by random polarization changes in optical fiber [41]. For intensity- or phase-modulated DMFs and direct-detection receivers, polarization management is only required in the presence of substantial PMD (Section VI-F). The additional receiver complexity associated with Pol-SK could

[5]Single-mode optical fibers are weakly guiding, circular dielectric waveguides supporting a single transverse mode in two orthogonal linear polarizations. The optical power carried by a mode is proportional to the squared magnitude of the transverse electric field or, equivalently, the transverse magnetic field [38]; thus, the term *optical field* denotes either of these field components, normalized such that its squared magnitude corresponds to the transported optical power. The optical field is usually referenced to some optical frequency, which for a single WDM channel is typically the signal's carrier frequency, leading to a complex baseband notation.

Table 2 Examples for Different Symbol Encodings

Data sequence	0	0	1	0	1	1	1	0	0	1	0	1
Multilevel (DQPSK)	0		$+\frac{\pi}{2}$		π		$+\frac{\pi}{2}$		$-\frac{\pi}{2}$		$-\frac{\pi}{2}$	
Pseudo-multilevel (CSRZ)	0	0	+1	0	+1	−1	+1	0	0	−1	0	−1
Partial-response (DB)	0	0	+1	0	−1	−1	−1	0	0	−1	0	+1
Alternate-mark inv. (AMI)	0	0	+1	0	−1	+1	−1	0	0	+1	0	−1

be acceptable if Pol-SK offered a significant receiver sensitivity improvement over intensity modulation, which it does *not* [20], [39]. However, the polarization degree of freedom *can* be used to improve the propagation properties of a format by pseudo-multilevel or correlative coding [42], [43], similar to an auxiliary optical phase modulation (see Section II-B). Furthermore, polarization is sometimes used in research experiments to increase spectral efficiency, either by transmitting two different signals at the same wavelength but in two orthogonal polarizations (*polarization-multiplexing*), or by transmitting adjacent WDM channels in alternating polarizations to reduce coherent WDM crosstalk or nonlinear interactions between the channels (*polarization-interleaving*). None of these methods are currently used in commercial systems due to the complexity associated with polarization maintaining system components and the wavelength-dependent random polarization rotations in transmission fiber [44].

B. Symbol Alphabet Size

Using *multilevel* signaling, $\log_2(M)$ data bits are encoded on M symbols, and are then transmitted at a reduced *symbol rate* of $R/\log_2(M)$, where R is the bitrate. In general, a symbol is assigned irrespective of the symbols sent before or after it (*memory-less* modulation [45]). Multilevel signaling offers the benefits of higher spectral efficiencies at the cost of a reduced tolerance to noise [45]–[47]. Multilevel signaling allows single-channel data rates to exceed the limits of high-speed optoelectronics technology. Alternatively, multilevel signaling allows for lower symbol rates at a fixed data rate, which is beneficial in the presence of dispersive signal distortions, such as CD (Section VI-E) or PMD (Section VI-F), as well as for implementing digital electronic signal processing.

Multilevel intensity modulation [25], [48], multilevel phase modulation [49]–[51], as well as hybrid multilevel intensity/phase modulation [52], [53] have been discussed in the context of multigigabit transmission. Multilevel intensity modulation (M-ASK) has not proven beneficial for fiber-optic transport applications so far, mainly due a substantial back-to-back receiver sensitivity penalty compared to binary OOK. For example, the four-level 4-ASK format incurs a penalty of about 8 dB due to the unequal amplitude level spacings necessitated by signal-dependent noise arising from square-law detection [25], [48]. One of the most promising multilevel optical modulation formats is DQPSK (Section V-B); an example for the mapping of a bit sequence into the 4-ary DQPSK symbol alphabet $\{0, +\pi/2, -\pi/2, \pi\}$ using Gray coding [45] is given in Table 2. Note that throughout this paper, `0` and `1` (set in Typeface font) denote *logical bits*, while Roman font (e.g., $\{0, \pm 1\}$ or $\{0, \pi\}$) denotes *modulation symbols*.

Within the class of modulation formats with more than two symbols in the symbol alphabet, *correlative coding* and *pseudo-multilevel modulation* have received substantially more attention in optical communications than multilevel formats. For these two classes of formats, the symbol alphabet is not enlarged in order to increase the data rate or to reduce the symbol rate at a fixed data rate; rather, all symbols are transmitted *at the bitrate*, and the additional degrees of freedom gained by using an increased symbol alphabet are exploited to shape the spectrum and to improve the tolerance of a format to specific propagation impairments by means of introducing *memory* into the modulation scheme, also referred to as *line coding* [45], [54]–[57]. If more than two symbols are used to represent a single bit, and if the assignment of redundant symbols to transmitted bits is *data-independent*, we refer to *pseudo-multilevel* DMFs. If the assignment of symbols depends on the transmitted data information, we generally refer to *correlative coding* DMFs, the most important subcategory being *partial-response* DMFs.

The most widespread (since easiest to generate) pseudo-multilevel format is CSRZ (Section IV-C), where the information is encoded on the intensity levels {0,1}, but the phase is changed by π *every* bit, regardless of the data information, as visualized in Table 2. The most important partial-response DMF is optical DB (Section IV-F1). As for CSRZ, information is conveyed by the intensity levels {0,1}, but π-phase shifts occur only for `1`-bits separated by an *odd* number of `0`-bits. This *correlation* between auxiliary phase flips and information encoding is characteristic of partial response formats. Note, however, that the phase information is generally *not* used for detection due to the phase insensitive nature of direct-detection (square-law) receivers. More advanced line coding schemes (both pseudo-multilevel and correlative coding) are being designed to combat fiber nonlinearity, as discussed in Section VI-H.

Fig. 3 shows the four most important *symbol diagrams* encountered in optical communications, comprising almost all formats categorized in Fig. 2. As visualized in Fig. 3(a) for the case of OOK, a "symbol diagram" captures the intensity and phase levels of all digital data symbols

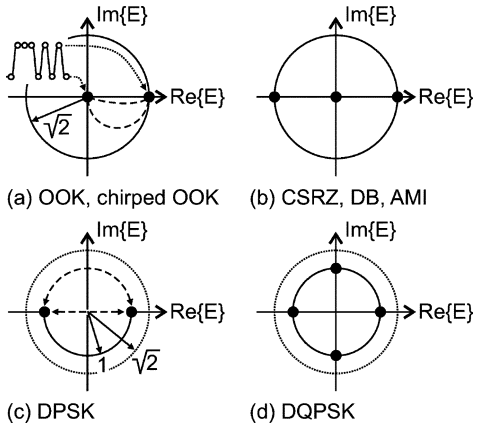

Fig. 3. *Symbol diagrams capture the complex optical field values of data symbols, used either for data transport or for improving specific format properties. All diagrams are shown on the same scale, normalized to unity average optical power. In (a), dashed lines show examples for transitions between symbols for chirped formats; in (c), dashed double-arrows represent different phase modulator implementations (Section V-A).*

(+1 and 0 in the case of OOK), and maps them into the complex optical field plane; idealized waveforms and optimum sampling instant are assumed. If *bit transitions* are of interest in studying a modulation format, curves joining the symbol set can be shown in a symbol diagram as well; such transitions appear as dashed curves in Fig. 3(a), and represent *chirped* OOK modulation (C-NRZ or CRZ, Sections IV-D and IV-E). Note, however, that symbol diagrams do not specify the *dynamics* of the transition between symbols, e.g., pulse rise and fall times or the duration of optical pulses. (In the example of Fig. 3(a), it is not possible to tell whether the dashed lines represent C-NRZ or CRZ.)

The symbol diagram in Fig. 3(b) represents CSRZ as well as DB and AMI. Fig. 3(c) and (d) represent DPSK and DQPSK, respectively. The two phase modulation formats are shown for the same average optical power as the intensity modulation formats of (a) and (b).

While Fig. 3 only shows symbol diagrams in two dimensions (intensity and phase of the optical field), multidimensional symbol constellations are possible by adding a polarization axis to the symbol diagram.

Note that DMFs with memory most beneficially use the symbol set $\{-1, 0, +1\}$, because optical receivers almost exclusively use *square-law detection*, i.e., they make use of the optical *power* $P = |E|^2$, the squared magnitude of the complex optical field E. As a consequence, a direct-detection receiver is unable to distinguish between the two received symbols $E_{1,2} = \pm|E|$, since they both have the same optical power, $P_1 = P_2 = |\pm E|^2$. Therefore, the ternary symbol set $\{+|E|, 0, -|E|\}$ is automatically mapped to the binary set $\{0, |E|^2\}$ at the receiver.

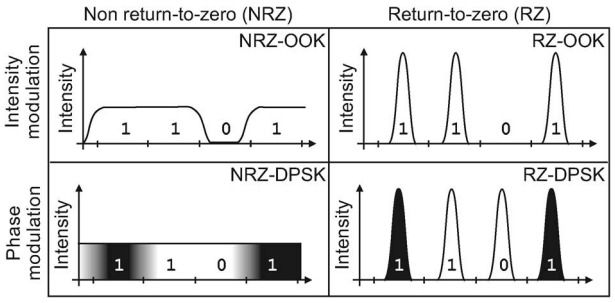

Fig. 4. *If data information is imprinted on a periodic optical pulse train, a format gets the qualifier RZ. (Grayscale indicates the optical phase.)*

C. Pulsed Modulation (RZ Versus NRZ)

If information is imprinted on the intensity, phase, or polarization of optical *pulses*, a DMF gets the qualifier *pulsed* or RZ, the latter referring to the fact that the optical intensity "returns to zero" within each bit slot. In contrast, NRZ formats permit constant optical intensity over several consecutive bits. Fig. 4 shows examples for RZ and NRZ versions of OOK and DPSK, respectively, with the optical phase encoded in grayscale. The differentially encoded relation between phase shifts and information bits for DPSK is explained in Section V-A.

As detailed in Section IV-B, RZ formats usually require a slightly more complex transmitter structure, but are generally more robust to ISI caused by imperfections in the frequency response and the limited bandwidth of opto-electronic transmitter and receiver hardware [58]–[61]. In addition, RZ formats tend to be more robust to many nonlinear propagation distortions (Section VI-G) as well as to MPI (Section VI-D) and PMD (Section VI-F).

III. MODULATOR TECHNOLOGIES

As data rates in optical communication systems have traditionally been limited by the speed of available optoelectronic components, it is of utmost importance to always consider practical aspects of modulation and detection hardware when designing optical modulation formats. More than often in optical communications, a new way of using existing modulator structures has given birth to novel optical modulation formats.

Finding the most cost-effective modulation technique for a particular system application involves aspects of *modulation format* and *modulator technology*. Three basic modulator technologies are widely in use today: *directly modulated lasers* (DMLs), EAMs, and MZMs.

A. Directly Modulated Lasers (DMLs)

Direct modulation of lasers is the easiest way to imprint data on an optical carrier. Here, the transmit data

is modulated onto the laser drive current, which then switches on and off the light emerging from the laser [62], [63]. The resulting modulation format is binary intensity modulation (OOK). Due to their compactness and low cost, DMLs ideally lend themselves to dense integration in small form factor pluggable transponders (XFPs). Today, DMLs are widely available up to modulation speeds of 2.5 Gb/s, with some limited availability up to 10 Gb/s and research demonstrations up to 40 Gb/s [64], [65]. The main drawback of DMLs for high-bitrate transmission beyond short-reach access applications is their inherent, highly component-specific *chirp*, i.e., a residual phase modulation accompanying the desired intensity modulation; laser chirp broadens the optical spectrum, which impedes dense WDM channel packing and can lead to increased signal distortions caused by the interaction with fiber CD [62], [63].

B. Electroabsorption Modulators (EAMs, EMLs)

EAMs are *pin* semiconductor structures[6] whose bandgap can be modulated by applying an external voltage, thus changing the device's *absorption* properties [63]. EAMs feature relatively low drive voltages (typically 2 V), and are cost-effective in volume production. They are available for modulation up to 40 Gb/s today, with research demonstrations up to 80 Gb/s [66]. However, similar to DMLs, they produce some residual *chirp*. They have wavelength-dependent absorption characteristics, dynamic extinction ratios (maximum-to-minimum modulated light power) typically not exceeding 10 dB, and limited optical power-handling capabilities. Their fiber-to-fiber insertion loss is about 10 dB. "On-chip" integration with laser diodes avoids the high loss at the input fiber-to-chip interface, and leads to compact transmitter packages. The resulting EMLs, with output powers on the order of 0 dBm, are widely available today for modulation up to 10 Gb/s. Another way of eliminating the high insertion losses of EAMs is the integration with semiconductor optical amplifiers (SOAs), which can even yield some net fiber-to-fiber gain [67]. Fig 5(a) shows the typical exponential transmission characteristics of an EAM as a function of drive voltage.

C. Mach–Zehnder Modulators (MZMs)

Unlike EAMs, which work by the principle of *absorption*, MZMs work by the principle of *interference*, controlled by modulating the optical *phase*. The modulator structure is shown in the inset to Fig. 5(b): the incoming light is split into two paths at an input coupler. One (or both) paths are equipped with *phase modulators* that let the two optical fields acquire some phase difference relative to each other, controlled by the applied phase modulation voltages $V_{1,2}$. Finally, the two fields interfere at an output

[6]The letters "pin" stand for "positive–intrinsic–negative," and describe the way these three layers of semiconductor material are doped.

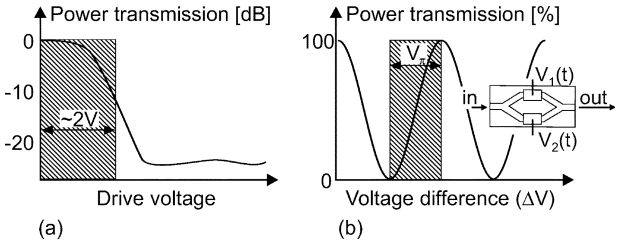

Fig. 5. *Transmission functions of: (a) EAMs and (b) MZMs.*

coupler. Depending on the applied electrical voltage, the interference varies from destructive to constructive, thereby producing intensity modulation.

The optical field transfer function $T_E(V_1, V_2)$ of the MZM reads (see, e.g., [25])

$$T_E(V_1,V_2) = \frac{1}{2}\left\{e^{i\phi(V_1)} + e^{i\phi(V_2)+i\psi}\right\} = e^{\frac{i(\phi(V_1)+\phi(V_2)+\psi)}{2}} \cos\left[\frac{(\phi(V_1)-\phi(V_2))}{2} - \frac{\psi}{2}\right] \quad (1)$$

where $\phi(V_{1,2})$ are the voltage-modulated optical phases of the two MZM arms, and ψ is an additional, temporally constant phase shift in one of the arms, referred to as the *modulator bias*. If the phase modulation depends linearly on the drive voltage ($\phi = \kappa V$), which is true for most materials used for MZMs, the MZM *power* transfer function depends only on the drive voltage difference (ΔV) : $T_P(V_1, V_2) = |T_E(V_1, V_2)|^2 = T_P(\Delta V) = \cos^2(\kappa \Delta V/2 + \kappa V_{\text{bias}}/2)$. The characteristic sinusoidal MZM power transfer function is shown in Fig. 5(b). The modulation voltage that is required to change the phase in one modulator arm by π, thereby letting the MZM switch from full transmission to full extinction, is called *switching voltage* V_π.

For a given drive voltage difference ΔV according to the desired modulated intensity, the additional degree of freedom in choosing $V_1(t) + V_2(t)$ can be exploited to imprint phase modulation (chirp) on the signal [68]–[70]. If chirp is not desired (which is often the case), the two modulator arms are driven by the same amount, but in opposite directions $[V_1(t) = -V_2(t)]$, and the phase term in (1) vanishes. This driving condition is known as *balanced driving* or *push–pull operation*. Some modulator structures, e.g., x-cut lithium niobate ($LiNbO_3$) use only a *single* drive signal, which modulates both arms of the MZM simultaneously and has the condition $V_1(t) = -V_2(t)$ for chirp-free operation built in by appropriate drive electrode design.

MZMs are most conveniently implemented in $LiNbO_3$ [71], [72]. Gallium arsenide (GaAs) [73], and indium phosphide (InP) [74], [75]. $LiNbO_3$-based devices are bulkier than their semiconductor equivalents, but offer easier

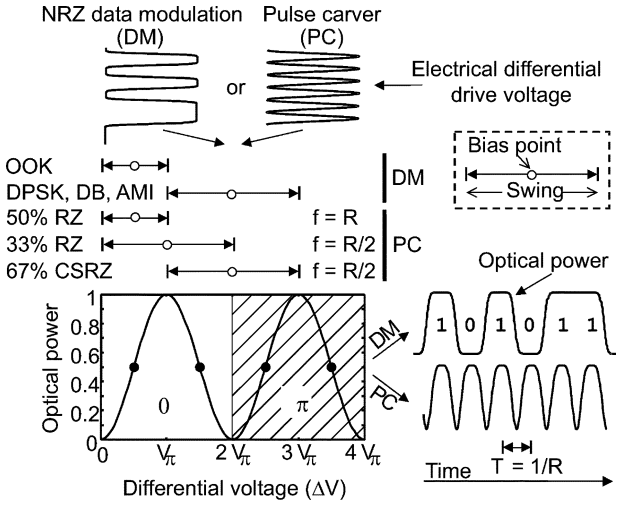

Fig. 6. ***Overview of different ways to drive an MZM, resulting in different optical modulation formats (black circles: MZM quadrature points). See Sections IV and V for details. PC: Pulse carver.***

fiber-to-chip coupling and no residual intensity modulation accompanying the desired phase modulation. On the other hand, semiconductor devices, and in particular InP, lend themselves to much denser integration [76], [77].

MZMs, especially $LiNbO_3$-based devices, feature wavelength-independent modulation characteristics, excellent extinction performance (typically 20 dB), and lower insertion losses (typically 5 dB) than EAMs. The required (high-speed) peak-to-peak drive voltages of up to 6 V, however, ask for broadband driver amplifiers, which can be challenging to build at data rates in excess of 10 Gb/s. Today, $LiNbO_3$-based MZMs are widely available for modulation up to 40 Gb/s.

Due to their well-controllable modulation performance and the possibility of independently modulating intensity and phase of the optical field, MZMs form the basis of many advanced optical modulation formats. Fig. 6 gives an overview of the different ways of driving an MZM to generate a variety of important modulation formats, and will be discussed in detail in Sections IV and V.

IV. INTENSITY MODULATION FORMATS

A. Nonreturn-to-Zero On/Off Keying (NRZ-OOK)

The simplest way to generate optical modulation format is NRZ-OOK, often just referred to as NRZ. At bitrates of 10 Gb/s and above, NRZ is most conveniently generated using DMLs or EAMs (for short-reach and intermediate reach transponders) or chirp-free MZMs (for long-haul applications). When using an MZM, the modulator is biased at 50% transmission (often referred to as the *quadrature point*, and indicated by black circles in Fig. 6), and is driven from minimum to maximum transmission with a voltage swing of V_π, as visualized in Fig. 6. Note that the nonlinear compression of the MZM transfer function at high and low transmission can suppress overshoots and ripple on the electrical NRZ drive signal upon conversion to optical power.

Fig. 7(a) shows the optical spectrum[7] and the optical intensity eye diagram[8] of an idealized NRZ signal. The NRZ optical spectrum is composed of a continuous portion, which reflects the shape of the individual NRZ data pulses, and a strong discrete tone at the carrier wavelength. The residual tones at multiples of the data rate R are generally much weaker than the tone at the carrier frequency, as determined by the spectrum of an individual NRZ data pulse.

B. Return-to-Zero On/Off Keying (RZ-OOK)

RZ-OOK transmitters can be implemented either by *electronically* generating RZ waveforms, which are then modulated onto an optical carrier, or by carving pulses out of an NRZ signal using an additional modulator, called *pulse carver* (see Fig. 8). While the first option [78] is feasible up to data rates of 10 Gb/s with today's technology [79], [80], a pulse carver has to be employed at 40 Gb/s and beyond. Typically, pulse carvers are implemented as *sinusoidally* driven EAMs or MZMs, since multigigahertz sinusoidal signals of appreciable drive amplitude are easily generated.

Using sinusoidally driven EAMs, low duty cycle optical pulses can be realized. This makes EAM-based pulse carvers well suited for optical time-division multiplexed (OTDM) systems, which are used in laboratory experiments to demonstrate per-channel data rates beyond the capabilities of high-speed optoelectronics [81], [82]. Due to the variable absorption characteristics and residual chirp of EAMs, advanced RZ modulation formats are typically implemented using MZM-based pulse carvers. At 10 and 40 Gb/s, one of the following three carving methods is usually employed.

- Sinusoidally driving an MZM *at the data rate* between minimum and maximum transmission results in optical pulses with a full-width at half-maximum (FWHM) of 50% of the bit duration (a duty cycle of 50%), as shown in Fig. 9 (dashed). Decreasing the modulation swing while lowering the modulator bias in order to still reach good extinction between pulses, the duty cycle can in principle be reduced to 36%—however, with significant excess insertion loss, since the modulator is then no longer driven to its transmission maximum.

[7]The *optical spectrum* is the absolute magnitude squared of the optical field's Fourier transform. As such, the optical spectrum contains information on the *temporal phase* of the optical field. An optical spectrum analyzer scans the optical power within a narrow optical resolution bandwidth.

[8]The *optical intensity eye diagram* is a time-domain representation of the optical intensity (or power). It only contains information on the optical field's *intensity*, and is typically recorded using a photodiode in combination with a high-speed digital sampling oscilloscope.

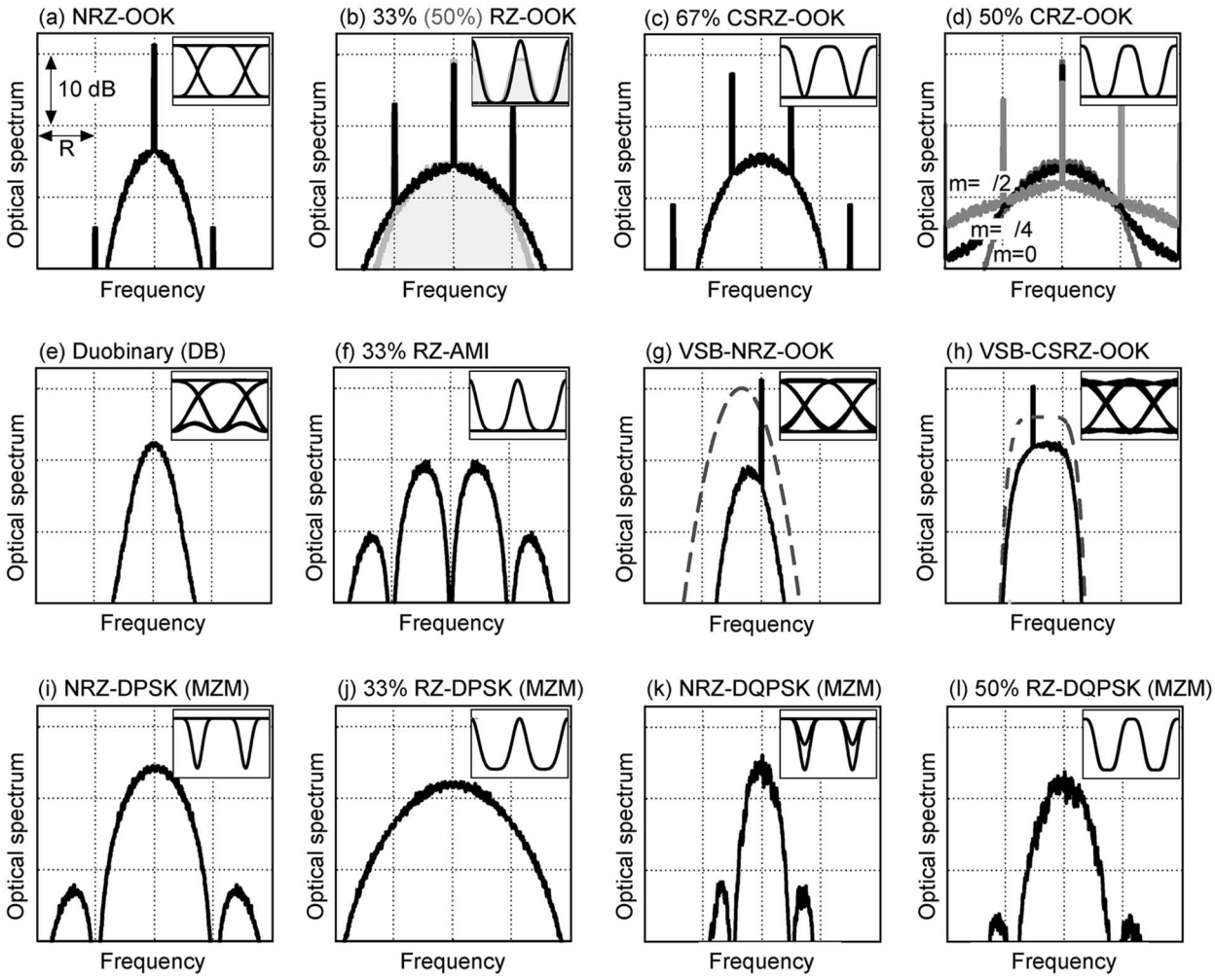

Fig. 7. ***Optical spectra and optical intensity eye diagrams of important modulation formats. Acronyms are defined in the list of acronyms at the beginning of this paper.***

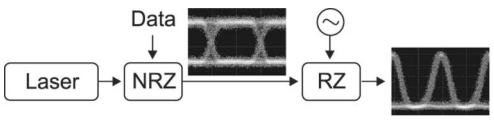

Fig. 8. ***Structure of a typical high data rate RZ transmitter, consisting of a laser source, an external NRZ modulator, and an RZ pulse carver.***

- Sinusoidally driving an MZM at *half the data rate* between its transmission minima produces a pulse whenever the drive voltage passes a transmission maximum, as visualized in Fig. 9 (solid). This way, duty cycles of 33% can be realized. The pulses may be broadened at the expense of extinction ratio between pulses by lowering the drive voltage.
- Sinusoidally driving an MZM at *half the data rate* between its transmission maxima results in pulses with 67% duty cycle and with alternating phase. The resulting format [83], [84] is called *carrier-suppressed RZ* (CSRZ, Section IV-C).

Spectra and intensity eye diagrams of 50%-duty-cycle RZ (gray) and 33%-duty-cycle RZ (black), as produced by an MZM in push–pull operation, are shown in Fig. 7(b).

C. Carrier-Suppressed Return-to-Zero (CSRZ)

CSRZ [83], [84] is a pseudo-multilevel modulation format, characterized by reversing the sign of the optical field at each bit transition. In contrast to the correlative coding formats detailed in Section IV-F, the sign reversals occur at *every* bit transition, and are completely *independent* of the information-carrying part of the signal. CSRZ is most conveniently realized by sinusoidally driving an MZM pulse carver at half the data rate between its transmission maxima, as visualized in Fig. 10. Since the

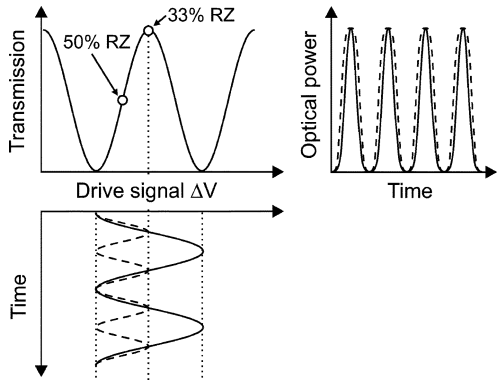

Fig. 9. *Sinusoidally driven MZM as pulse carver for 33%-duty-cycle RZ (solid) and 50%-duty-cycle RZ (dashed). The MZM bias points are indicated by an open circle.*

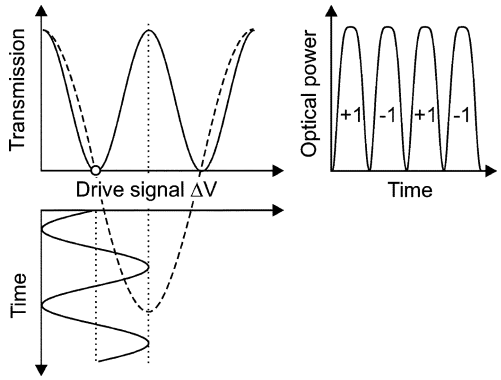

Fig. 10. *Sinusoidally driven MZM as pulse carver for 67%-duty-cycle CSRZ. The solid and dashed transmission curves apply for the optical power ($T_P(\Delta V)$) and field ($T_E(\Delta V)$), respectively. The MZM bias point is indicated by an open circle.*

optical *field* transfer function $T_E(\Delta V)$ (dashed) of the MZM changes its sign at the transmission minimum [cf. (1) for push–pull operation], phase inversions between adjacent bits are produced. Thus, on average, the optical field of half the 1-bits has positive sign, while the other half has negative sign, resulting in a zero-mean optical field envelope. As a consequence, the carrier at the optical center frequency vanishes, giving the format its name. Since the optical phase in a CSRZ signal is periodic at half the data rate, the CSRZ spectrum exhibits characteristic tones at $\pm R/2$. Spectrum and eye diagram of 67%-duty-cycle CSRZ, as generated by an MZM in push–pull configuration, are shown in Fig. 7(c).

Using an MZM to generate CSRZ results in a duty cycle of 67%, which can be brought down to 50% at the expense of excess insertion loss by reducing the drive voltage swing. It is important to note that, due to its most widely used practical implementation with MZMs, the duty cycle of CSRZ signals usually differs from the one of standard RZ. Thus, care has to be taken when comparing the two formats, since some performance differences result from the *carrier-suppressed* nature of CSRZ, while others simply arise from the *different duty cycles*.

D. Chirped Return-to-Zero (CRZ)

If a controlled amount of *analog phase modulation* is applied to a DMF, the qualifier *chirped* is added to describe the format. In the case of CRZ [85], [86], or ACRZ [70], [87], bit-synchronous periodic chirp spectrally broadens the signal bandwidth. Although this reduces the format's suitability for high spectral efficiency WDM systems, it generally increases its robustness to fiber nonlinearity [88], [89] and also enhances its resilience to MPI (Section VI-D). CRZ is predominantly used in ultralong-haul point-to-point fiber communications, as found in transoceanic (submarine) systems, with a typical phase modulation amplitude around 1 rad [85]. Optical spectra for CRZ with different phase modulation indices m are shown in Fig. 7(d).

CRZ signals are typically generated by sinusoidally modulating the phase of a RZ signal at the data rate using a separate phase modulator. This leads to a complex, three-modulator transmitter architecture, which requires careful synchronization of the three drive signals. Integrated GaAs/AlGaAs modulators for CRZ, combining NRZ data modulator, RZ pulse carver, and CRZ phase modulator in one package, have been reported [90]. Alternative implementations that take advantage of the phase-modulation properties of dual-drive MZMs [cf. phase term in (1)] have also been demonstrated [70].

E. Chirped NRZ (C-NRZ), Dispersion-Supported Transmission (DST), and Electronic Signal Predistortion (EPD)

Due to CD in positive-dispersion optical fiber (Section VI-E), higher frequency components contained in a modulated signal spectrum travel faster than lower frequency components. The resulting dephasing of spectral components leads to dispersive pulse broadening in time, which causes transmission penalties. To first order, this effect can be mitigated by introducing the appropriate amount of *chirp* across each optical pulse: *lowering* the frequency across the pulse's leading edge, and *raising* the frequency across the trailing edge, counteracts CD [91], [92].

Among several other techniques, prechirping of optical pulses can be performed by imbalancing a dual-drive MZM used for NRZ modulation [68], [69], or by properly driving a DML, taking advantage of a DML's residual FM [62], [63]. Chirp-controlled DML designs have achieved transmission distances in excess of 200 km at 10 Gb/s over SSMF [93]. As an extreme example for exploiting a DML's FM response, DST [94] predominantly modulates

the *phase* of the optical field, with the intent to have the correct amount of CD convert this phase modulation into intensity modulation upon transmission. Transmission distances of 250 km at 10 Gb/s have been achieved using DST [95].

Another, more advanced technique of prechirping pulses at the transmitter takes a *digital EPD* approach [17], [96]–[99]. Here, both intensity *and* phase of the optical field are independently modulated using a digitally precomputed analog waveform, such that propagation over a dispersive fiber reconstructs the desired, undistorted waveform at a specific target distance. This technique requires a two-times oversampled digital-to-analog converter at the transmitter (20-Gsamples/s DAC for 10-Gb/s channels), and is becoming possible to build at 10 Gb/s due to advances in high-speed digital electronic signal processing.

Note, however, that all heavily predistorted or prechirped signals (such as DST or EPD) are only detectable in the vicinity of the distance which they are predistorted for. This impedes some important features of advanced optical networking, such as broadcasting or optical $1 + 1$ protection [98]. Also, EPD can have severe impact on nonlinear fiber transport [99].

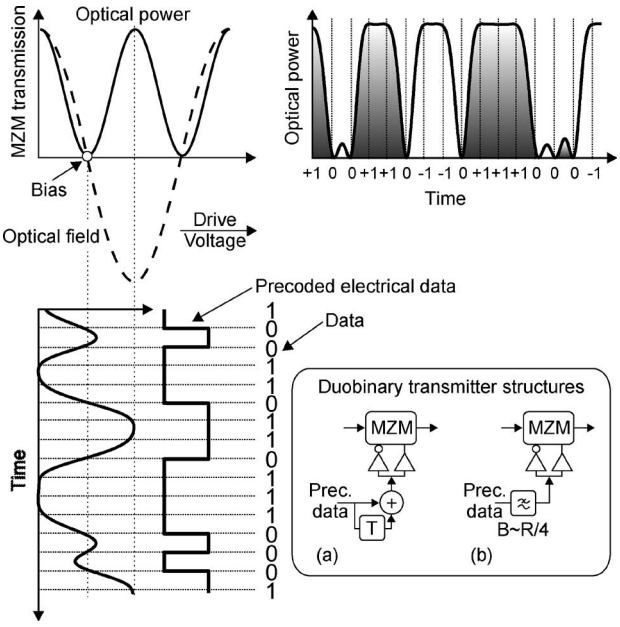

Fig. 11. ***Duobinary signals are generated by driving an MZM around its transmission minimum using a three-level electrical drive signal, generated from the precoded data signal by either: (a) a delay-and-add circuit or (b) some other appropriate low-pass filter.***

F. Correlative Coding and Partial Response Formats

Optical DB and AMI belong to the general class of *correlative coding* formats, a subclass of which being referred to as *partial response* signaling [25], [45], [46], [100]–[102].

As discussed in Section II-B, correlative coding formats most conveniently employ the signaling set $\{0, \pm|E|\}$ to take advantage of the power-detecting property of direct detection optical receivers, which automatically convert the three optical symbols to the two electrical symbols $\{0, |E|^2\}$. However, in contrast to CSRZ, correlative coding introduces a distinct *correlation* between the optical phase and the data information: in optical DB, a phase change occurs whenever there is an odd number of 0-bits between two successive 1-bits, whereas for AMI the phase changes for each 1-bit (even for adjacent 1-bits), independent of the number of 0-bits in between. Table 2 visualizes the phase correlation used by these formats.

1) Duobinary (DB, PSBT, PASS): The most prominent representative of partial response formats is DB. In optical communications, duobinary modulation [103], [104] is also promoted under the names PSBT [56] and PASS [57]; although PSBT and PASS, like the combined amplitude phase shift signaling (CAPS) [54], are meant to comprise more general correlative coding rules between amplitude and phase, PSBT and PASS are mostly used as synonyms for DB.

The main benefit of DB signals is their higher tolerance to CD and narrowband optical filtering compared to binary signaling formats. This can be understood both in the time domain [57], [105] and in the frequency domain [25], [106], [107]. The *time-domain explanation* considers a 1 0 1 bit pattern, which for duobinary is encoded as $+1\ 0\ -1$. If, due to dispersion or optical filtering, the two 1-bit pulses spread into the 0-bit between them, duobinary encoding lets them interfere *destructively*, thus maintaining a low 0-bit level. Conventional OOK formats, on the other hand, let the pulses interfere *constructively*, which raises the 0-bit level and closes the eye. The *frequency-domain explanation* is based on the narrower spectral extent of properly filtered DB signals [cf. Fig. 7(e)], which reduces dispersion induced signal distortions.[9] The spectral compression of DB results from the *smoother* $+1\ 0\ -1$ transition of properly filtered duobinary as compared to the *sharper* $+1\ 0\ +1$ transition of conventional OOK.

As shown in the inset to Fig. 11, duobinary transmitters use a differentially precoded version of the data signal [46], [107] at the input; this precoded data stream exhibits a level change for every 0-bit contained in the original data sequence. Although decoding at the receiver instead of precoding at the transmitter is also possible, precoding at the transmitter is preferable to avoid error propagation after detection [46], [102]. The precoded sequence is converted into a three-level electrical signal by means of severe electrical low-pass

[9]Note that it is the entire spectral shape rather than just the 3-dB bandwidth that influences the robustness of a format to CD.

filtering. The low-pass filter can either be implemented as a delay-and-add filter [Fig. 11(a)] or as some other type of filter with suitable roll-off characteristics and a 3-dB bandwidth of about 25% of the bitrate [Fig. 11(b)]. Delay-and-add filters typically result in a better back-to-back sensitivity, while carefully tailored low-pass characteristics yield higher tolerance to CD at the expense of some back-to-back sensitivity penalty [106] (cf. Section VI-B). The three-level electrical signal is then used to drive a chirp-free MZM between its transmission maxima, as shown in Fig. 11. Alternatively, an MZM designed for one-fourth of the desired data rate may be used to combine the functionality of low-pass filtering and modulation [108], [109], which has allowed MZM-based DB modulation up to 107 Gb/s [110].

Note that electrical low-pass filtering can equivalently be performed in the *optical* domain: passing a binary signal with levels $\{-1, +1\}$, also known as phase-shift keying (PSK, Section V-A), through a narrowband optical bandpass filter produces optical duobinary [111] (see Fig. 16).

2) Alternate-mark inversion (AMI, DCS): AMI, sometimes also classified as partial response due to the way it is generated [102], does not share the bandwidth limitation characteristic of other partial response formats. In optics, AMI is typically implemented in RZ form (RZ-AMI). Like other RZ-OOK formats using auxiliary phase coding, the additional phase modulation of AMI can help to reduce the effects of some fiber nonlinearities (see Section VI-H). Optical spectrum and intensity eye diagram of 33%-duty-cycle RZ-AMI are shown in Fig. 7(f).

One possible AMI transmitter implementation is identical to the DB transmitter of Fig. 11(a), except that it uses an electrical delay-and-*subtract* circuit (high-pass filter) instead of the delay-and-*add* (low-pass) filter used for DB. To obtain RZ-AMI, the data modulator is then followed by any standard RZ pulse carver. Another transmitter structure, shown in Fig. 12(a), first generates binary (phase or intensity) modulation in NRZ form ($\{-1, +1\}$ or $\{0, +1\}$), as shown in the upper plot of Fig. 12(b). This signal is then passed through an *optical* delay-and-subtract filter, implemented by an optical DI with delay $\tau \leq T$, where T is the bit period. To act as a delay-and-subtract filter, the DI is set for *destructive* interference at its output in the presence of an unmodulated input signal. As indicated by the hatched area and the double arrow in Fig. 12(b), optical pulses of alternating phase are produced at the DI output whenever the NRZ input signal differs from its τ-delayed version (dashed). By varying τ, RZ-AMI signals with different duty cycles can be generated without the need for an active, pulse carving modulator [112]–[114].

Yet another possibility of generating RZ-AMI is readily understood by comparing the DB and AMI phase encodings in Table 2: if a DB signal is passed through a CSRZ pulse carver, the bit-alternating phase reversals in-

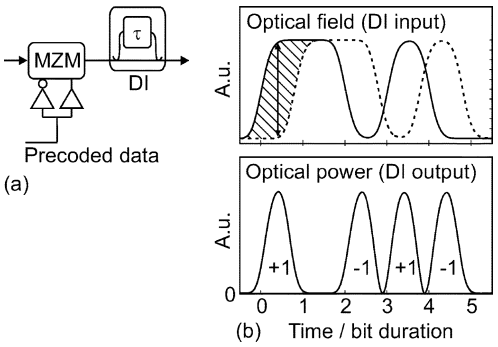

Fig. 12. *(a) Possible structure of a variable duty cycle RZ-AMI transmitter. (b) A signal in NRZ format interferes with its τ-delayed replica (dashed) in a DI, producing pulses of alternating phase.*

herent to CSRZ convert DB into AMI. This fact has lead to the name *duobinary-carrier-suppressed* as a sometimes encountered synonym for AMI [29], [113], [115]. In recent literature, the term "modified duobinary" has also been used to denote AMI. Note, however, that modified duobinary is *not* equivalent to AMI, but represents a distinctly different modulation format. Modified duobinary is a partial response format that is generated using a delay-and-subtract circuit with a *two-bit* delay ($\tau = 2T$) [45], [46], [102], [116].

G. Vestigial Sideband (VSB) and Single Sideband (SSB)

Apart from shaping (and compressing) the optical signal spectrum by means of (pseudo)-multilevel signaling or correlative coding, it is possible for some modulation formats to additionally suppress half of their spectral content by appropriate optical filtering. Since the spectrum of *real-valued* baseband signals is symmetric around zero frequency, filtering out the redundant half of the spectrum (i.e., one of the two spectral *sidebands*) preserves the full information content. This is exploited in SSB signaling, where one sideband is completely suppressed, and in VSB signaling, where an optical filter with a gradual roll-off is offset from the optical carrier frequency to suppress major parts of one sideband, while at the same time performing some filter action on the other [46]. As an important caveat, note that the vast majority of optical receivers uses *square-law detection* rather than coherent detection. In order to be a successful candidate for VSB or SSB filtering, a real-valued modulation format has to maintain square-law detectability after conversion into VSB or SSB. While SSB filtering is hard to implement in practice due to difficulties in realizing the appropriate optical or electrical filter functions [25], [117], [118], optical VSB has been successfully demonstrated on NRZ-OOK [4], [9], [119], [120],

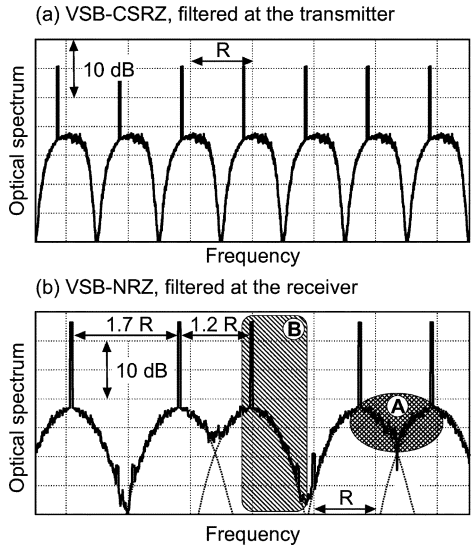

Fig. 13. *VSB transmission of optical signals using: (a) VSB filtering of CSRZ at the transmitter or (b) an unequally spaced frequency grid to avoid WDM channel crosstalk for NRZ [4], [9], [119], [120].*

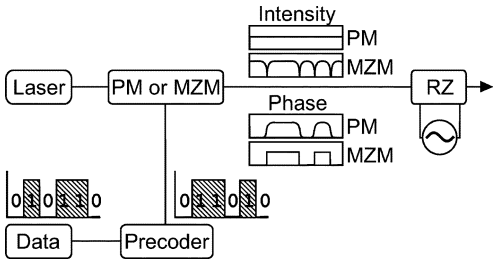

Fig. 14. *Setup of a RZ-DPSK transmitter. Phase modulation can either be achieved using an MZM or by means of a straight-line PM, resulting in different intensity and phase waveforms.*

RZ-OOK [121], and CSRZ-OOK [122], [123]. Fig. 7(g) and (h) show optical spectra and intensity eye diagrams of VSB-NRZ and VSB-CSRZ; the corresponding VSB filter shapes are also shown (dashed).

In a WDM system, VSB filtering can either be done at the *transmitter* (i.e., before or in combination with multiplexing the WDM channels) [122], [123] or at the *receiver* (i.e., after or in combination with demultiplexing) [4], [9], [119], [120]. Filtering at the transmitter, shown for VSB-CSRZ in Fig. 13(a), allows for ultimate spectral compression and highly spectrally efficient WDM transmission. The advantage of VSB filtering at the *receiver* comes from reduced WDM channel crosstalk for the desired sideband, if *unequal* WDM channel spacings are employed. This situation is visualized in Fig. 13(b) for VSB-NRZ [4], [9], [119], [120], showing the composite spectrum of five wavelength division multiplexed (double-sideband) NRZ-OOK signals with alternating channel spacings of 1.2 and 1.7 times the data rate R. Severe WDM crosstalk is introduced for the sidebands overlapping on the closer spaced sides (region A), making them useless for detection. On the other hand, significantly less crosstalk is found for the sidebands on the larger spaced sides (region B) than would be present if the channels were spaced on an equally spaced frequency grid for the same spectral efficiency of 0.7 b/s/Hz.

V. DIFFERENTIAL PHASE MODULATION FORMATS

In order to detect information carried by the optical field's *phase* by means of square-law detection, phase-to-intensity converting elements have to be inserted into the optical path prior to the photodiode. Due to the absence of an optical phase reference at such a (noncoherent) receiver, the phase reference has to be provided by the signal itself: each bit acts as a phase reference for another bit, which is at the heart of all DPSK formats [124].

A. Binary Differential Phase Shift Keying (DPSK)

Differential binary PSK (DBPSK, or simply DPSK) encodes information on the binary phase change between adjacent bits: a 1-bit is encoded onto a π phase change, whereas a 0-bit is represented by the absence of a phase change. Like OOK, DPSK can be implemented in RZ and NRZ format. The main advantage from using DPSK instead of OOK comes from a 3-dB receiver sensitivity improvement [20], [125], which can be intuitively understood from Fig. 3(c), showing that the symbol spacing for DPSK is increased by $\sqrt{2}$ compared to OOK for fixed average optical power [124]. This increased symbol distance makes DPSK accept a $\sqrt{2}$ larger standard deviation of the optical field noise than OOK for equal BER, which translates into a 3-dB reduction in OSNR.

An optical DPSK transmitter is shown in Fig. 14. Like for DB or AMI, the data signal is first differentially encoded at the transmitter, which avoids error propagation that may occur by differential decoding at the receiver [46], [102]. The precoding operation is visualized by the two bit patterns in Fig. 14. The phase of the optical field of a narrow-linewidth laser source is then flipped between 0 and π using the precoded data sequence.

To perform optical phase modulation, one can either use a *straight-line phase modulator* (PM) or an MZM [126]. The difference between the two phase modulation schemes is indicated by the dashed double-arrows in Fig. 3(c): a PM modulates the phase *along the unit circle* in the complex plane, leaving constant the intensity of the phase-modulated light. This is visualized in Fig. 14, where the upper intensity and phase waveforms apply to a PM. However, since the optical phase directly follows the electrical drive signal, the speed of phase transitions is

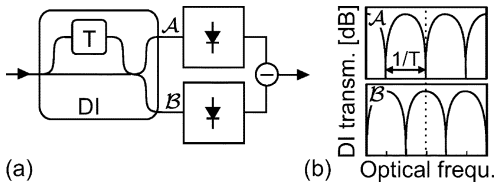

Fig. 15. ***(a) Balanced DPSK receiver using an optical DI to convert phase modulation to intensity modulation. (b) Periodic DI power transmission characteristics for the destructive port*** $(\mathcal{A})$ ***and the constructive port*** $(\mathcal{B})$**.**

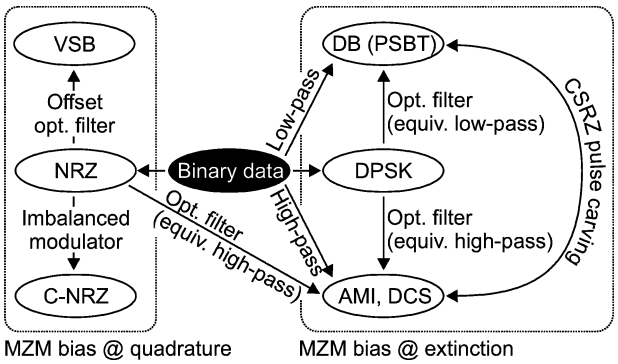

Fig. 16. ***Relationship between NRZ (including C-NRZ and VSB-NRZ), DPSK, DB, and AMI. Arrows indicate how to transition from one format to another, starting from the same binary electrical data stream.***

limited by the combined bandwidth of driver amplifier and phase modulator, and any overshoot or ringing in the drive waveform manifests itself in phase distortions. An MZM, symmetrically driven around zero transmission, modulates *along the real axis* through the origin of the complex optical field plane [cf. Fig. 3(c)], which always produces *exact* π phase jumps at the expense of residual optical intensity dips at the locations of phase transitions (see MZM waveforms in Fig. 14). Since exact phase modulation is more important for DPSK than a constant optical intensity, practical DPSK transmitters are most conveniently implemented using an MZM as a phase modulator [124]. Like for OOK, a pulse carver can be inserted to convert the NRZ-DPSK signal to RZ-DPSK, if desired.

Fig. 7(i) and (j) show optical spectra and intensity eye diagrams for NRZ-DPSK and 33%-duty-cycle RZ-DPSK, respectively. Note the absence of a 0-bit rail in the eye diagrams, which is characteristic of phase-modulated formats. The intensity dips between two bits in the NRZ-DPSK eye represent the residual intensity modulation of the MZM caused by the finite NRZ drive signal bandwidth (cf. Fig. 14).

Since DPSK cannot directly be received using square-law detection, a DI is inserted in the optical path at the *receiver* to convert the differential phase modulation into intensity modulation. As shown in Fig. 15(a), a DI splits the phase modulated signal into two paths, which experience a delay difference equal to the bit duration T (25 ps at 40 Gb/s) in order to let two neighboring bits interfere at the DI output. In practice, this differential delay is implemented by different physical path lengths within the DI, and needs to be designed to within $\pm 10\%$ for a 0.5-dB penalty [124], [127]. In addition, the DI path length difference has to be *fine*-tuned with subwavelength accuracy (i.e., on the order of 10 nm, corresponding to less than 0.1 fs, in the 1550-nm wavelength range) in order to control the interference conditions at the DI output [124], [127]. Maintaining good interference is the most critical aspect in the design of high-performance DPSK receivers, as discussed in more detail in the context of DQPSK receivers in Section V-B. At the DI output port $\mathcal{A}$ (the "destructive port"), the two optical fields interfere destructively whenever there is *no* phase change, and constructively whenever there *is* a phase change between subsequent bits, in agreement with the differential precoding rule. Due to energy conservation within the DI, the second DI output port $\mathcal{B}$ (the "constructive port") yields the *logically inverted* data pattern. In principle, one of the two DI output ports is sufficient to fully detect the DPSK signal (*single-ended detection*). However, the 3-dB sensitivity advantage of DPSK is *only* seen for *balanced detection* [124], [128], [129]; as shown in Fig. 15(a), a balanced receiver forms the difference of ports $\mathcal{A}$ and $\mathcal{B}$ to obtain the electrical decision variable. The reason for the superior performance of balanced detection compared to single-ended detection is the non-Gaussian noise statistics, characteristic of beat-noise limited systems [124], [128], [129].

Note that the DI used for DPSK demodulation is functionally equivalent to the DI discussed in the context of AMI. Fig. 15(b) shows, on a logarithmic scale, the sinusoidal transmission characteristics of ports $\mathcal{A}$ and $\mathcal{B}$ of a DI as a function of frequency. The laser carrier frequency is indicated by a dotted line. Both transmission spectra are periodic with period $1/T$. The destructive DI output port $\mathcal{A}$ acts as a delay-and-subtract filter (high-pass characteristics to first order), while the constructive port $\mathcal{B}$ is a delay-and-add filter (low-pass characteristics to first order) [111]. Not surprisingly, the formats seen at ports $\mathcal{A}$ and $\mathcal{B}$ are AMI and DB, respectively. Fig. 16 summarizes the interesting relationship between the modulation formats discussed so far, all starting from the same binary transmit data stream. The apparent lack of symmetry in Fig. 16 (no arrow from NRZ to DB) is due to the fact that narrowband optical filtering of NRZ-OOK results in a duobinary signal with three *intensity levels* [130], in analogy to the three-level electrical drive waveform shown in Fig. 11. Such a signal cannot take advantage of the square-law detecting property of photodiodes and requires special detection schemes [131], [132].

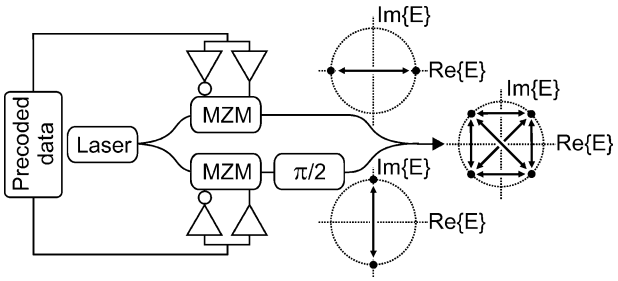

Fig. 17. *Structure of a DQPSK transmitter. Two MZMs are used as phase modulators, and the two separately modulated fields are combined with a $\pi/2$ phase shift [49], [50].*

Table 3 Classification of WDM Systems

System	Distance [km]
Access	< 100
Metro	< 300
Regional	300 – 1,000
Long-haul	1,000 – 3,000
Ultra long-haul	>3,000

B. Differential Quadrature Phase Shift Keying (DQPSK)

DQPSK is the only true multilevel modulation format (more than one bit per symbol) that has received appreciable attention in optical communications so far [49]–[51], [133]–[138]. It transmits the four phase shifts $\{0, +\pi/2, -\pi/2, \pi\}$ at a symbol rate of *half* the aggregate bitrate (cf. Table 2).

As in the case of DPSK, a DQPSK transmitter is most conveniently implemented by two nested MZMs operated as phase modulators. Fig. 17 shows the corresponding transmitter setup [50], [90], consisting of a continuously operating laser source, a splitter to divide the light into two paths of equal intensity, two MZMs operated as phase modulators, an optical $\pi/2$-phase shifter in one of the paths, and a combiner to produce a single output signal. The symbol constellations of the upper and lower paths as well as at the modulator output are also shown, together with the symbol transitions. Using this transmitter structure, one first takes advantage of the exact π-phase shifts produced by MZMs, independent of drive signal overshoot and ringing. Second, this transmitter structure requires only *binary* electronic drive signals, which are much easier to generate at high speeds than multilevel drive waveforms. Optionally, a pulse carver can be added to the structure to produce RZ-DQPSK.

Optical spectrum and intensity eye diagram for NRZ-DQPSK and 50%-duty-cycle RZ-DQPSK are shown in Fig. 3(k) and (l). Note that the *shape* of the DQPSK optical spectrum is identical to that of DPSK, but the DQPSK spectrum is compressed in frequency by a factor of two due to the halved symbol rate for transmission at fixed bitrate. The compressed spectrum is beneficial for achieving high spectral efficiencies in WDM systems [47], [49], [136] (Section VI-C), as well as for increased tolerance to CD [49], [139] (Section VI-E); the longer symbol duration compared to binary modulation formats makes DQPSK more robust to PMD (Section VI-F) [49], [139].

Like at the transmitter, one also strives to work with *binary* electrical signals at the DQPSK receiver due to implementation benefits in high-speed electronics. At the receiver, the DQPSK signal is thus first split into two equal parts, and *two* balanced receivers of the form depicted in Fig. 15(a), but with differently biased DIs, are used in parallel to simultaneously demodulate the two binary data streams contained in the DQPSK signal [49]. Note that the DI delay has to equal the *symbol* duration for DQPSK demodulation, which is *twice* the bit duration. The price of this receiver structure is a *six times* lower tolerance to frequency drifts between transmit laser and DI compared to DPSK [124], [140]. For example, at 40 Gb/s and for a 1-dB penalty, DPSK tolerates ± 1.2 GHz of laser-to-DI frequency mismatch, whereas DQPSK only allows for ± 200 MHz. At 10 Gb/s, the tolerances are even tighter by a factor of four. Note in this context that the end-of-life stability of wavelength-locked DFB lasers used in commercial optical transmitters amounts to ± 2.5 GHz, which requires feedback-controlled DI tuning within the receiver. Furthermore, any *polarization*-dependent frequency shift of the DI transfer characteristics has to be kept below the respective format's tolerance to frequency offsets [124], [127], [140]. An innovative DI design that simultaneously demodulates both binary bit streams of a DQPSK signal mitigates the problem [141].

VI. OPTICAL NETWORKING WITH ADVANCED MODULATION FORMATS

WDM systems require optical signals to propagate over long distances of optical fiber without optical-to-electrical-to-optical (O/E/O) regeneration; as mentioned in the introduction, the very value proposition of WDM lies in *sharing* optical components among many channels for as long an optical transmission distance as possible. This includes *optical routing* of densely packed WDM channels by means of OADMs. Typical transmission distances of different types of WDM systems are listed in Table 3.

The basic structure of a WDM system is shown in Fig. 18. The optical signals generated by N TXs at wavelengths λ_i are multiplexed onto a single optical fiber using a WDM multiplexer (mux). Acting as an optical bandpass filter for each channel, a mux confines the spectral extent of a modulation format in order to avoid WDM crosstalk with neighboring channels (see Section VI-C). After propagating over a series of transmission fiber spans and periodically spaced OAs (Section VI-A), the WDM channels are

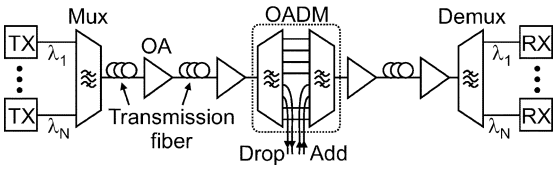

Fig. 18. *Generic setup of a WDM optical line system, consisting of N TXs and RXs at wavelengths λ_i. Wavelength channels are combined and separated by WDM multiplexers (mux) and demultiplexers (demux). Each transmission span is followed by an OA. Intermediate wavelength routing is enabled by OADMs.*

separated using a WDM demultiplexer (demux), and detected by per-channel RXs. The demux, again, acts as an optical bandpass filter for each channel to suppress both interference from neighboring WDM channels and OA noise (see Section VI-B). A possible OADM architecture, consisting of a demux followed by a mux, with intermediate access to the individual WDM channels, is also shown in Fig. 18.

In the remainder of this section, we address the question of how advanced optical modulation formats can help to combat impairments found in highly spectrally efficient optically routed WDM networks. In general, modulation formats *simultaneously* need to be:

- resilient to noise from OAs and in-band crosstalk;
- tolerant to CD and PMD;
- robust to fiber nonlinearity and inaccuracies in dispersion maps;
- amenable to repeated optical filtering due to OADMs;
- narrowband to enable high SE.

A. Single-Mode Fiber: Loss and Amplification

Optical fiber is classified into *multimode fiber* (supporting many transverse propagation modes) and *single-mode fiber* (supporting propagation of only a single transverse mode) [142]. Whether a fiber is single-mode or multimode depends on the waveguide geometry and on the transmitted optical wavelength. Because of severe *modal dispersion* in multimode optical fiber, transmission beyond a few hundred meters at multigigabit/s data rates requires single-mode optical fiber [143], which all systems listed in Table 3 are based on.

Single-mode optical fiber is an exceptionally transparent medium. Modern telecom fiber features attenuation coefficients below 0.2 dB/km across a bandwidth of many THz. This value should be compared to typical coaxial cable losses of several tens of dB/km for only a few hundred MHz bandwidth. Nevertheless, after substantial propagation distances, fiber loss reduces the signal power below the detectability threshold of optical receivers, which makes systems require *optical amplification*. Optical amplifiers can either be designed as *lumped* elements (e.g., erbium-doped fiber amplifiers, EDFAs [144], [145]), typically spaced 80 to 100 km apart in terrestrial long-haul systems, and 40 to 60 km in submarine systems, or amplification can be *distributed* by introducing gain along the transmission fiber (e.g., distributed Raman amplification [146], [147]). Widely independent of the amplification scheme, and in contrast to many RF amplifiers, most OAs do *not* distort optical signals; they exhibit constant gain across the spectrum of a single WDM channel, even at per-channel bitrates of 40 Gb/s; the main impact of optical amplification is the generation of ASE [144], [145].

B. Amplified Spontaneous Emission (ASE)

From a modulation format point of view, ASE by itself represents an optical source of *Gaussian noise*. Like the OA gain, the ASE spectrum is typically constant ("white") across the signal spectrum [145]. Note, however, that the statistical properties of ASE can be modified by nonlinear interactions during fiber propagation (cf. Section VI-G). If multiple optical amplifiers are concatenated to periodically compensate for fiber loss, ASE builds up in the system, in analogy to the noise build-up in an electrical amplifier chain [148]. This noise build-up is captured by the OSNR, which degrades with every amplifier along the propagation path [144], [145]. The OSNR is typically defined as the average optical signal power divided by the ASE power, measured in both polarizations and in a 12.5-GHz optical reference bandwidth.[10]

In converting the optical signal into an electrical signal $S(t)$, a square-law detecting optical receiver lets the ASE field $N(t)$ beat against the optical signal field $E(t)$ to yield $S(t) \propto |E(t)+N(t)|^2 = |E(t)|^2 + |N(t)|^2 + 2\mathrm{Re}\{E(t)N^*(t)\}$. The first term on the right-hand side represents the desired electrical signal, while the second and third terms represent, respectively, *ASE-ASE beat noise* and *signal–ASE beat noise* [145], [148], [149]. Note that the signal–ASE beat noise term depends on the optical signal, in particular on the optical signal power. This *signal-dependent* nature of detection noise is typically not found in RF engineering, but is characteristic of many optical communication systems.

In well designed fiber-optic receivers, the two beat noise terms dominate all other noise terms (e.g., thermal noise), and the receiver is called *beat-noise limited* [26]. The noise performance of a beat-noise limited receiver is fully characterized by the *required OSNR* ($\mathrm{OSNR}_{\mathrm{req}}$), which is the OSNR that is needed to obtain a specified target BER [26]. Obviously, detection noise in a beat-noise limited receiver is neither Gaussian nor stationary; the noise statistics depend markedly on the optical signal power, signal waveform, and receive filter characteristics [26], which has serious implications for numerical BER predictions.

[10]The data rate *independent* choice of this reference bandwidth has historic reasons: 0.1 nm (corresponding to 12.5 GHz at a wavelength of 1550 nm) is a convenient resolution bandwidth of optical spectrum analyzers that are used to measure the OSNR.

Table 4 Overview of Modulation Formats and Some Performance Values at 42.7 Gb/s. (Required OSNR at BER = 10^{-3})

Modulation format	TX complexity	RX complexity	$OSNR_{req}$			CD [ps/nm]		DGD [ps]
			Back-to-back	10 OADMs (0.4 b/s/Hz)	5 OADMs (0.8 b/s/Hz)	(2-dB pen.)		(1-dB pen.)
NRZ-OOK	1 MZM	1 PD	15.9 dB	18.2 dB	n/a	54		8
50% RZ-OOK	1-2 MZMs	1 PD	14.4 dB	15.8 dB	n/a	48		10
67% CSRZ-OOK	2 MZMs	1 PD	14.9 dB	14.2 dB	n/a	42		11
DB	1 MZM	1 PD	16.6 dB	14.2 dB	18.4 dB	211	(152)	6
33%RZ-AMI	1-2 MZMs, 1 DI	1 PD	13.4 dB	14.8 dB	n/a	49		10
VSB-NRZ-OOK	1 MZM + 1 OF	1 PD	16.4 dB	15.6 dB	17.3 dB	63	(155)	6
VSB-CSRZ	2 MZMs + 1 OF	1 PD	14.8 dB	14.7 dB	16.7 dB	51	(154)	11
NRZ-DPSK	1 MZM	1 DI + 2 PDs	11.7 dB	12.1 dB	17.6 dB	74	(161)	10
50% RZ-DPSK	1-2 MZMs	1 DI + 2 PDs	11.1 dB	11.5 dB	17.0 dB	50	(161)	10
NRZ-DQPSK	2 nested MZMs	2 DIs + 4 PDs	13.2 dB	12.6 dB	12.9 dB	168	(176)	20
50% RZ-DQPSK	2 nested MZMs + 1 PC	2 DIs + 4 PDs	12.2 dB	12.0 dB	12.0 dB	161	(186)	21

PD: photodiode; OF: optical filter; PC: pulse carver.

Table 4 gives an overview of some key characteristics of most optical modulation formats discussed in Sections IV and V. The second and third columns summarize TX and RX hardware complexity in terms of the optoelectronic component requirements. The fourth column specifies $OSNR_{req}$, based on semianalytic BER simulations that properly take into account the *non-Gaussian* noise statistics of beat-noise limited detection through Karhunen–Loève series expansions [124], [128]. The assumed 42.7 Gb/s are representative of a 40-Gb/s per-channel bitrate, including a 7% overhead for FEC, as standardized for terrestrial[11] fiber transmission systems [151]. Since enhanced FEC schemes for multigigabit/s optical communications are able to correct BER values of 10^{-3} to values below 10^{-16} [16], Table 4 is based on 10^{-3} as the target BER for stating $OSNR_{req}$. The TX implementations correspond to the ones underlying Fig. 7. All simulations assume an optical line system according to Fig. 18 with second-order super-Gaussian [91] mux and demux, having 3-dB bandwidths of 85 GHz each; such filters are characteristic of a WDM system with 100 GHz ITU channel spacing [10]. The receiver electronics are assumed to have a fifth-order Bessel low-pass characteristics with 30-GHz bandwidth. Nonideal component characteristics (e.g., group delay ripple of filters, undesired frequency offsets of filters or DIs) are neglected.

While actually measured values for $OSNR_{req}$ may differ somewhat from the numbers given in Table 4 due to various optical and electronic hardware implementation aspects, including drive waveforms, filter characteristics [60], and modulator extinction ratio [152], some general facts are worth mentioning. First, we note that *RZ formats* in general require 1–3 dB less OSNR for identical BER than their NRZ equivalents [58], [59], [61]. For beat-noise limited receivers, this is mostly due to the reduced impact of ISI on RZ formats. RZ-AMI turns out to be particularly well performing among all OOK formats, which has also been proven experimentally [114].

The spectrally narrow DB format exhibits a back-to-back penalty of typically 1–2 dB compared to OOK formats. This penalty is generated by the V-shaped eye opening [cf. Fig. 3(e)] leading to poor 0-bit detection performance, as well as by the wider-than-optimum optical filtering assumed [153]. As such, the penalty depends on the choice of filters at transmitter and receiver; for the numbers given in Table 4, an 11-GHz fifth-order Bessel electrical lowpass filter was used to implement the duobinary transmitter. As discussed below, the penalty can be reduced by tighter optical filtering (acting on the eye shape and on detection noise) or by residual CD (acting on the eye shape only).

Using DPSK instead of intensity modulation, OSNR requirements are significantly reduced. The gain of balanced-detection DPSK over OOK is generally *independent* of the target BER and typically amounts to around 3 dB (cf. RZ-OOK and RZ-DPSK in Table 4). Depending on the modulation waveforms and optical as well as electrical filters, the gain of DPSK can also *exceed* 3 dB (cf. NRZ-OOK and NRZ-DPSK in Table 4). The most sensitive modulation format practically suitable for multigigabit/s operation that is known today[12] is RZ-DPSK.

It is worth noting from Table 4 that DQPSK requires only 1–1.5 dB higher OSNR than DPSK at *poor BER* (e.g., 10^{-3}). At *good BER* (e.g., 10^{-12}), the OSNR gap between DPSK and DQPSK increases, and DQPSK approaches the performance of OOK [45]. Leaving aside TX/RX complexity aspects, the good OSNR performance at FEC error ratios makes DQPSK an attractive candidate for optically routed networks that require narrow optical signal spectra.

[11]Submarine systems use FEC schemes with overheads of up to 25% [150].

[12]In principle, pulse position modulation (PPM) is known to have even better performance for some (space-borne) applications [154]; however, its use is limited to a few Gb/s by high-speed modulation and detection electronics.

Finally, we want to remind the reader that all OSNR requirements listed in Table 4 are *bitrate specific* due to the convention of assuming a fixed optical noise reference bandwidth of 12.5 GHz. The OSNR numbers increase by 3 dB for every doubling in bitrate.

C. Filter Narrowing and WDM Crosstalk

One of the most striking differences among the modulation formats displayed in Fig. 7 is their different spectral extent. Not surprisingly, some formats are better suited than others when it comes to tight WDM channel packing, quantified by the SE or ISD defined in the introduction. Over the past few years, optical transport systems have been pushed to SEs of 0.8 b/s/Hz, and in some research experiments even beyond by means of polarization multiplexing or polarization interleaving.[13] Apart from important SE-dependent nonlinearity considerations (see Section VI-G), the two dominant impairments arising from dense WDM channel spacings in optically routed networks are *coherent WDM crosstalk* and *filter narrowing*.

Similar to signal–ASE beat noise, coherent WDM crosstalk between an optical signal field $E(t)$ and the residual optical field $R(t)$ of a neighboring WDM channel after WDM demultiplexing produces interference at square-law detection: $S(t) \propto |E(t)+R(t)|^2 = |E(t)|^2 + |R(t)|^2 + 2\mathrm{Re}\{E(t)R^*(t)\}$. For copolarized WDM channels, degradations come mostly from the beat interference term $2\mathrm{Re}\{E(t)R^*(t)\}$, which depends on the polarization between adjacent WDM channels, and is largely suppressed by *polarization-interleaving*, where adjacent WDM channels are transmitted in orthogonal polarizations. The beat interference term also depends on the optical waveform of the interfering channel, carrying a randomly different data stream, as well as on the random carrier-phase difference between WDM channels [155]. Careful mux and demux design has to ensure that WDM crosstalk is suppressed as much as possible, while signal distortions through overly narrow optical filtering are kept to a minimum [156]–[159].

Multiple OADMs in optically routed networks with high SE represent a *concatenation* of several mux–demux filters to the express channels (cf. Fig. 18); this concatenation narrows the overall optical filter bandwidth and distorts the signal. For example, concatenating five perfectly aligned OADMs, each containing two second-order super-Gaussian filters, reduces the effective 3-dB bandwidth to 56% of the bandwidth of a single filter. Practically unavoidable wavelength offsets between multiple filters or between filters and laser wavelengths exacerbate the bandwidth reduction effect.

The fifth and sixth columns in Table 4 give, respectively, the required OSNR for the concatenation of 10 OADMs in a system suitable for 0.4 b/s/Hz SE (85-GHz bandwidth for mux and demux filters at the TX, RX, and within each OADM) and 5 OADMs for 0.8 b/s/Hz SE (43-GHz bandwidth for mux and demux filters at the TX, RX, and within each OADM). It can be seen that some formats, most notably DB, exhibit an OSNR *improvement* when tightly filtered. This phenomenon arises both from ASE truncation and from beneficial waveform shaping through filtering [153], [160]. It can also be seen that supposedly narrowband modulation formats (most notably NRZ-OOK) do not lend themselves well to concatenated filtering at high spectral efficiencies, the reason being their high susceptibility to ISI and hence their low robustness to filter-induced signal distortions. Offsetting the laser frequency and properly shaping the mux filter to produce VSB enables 0.8 b/s/Hz for both VSB-NRZ and VSB-CSRZ. (In Table 4, both VSB mux and laser frequency offset were numerically optimized for 5 OADMs in a system suitable for 0.8 b/s/Hz SE.) One of the best suited formats for high-SE channel packing is RZ-DQPSK.

Note that the simulation results shown in Table 4 represent the effect of *filter concatenation only*, as they were carried out for a *single* WDM channel. The values therefore apply to a WDM system using polarization interleaving. Depending on the modulation format, coherent WDM crosstalk can lead to further penalties, especially at 0.8 b/s/Hz SE; properly capturing coherent WDM crosstalk in numerical simulations for various modulation formats is still a topic of active research [155], [159]. However, it has been shown experimentally that RZ-DQPSK [136] and VSB-CSRZ [123] show no penalty in a 0.8-b/s/Hz SE WDM networking environment.

Another aspect of filter narrowing is closely related to nonlinear fiber propagation: since OADMs can be spaced by several hundred kilometers in optically routed networks, a modulation format suitable for high-SE networks has to simultaneously lend itself to multiple passes through OADMs *and* to nonlinear fiber propagation over appreciable distances. The impact of joint impairments incurred in this scenario has been experimentally studied for 40-Gb/s systems with 0.4 and 0.8 b/s/Hz SE using a variety of modulation formats [27], [161]–[164]. In these studies, DB, VSB-CSRZ, and RZ-DQPSK are identified as the best suited formats for optically routed networks at 0.8 b/s/Hz SE.

D. Multipath Interference (MPI)

MPI describes the coherent interference of a signal with residual signals at the same wavelength [165]. As shown in Fig. 19(a), these residual signals can be multiple reflections of the desired signal due to imperfect, reflective fiber connectors or, more fundamentally, due to double-Rayleigh backscattering (DRB), e.g., in Raman-amplified systems. In optically routed networks, MPI can also arise from imperfect drop capabilities of OADMs [Fig. 19(b)].

[13]Record transmission results are typically reported in the postdeadline sessions of the annual Optical Fiber Communication Conference (OFC) and the annual European Conference on Optical Communication (ECOC).

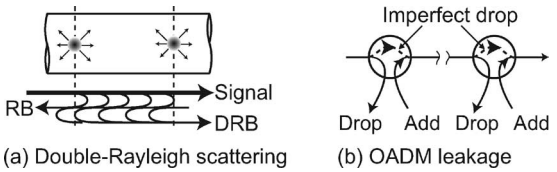

Fig. 19. *MPI can result from (a) DRB in fibers or from (b) imperfect channel dropping within OADMs.*

In complete analogy to signal–ASE beat noise and coherent WDM crosstalk, MPI gives rise to signal-MPI beat noise at square-law detection. The impact of MPI on system performance depends on the number of interferers causing MPI [165]–[167], the OSNR due to ASE [165], [168], the modulation format [165], [168], [169], the employed signal waveform (in particular the signal extinction ratio) [165], [169], [170], and the phase coherence of the interfering signal(s) in combination with the burst-error correction properties of the underlying FEC scheme [155], [171]. In general, broadband modulation spectra (RZ formats or chirped modulation) are less susceptible to MPI due to reduced signal-MPI beat noise [165], [172], [173].

E. Chromatic Dispersion (CD)

The equation for the evolution of an optical field $E(z,t)$, representing a modulated optical signal propagating in z-direction along a dispersive fiber is given by [91]

$$\frac{\partial E}{\partial z}+\frac{i}{2}\beta_2(z)\frac{\partial_2 E}{\partial t^2}-\frac{1}{6}\beta_3(z)\frac{\partial_3 E}{\partial t^3}+\frac{\alpha(z)}{2}E=0 \qquad (2)$$

where $\alpha(z)$ denotes the fiber loss coefficient (or gain coefficient, if distributed amplification is used), and captures the signal power evolution along the fiber. For a transmission fiber with uniform loss, we have $\alpha(z)=\alpha_0$. The parameter $\beta_2(z)$ is called group velocity dispersion (GVD), and represents the change in group velocity with angular frequency ω. The GVD is obtained from the propagation constant $\beta(\omega)$ using $\beta_2 \equiv [d_2\beta/d\omega^2]_{\omega=\omega_0}$ where ω_0 is the angular reference frequency at which the GVD is evaluated. The coefficient $\beta_3(z)$ accounts for the change of GVD with angular frequency ($\beta_3 \equiv [d\beta_2/d\omega]_{\omega=\omega_0} \equiv [d_3\beta/d\omega^3]_{\omega=\omega_0}$), and is referred to as the *third-order CD* parameter. In the engineering community, the dispersion parameter D, given in units of $[\mathrm{ps}/(\mathrm{km}\cdot\mathrm{nm})]$, is more commonly used than β_2 for the specification of fiber dispersion, as it relates more directly to measurements [91], [92]. Its relation to the GVD is given by

$$D(z)=-\frac{2\pi c}{\lambda^2}\beta_2(z) \qquad (3)$$

Table 5 Dispersion Parameters of Commercial Fiber at 1550 nm

Fiber type	D [ps/(km nm)]	S [ps/(km nm^2)]
NZDF	+4 to +8	+0.04 to +0.09
SSMF	+17	+0.06
DCF	−100	−0.22 to −0.67

where c is the speed of light in vacuum, and λ is the signal wavelength. Note from (3) that D and β_2 have opposite signs. The coefficient $\beta_3(z)$ of (6) is related to the more easily measurable *dispersion slope* $S(z)$ through the relation

$$S(z)\equiv\frac{dD}{d\lambda}=\frac{4\pi c}{\lambda^3}\beta_2(z)+\left(\frac{2\pi c}{\lambda^2}\right)^2\beta_3(z). \qquad (4)$$

The bandwidths of most signals at bitrates of 2.5, 10, and 40 Gb/s are much narrower than the bandwidth over which β_2 varies for the most common fiber types (see Table 5, and note that a bandwidth of 1 nm corresponds to 125 GHz at 1550 nm wavelength). As a result, β_3 represents an effective change of β_2 from channel to channel in a WDM system rather than having a noticeable impact within a WDM channel itself.

Since CD depends both on the fiber material (*material dispersion*) and on the waveguide geometry (*waveguide dispersion*), the dispersion of optical fiber can be engineered to achieve a wide range of positive and negative values. Optical fiber with negative dispersion (DCF) is used to compensate for the dispersion accumulated along the typically positive-dispersion transmission fiber. Dispersion parameters for commercial transmission fiber and DCF are given in Table 5. DCF have highly negative dispersion values to achieve high dispersion compensation with short lengths of DCF, and thus low DCF loss [174]. A large amount of installed fiber infrastructure is SSMF. Newer fiber plant is often based on NZDF.

As mentioned in Section IV-E, CD produces a spread in the propagation speed for different spectral components contained in a modulated optical signal; the effect of dispersion due to propagation over a fiber of length L is captured by multiplying the Fourier transform $E_{\mathrm{in}}(f)$ of an optical field $E_{\mathrm{in}}(t)$ by a quadratic phase term

$$E_{\mathrm{out}}(f)=E_{\mathrm{in}}(f)\exp\left[-\frac{i\pi\lambda^2 f^2 DL}{c}\right] \qquad (5)$$

which in the time domain results in signal distortions and typically in pulse broadening [91]. The resulting ISI degrades the signal quality by corrupting the peak amplitude of the 1-bits and by raising the amplitude within the 0-bits through optical interference of neighboring 1-bits. Due to the symmetric transfer function of CD, optical signal fields

whose spectral phase is symmetric (or anti-symmetric) around zero frequency experience the exact same amount of distortion for equal *positive* and *negative* values of dispersion. This applies in particular to real-valued, unchirped modulation formats. In contrast, chirped formats are distorted differently for positive and negative dispersion [91], as discussed in Section IV-E.

The seventh column in Table 4 quantifies the accumulated CD $D \cdot L$ [ps/nm] that yields a 2-dB penalty in $\mathrm{OSNR}_{\mathrm{req}}$ at 42.7 Gb/s, assuming no OADMs and mux/demux bandwidths of 85 GHz. Most modulation formats exhibit dispersion tolerances on the order of 50 ps/nm, the exception being some *spectrally narrow*[14] formats, which in general yield significantly better dispersion tolerance [25], [48]. This is reflected by the high values for DB and DQPSK. Note that dispersion tolerance values, like back-to-back OSNR requirements, can depend to an appreciable extent on the waveforms and filters used in the system. Where applicable, the numbers in brackets in the seventh column of Table 4 refer to the dispersion tolerance in a system with five OADMs at 0.8 b/s/Hz SE (cf. Section VI-C). Since filter narrowing curtails the signal spectrum, an *increase* in dispersion tolerance is typically observed. Only DB, tailored (by optimized electrical low-pass filtering at the receiver) for high dispersion tolerance in the *absence* of severe optical filtering, sees a reduction in dispersion tolerance (albeit an improvement in sensitivity) when tightly filtered. This discussion shows that the performance of a modulation format to various impairments cannot be taken in isolation, but has to be evaluated in the context of the system it is operating in. Another important example is the format-dependent shrinkage of dispersion tolerance in the presence of fiber nonlinearity, which, for example, is more pronounced for DB than for NRZ-OOK (see Section VI-H). Furthermore, we want to point out that advanced *digital signal processing* at the receiver can significantly increase the dispersion tolerance. For example, by using an MLSE at 10.7 Gb/s, an increase in dispersion tolerance by up to a factor of 2.6 has been reported for NRZ-OOK [15], [175]. Note, however, that the amount of increase in dispersion tolerance due to equalization depends on the equalization technique as well as on the modulation format [13]–[15], [32], [175]. For example, MLSE reception of DB improves the dispersion tolerance by a factor of 1.3 only [175].

Note that the CD values given in Table 4 apply for 42.7 Gb/s and scale *quadratically* with bitrate: a fourfold increase in bitrate is accompanied by a 16-fold reduction in dispersion tolerance. This quadratic scaling is evident from (5), and may be intuitively understood from the fact that the amount of temporal pulse spreading is inversely proportional to the pulsewidth [82], and the amount of pulses per unit time interval increases linearly with bitrate. As a useful coincidence, we want to mention that the numerical value of the dispersion tolerance (in [ps/nm]) at 40 Gb/s is almost identical to the dispersion tolerance (in km SSMF, $D = 17$ ps/nm) at 10 Gb/s. For example, if a signal tolerates 54 ps/nm at 42.7 Gb/s, it can propagate over roughly 54 km of SSMF at 10.7 Gb/s for the same OSNR penalty.

From a systems perspective, the resistance of a signal to CD helps to relax fiber specifications and minimizes the need for installing DCFs. Note that CD is a *linear* phenomenon. Hence, DCF can be located or distributed anywhere in an optical path in the absence of fiber nonlinearity, since order or placement of fiber types does not affect linear system performance. However, most optical communication systems operate under *fiber nonlinearity*, which makes the proper placement of DCF an important system design aspect, as discussed in detail in Section VI-G.

F. Polarization-Mode Dispersion (PMD)

Because of its circular symmetry, the single transverse propagation mode of single-mode fiber exists in two degenerate *polarization modes*, which have identical propagation properties in ideal optical fiber. In reality, however, minute waveguide asymmetries, either due to manufacturing imperfections or due to stress imposed by mechanical vibrations or temperature variations let the two polarization modes become slightly nondegenerate. The resulting two polarization-eigenstates are called *principal states of polarization*, exhibiting different group velocities, and giving rise to a DGD. The DGD manifests itself in dispersive pulse broadening: after square-law detection, the electrical signal is given by the sum of the signal powers in both (x and y) polarizations, $S(t) = |E_x(t)|^2 + |E_y(t - \mathrm{DGD})|^2$. This phenomenon is called polarization-mode dispersion (PMD) [176]. If the DGD is constant over wavelength, we refer to *first-order* PMD, while we use the term *higher order* PMD if the DGD changes with wavelength. For many applications, the DGD can be considered constant across a single WDM channel but varying across multiple channels.

The eighth column in Table 4 quantifies the tolerance of different modulation formats to first-order PMD. It shows the DGD [ps] that leads to a 1-dB OSNR penalty. For most modulation formats, a 1-dB penalty occurs at a DGD between 30 and 40% of the symbol duration, with RZ formats being in general more resilient to PMD than NRZ formats [176], [177]. Note that the resilience to PMD, in addition, depends to an appreciable extent on the waveforms [178], [179] and filters [178], [180], as well as on other residual distortions. For example, the tolerable amount of DGD for DB is almost doubled (1-dB penalty at 11 ps DGD) when operated at 211-ps/nm residual CD [181]. A similar effect is seen for VSB-NRZ when passing through 5 OADMs at 0.8 b/s/Hz SE (1-dB penalty at 10 ps DGD). Note that the tolerance to first-order PMD scales linearly

[14]Note that it is the entire spectral shape rather than just the 3-dB bandwidth that influences the robustness of a format to CD.

with symbol duration. Therefore, DQPSK has about twice the PMD tolerance of binary modulation formats at the same bitrate. The tolerance to first-order PMD shrinks linearly with bitrate.

The main problem with PMD in optical fiber systems is its stochastic nature, letting PSPs and DGD vary on timescales between milliseconds (acoustic vibrations) and months (temperature variations of buried fiber) [182]. The rare occurrence of exceedingly high DGD values prohibits worst case system design; instead, systems are allocated some margin (e.g., 1 dB), and the rare occurrence of DGDs exceeding the margin results in *system outage*. Properly specifying the *outage probability* is an important interface between fiber manufacturers, systems integrators, and service providers [176]. If outage requirements cannot be met, PMD has to be *compensated* on a per-channel basis at the receiver, or the PMD tolerance of the respective modulation format has to be increased using optical [183] or electronic [14], [15], [184], [185] *equalization* techniques.

G. Fiber Kerr Nonlinearity

The transverse mode of signals propagating in single-mode optical fibers is highly confined to the fiber core. The effective area of the modes typical ranges from 20 to 110 μm^2. As a result of this very strong confinement, light intensities within optical fibers can exceed a MW/cm^2. At such high optical intensities, the fiber's index of refraction is affected by the presence of optical signals through the Kerr effect [91], and signal-induced refractive index changes translate into changes of the signals' optical phases. These phase rotations, in conjunction with fiber dispersion, result in waveform distortions that increase with signal power.

1) Equation of Propagation: The evolution of a single-polarization optical field $E(z,t)$ in the presence of instantaneous Kerr nonlinearity in an optical fiber can be written as [91]

$$\frac{\partial E}{\partial z}+\frac{i}{2}\beta_2(z)\frac{\partial_2 E}{\partial t^2}-\frac{1}{6}\beta_3(z)\frac{\partial_3 E}{\partial t^3}+\frac{\alpha(z)}{2}E=i\gamma|E|^2E. \quad (6)$$

The Kerr nonlinearity coefficient γ is defined as $\gamma = n_2\omega_0/(cA_{\text{eff}})$, where n_2 is the nonlinear refractive index coefficient and A_{eff} is the effective mode area. Equation (6) is often referred to as the *generalized nonlinear Schrödinger equation* (GNSE). Note that the field E in the GNSE can contain *all* the fields present in the optical fiber, including the optical field of many WDM channels as well as ASE.

2) Nonlinear Transmission Regimes: If fiber loss or gain as well as third-order dispersion are neglected (i.e., α and β_3 are 0), and if $\beta_2(z)$ is a z-independent constant (i.e., the fiber has constant dispersion along its length), (6) is known as the *nonlinear Schrödinger equation* (NSE) which has *soliton* solutions if dispersion is anomalous (i.e., $\beta_2 < 0$ or $D > 0$). Soliton solutions all have the same temporal pulse profile (hyperbolic-secant-squared power profile), specific pulsewidths, and power levels that produce a periodic power evolution along the fiber length [186]. The most important soliton in optical communications is the *fundamental soliton* (i.e., the lowest-power soliton) that propagates undistorted along the propagation path [91], [187]–[189]. From a modulation format point of view, solitons do *not* represent a distinct modulation format, but fall within the broader class of RZ-OOK. During fiber propagation, fundamental solitons achieve an *exact* balance between dispersion and nonlinearity, as first demonstrated in 1980 [190]. Optical solitons have later been used in many system experiments [191]–[194] (see also [35], [188], [189], [195] for reviews). A drawback of soliton communication systems is that they require transmission fibers with low dispersion ($D \lesssim 3$ ps/(km–nm) at bitrates near 10 Gb/s; at these low dispersion values, the phenomenon of FWM between WDM channels becomes important and limits transmission [196], [197]. For this reason, fundamental solitons are not attractive for commercial systems.

For nonlinearity-resistant transmission at per-channel data rates of 10 Gb/s and above, three regimes of transmission over optical fibers are prominent: *dispersion-managed solitons*, *quasi-linear transmission*, and *pseudolinear transmission*.

It was found in 1995 [198] that the solitonic effect can still play a significant role, even for transmission fibers with high dispersion [$D \gtrsim 3$ ps/ (km–nm)], where fundamental solitons cannot be used, if one periodically distributes DCFs with positive GVD β_2 (or negative dispersion D) along the transmission line. If $\beta_2(z)$ is a *periodic* function with sufficiently low path-averaged dispersion,[15] (6) has an approximate solution called *dispersion-compensated soliton* or *dispersion-managed soliton* [199]–[201]. Dispersion-managed solitons are the solitons that best fit fiber-optic communication systems using dispersion compensation, and have been used in many system experiments [198], [202]–[207]. Note that the dynamics associated with dispersion-managed solitons still require an average balance of dispersive effects and nonlinear effects in the transmission fiber (in contrast to the *exact* balance needed for fundamental solitons). This average balance occurs at a per-channel bitrate of about 10 Gb/s over the majority of commercial fiber, and explains why all dispersion-managed soliton experiments have been performed near this bitrate.

Even though dispersion-managed solitons are conceptually attractive, alternative regimes of transmission have

[15]The path-averaged dispersion is the CD averaged over the propagation path length.

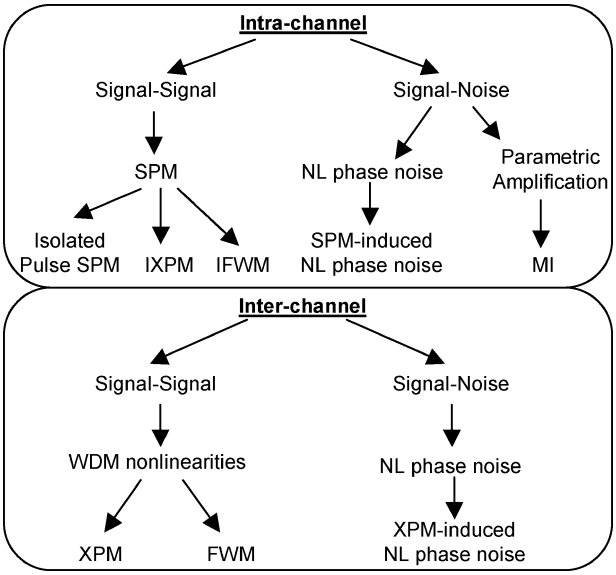

Fig. 20. *Classification of nonlinearities in optical fibers. Intrachannel and interchannel stand for nonlinearities occurring within or between WDM channels, respectively.*

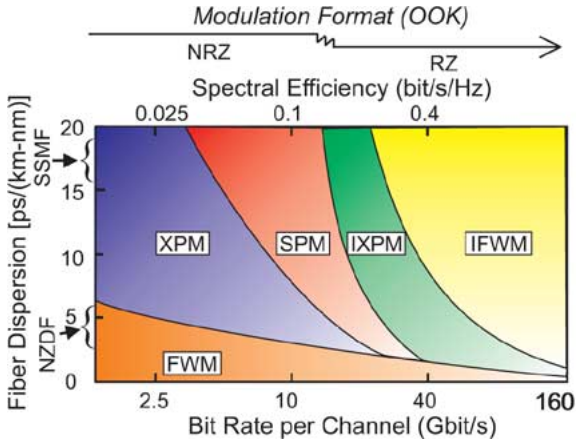

Fig. 21. *Significance of inter- and intrachannel nonlinear impairment in WDM systems of different per-channel bitrates. For high-speed TDM systems exceeding 10 Gb/s per channel, the dominant nonlinear interactions are intrachannel cross-phase modulation and intrachannel four-wave mixing.*

demonstrated similar or superior resistance to fiber nonlinearity. One such alternative regime is the *CRZ regime* [88], [89], which is also referred to as the *quasi-linear regime*. As mentioned in Section IV-D, analog periodic phase modulation is imprinted on the RZ-OOK signal, with a phase modulation index tailored to the length of the transmission line. This allows to decrease the solitonic effect in the line, generally resulting in slightly better performance than for dispersion-managed soliton systems [89]. Like for dispersion-managed solitons, this regime of transmission is best suited for per-channel bitrates around 10 Gb/s.

Another regime of transmission, referred to as *pseudolinear transmission* [82], [208], [209] allows efficient nonlinear transmission for high-speed signals ($\gtrsim$10 Gb/s). In this regime, the signal waveform *evolves very fast* along the fiber length, which averages out the nonlinearities between bits from the same channel as well as the nonlinearities between different channels. The pseudolinear regime has been demonstrated at per-channel bitrates as high as 320 Gb/s [210].

3) Types of Nonlinear Distortions: In order to better understand the origin and performance of different nonlinear transmission regimes, we decompose the Kerr nonlinearity in (6) into more specific nonlinear interactions that can distort optical signals in different ways. A summary of nonlinear interactions is presented in Fig. 20, and in Sections VI-G4 and VI-G6.

Fiber nonlinearities occuring between pulses of the *same* WDM channel or between a WDM channel and ASE are referred to as *intrachannel* nonlinearities. When the nonlinearities occur among two or more WDM channels, we use the expression *interchannel* nonlinearities. The importance of each class of nonlinearities depends significantly on the per-channel bitrate. As a rule of thumb, interchannel effects affect WDM systems most strongly at per-channel bitrates of 10 Gb/s and below (i.e., dispersion-managed solitons and quasi-linear regime), while intrachannel nonlinearities affect systems most strongly at bitrates above 10 Gb/s (i.e., pseudolinear transmission). The impact of fiber nonlinearity also depends on the local fiber dispersion: in general, lower dispersion fiber [$|D| \lesssim$ 10 ps/(km-nm)] has stronger interchannel effects than fiber with high local dispersion [$|D| \gtrsim$ 10 ps/(km-nm)]. Nonlinear interactions between signal and noise depend significantly on the noise level, and become stronger if the OSNR is *poor during propagation*, which has become particularly important with the use of FEC.

The impact of fiber nonlinearity on various modulation formats depends strongly on the physical characteristics of the underlying optical network. Fig. 21 presents the results of an extensive numerical study, showing the dominant nonlinearity for a given spectral efficiency and fiber dispersion for plain OOK modulation formats with various duty cycles. The figure should be read as follows: for a given spectral efficiency (upper x-axis), the figure gives the optimum per-channel bitrate (lower x-axis) that allows for maximum signal launch power at a fixed penalty due to nonlinearities; maximizing the signal launch power also maximizes the OSNR delivered at the receiver, and for equal signal distortion minimizes the BER. The figure then shows the most important nonlinearity that limits transmission for various local fiber dispersion values (vertical

axis). For instance, at bitrates of 2.5 or 10 Gb/s, and as explained in more detail in Section VI-G4, OOK signals are mostly limited by FWM, XPM, or SPM. At 40 Gb/s and above, intrachannel nonlinearities are dominating for OOK as soon as fiber dispersion exceeds a few ps/(km-nm). The broken arrow at the top of Fig. 21 shows that the optimum modulation format in terms of nonlinear transmission changes from NRZ to RZ (50% and 33% duty cycles) around 10 Gb/s per channel.

4) Signal–Signal Interactions: Starting from (6), we can analytically break down nonlinear effects into more elementary nonlinear interactions, as displayed in Fig. 20. To this end, we decompose an aggregate of WDM channels into the sum of individually interacting WDM channels (for *interchannel* nonlinearities), or a single WDM channel into the sum of individually interacting bits (for *intrachannel* nonlinearities). For instance, by decomposing a WDM multiplexed field E into three of its interacting field components E_1, E_2 and E_3, we rewrite (6) in terms of the three fields E_1 through E_3. Under the condition of small signal distortions, the equation can be separated into three coupled equations, one for each field component. For example, the equation describing the evolution of E_1 is given by

$$\frac{\partial E_1}{\partial z}+\frac{i}{2}\beta_2(z)\frac{\partial_2 E_1}{\partial t^2}-\frac{1}{6}\beta_3(z)\frac{\partial_3 E_1}{\partial t^3}+\frac{\alpha(z)}{2}E_1 = \underbrace{i\gamma|E_1|^2E_1}_{\text{SPM}}+\underbrace{2i\gamma\left(|E_2|^2+|E_3|^2\right)E_1}_{\text{(I)XPM}}+\underbrace{i\gamma E_2^2E_3^*}_{\text{(I)FWM}} \quad (7)$$

where the terms on the right-hand side involving E_2 and E_3 are responsible for the nonlinear effects of XPM and FWM if the fields E_1 through E_3 represent individual WDM channels; if the fields E_1 through E_3 represent individual bits from a single WDM channel, these terms are responsible for IXPM and IFWM. Note that SPM sometimes refers to SPM that an entire channel is experiencing and sometimes refers to SPM that a pulse is producing on itself.

Intrachannel nonlinearities are particularly important to advanced optical modulation formats at high per-channel bitrates. Numerous detailed analyses reveal how these nonlinearities impact transmission [82], [211]–[216]. Figs. 22 and 23 show the effects of IXPM and IFWM, respectively, as experienced by a 40-Gb/s RZ-OOK signal after nonlinear propagation. In the case of dominating IXPM [208] (Fig. 22), *timing jitter* is present after transmission. In a system limited by IFWM (Fig. 23), *shadow pulses* (*ghost pulses*) [208], [209] are created in originally empty time slots. Amplitude jitter is also present, and both effects impair transmission for systems limited by IFWM [82]. Most advanced modulation formats are geared toward a reduction of intrachannel nonlinearities; IXPM and IFWM

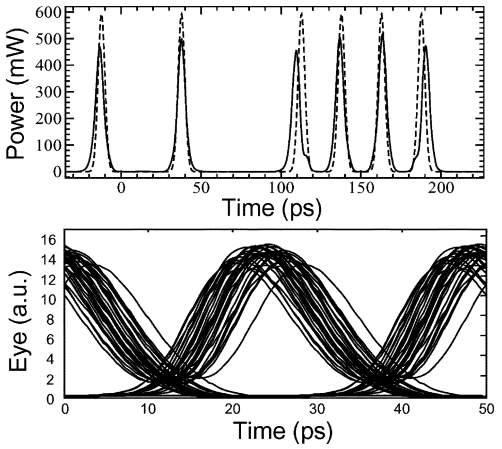

Fig. 22. *Effect of IXPM on a 40-Gb/s RZ-OOK signal. The upper graph shows the signal waveform before (dashed line) and after (solid line) transmission. The main effect of IXPM is to produce timing jitter, as observed on the eye diagram in the lower graph.*

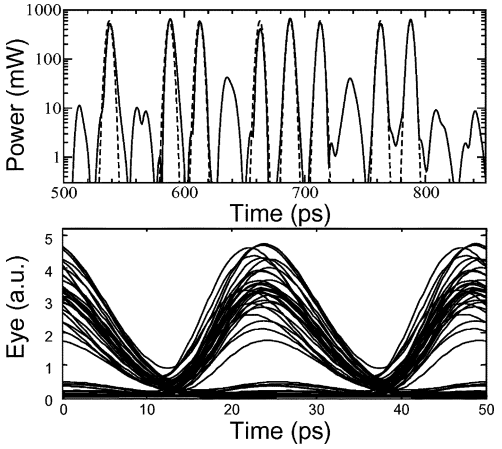

Fig. 23. *Same as Fig. 22 but for a system limited by IFWM. In the upper graph, one can observe the presence of small pulses in the location of initially empty slots ("zeros"). Such pulses are referred to as shadow pulses (ghost pulses).*

are sensitive to auxiliary phase coding (pseudo-multilevel or correlative coding) used by advanced modulation formats [212].

5) Dispersion Mapping: One of the most powerful and most widely used techniques to reduce the impact of fiber nonlinearity is the use of *dispersion mapping*, referring to the precise placement of DCFs in optical networks [82], [217], [218]. One can understand dispersion mapping by noting that the effect of fiber nonlinearity at a given point in a network depends on the characteristics of the optical signal fields at that point. Furthermore, the waveform conditions at a given point in a network are largely

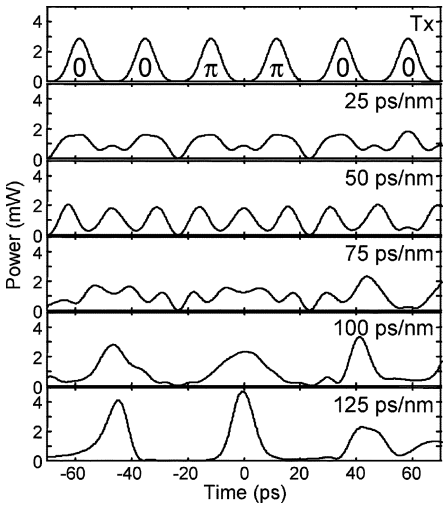

Fig. 24. *Evolution of an RZ-DPSK waveform as a function of cumulative dispersion. The data-encoded phases are indicated on upper graph. Despite having identical pulses intensities at the TX, the phase coding creates a waveform without periodic structures after dispersion. The average power is 1 mW.*

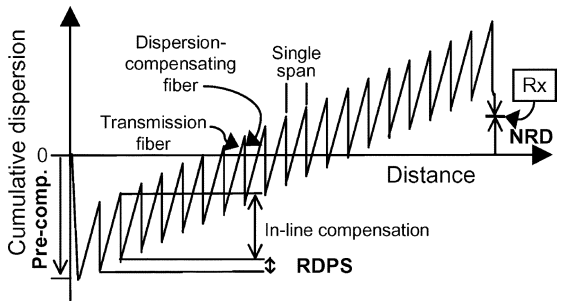

Fig. 25. *Example of a dispersion map showing the cumulative dispersion as a function of distance.*

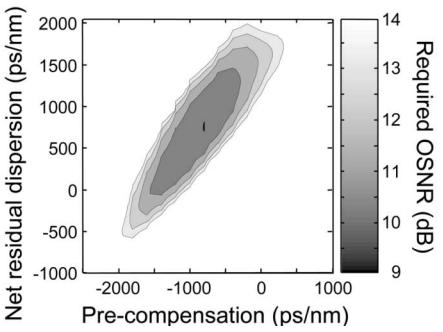

Fig. 26. *Example of a robustness analysis for a singly periodic dispersion map and NRZ-OOK. The contour lines represent the required OSNR. The back-to-back required OSNR is 10.9 dB.*

dependent on the accumulated dispersion the signal has experienced from the transmitter up to that point in the network (see Fig. 24). Consequently, a judicious placement of DCFs can be used to control the signal accumulated dispersion in a network in order to reduce the impact of fiber nonlinearity. Dispersion mapping is a significant part of the design of virtually all optical communication systems, from metro to ultralong haul (cf. Table 3).

Fig. 25 shows an example of a dispersion map. This type of dispersion map, having the same *residual dispersion* for every span, is referred to as *singly periodic dispersion map*. Only three parameters are necessary to define a singly periodic dispersion map: dispersion *precompensation*, RDPS, and NRD. The optimization of these three parameters for a given fiber type, bitrate, channel spacing and modulation format allows for maximum signal launch power and thus largest delivered OSNR at the receiver and best BER [219] while keeping low nonlinearity-induced signal distortions.

Other types of dispersion maps are also possible and have been studied [212], [220], [221]. An example for an advanced dispersion map is the *doubly periodic dispersion map* [222], [223] where periodic corrections of the dispersion map improve nonlinear transmission or adjust the dispersion level for optimum detection at periodically spaced OADM sites. Achieving a certain value of dispersion may be challenging, since the dispersion of fibers is often known only to a certain accuracy. Variations in the fiber manufacturing process, inaccurate dispersion measurements of installed fiber infrastructure, effects of temperature variations on dispersion [224], [225], and a finite number of commercially available DCF modules ("granularity" of DCFs) are factors that contribute to a reduction in dispersion map accuracy. Because of these uncertainties, it is important to consider the resistance of various modulation formats to dispersion map inaccuracies [226].

An example of the way dispersion maps are analyzed is given in Fig. 26 for NRZ-OOK at 10.7 Gb/s. The required OSNR for the center channel of an 11-channel WDM transmission simulation is presented as a function of precompensation and NRD, two of the three parameters defining a singly periodic dispersion map. The third parameter, the RDPS, was set to a fixed value of 100 ps/nm; 15 spans of 80-km SSMF and a per-channel fiber launch power of 2.6 dBm were assumed. Such plots allow finding optimally robust dispersion map parameters for a given modulation format.

6) Signal–Noise Interactions: In addition to the signal–signal interactions described in previous sections, the signal can also interact with optical noise through fiber nonlinearities. The dominant source of optical noise in a transmission line is typically the ASE generated by in-line

optical amplification. One can distinguish between two forms of nonlinear interactions that involve signal and noise.

A first form of nonlinear signal–noise interaction that can affect transmission in optical fibers falls in the category of *parametric amplification* [91]. In such a process, noise amplification occurs through the presence of one or many signals in a passive nonlinear medium. When a single wave is involved in this process, one uses the term *modulation instability*. In the context of fiber-optic communication systems, parametric amplification of noise and modulation instability manifest themselves mainly by the amplification of noise in a limited frequency band (up to $\sim$ 50 GHz) around the signal central frequency [227], [228]. XPM can also induce modulation instability in fibers [229], [230]. Modulation instability and parametric amplification have more impact on signals propagating at low OSNR, like systems using FEC [231].

A second form of nonlinear signal–noise interactions manifests itself in noise-induced nonlinear distortions of *specific* signal characteristics (e.g., amplitude, timing, phase, or frequency [148], [232]. Upon nonlinear propagation, the temporal pulse profile can be well preserved, but fluctuations in other pulse characteristics due to nonlinear interactions can largely exceed the fluctuations induced by the linear presence of noise. A classic example is the nonlinear interaction between optical solitons and ASE that leads to wandering of the soliton positions in their respective bit slots (*Gordon–Haus timing jitter* [233]). Another example, particularly relevant to advanced phase modulation formats, is *nonlinear phase noise*, sometimes referred to as the *Gordon–Mollenauer* effect [234]. This effect can be explained as follows: noise that happens to add constructively to some bits in a pulse train results in an *increase* in amplitude for these bits, while noise that adds destructively to some other bits results in *reduced* pulse amplitudes. These noise-induced random differences in pulse amplitudes among different bits affect SPM-induced phase rotations. Random amplitude differences are therefore translated into random phase differences by fiber nonlinearity. This bit-to-bit randomization of the optical phase is particularly harmful to modulation formats that use *phase coding* to transmit data, such as DPSK [235], [236] and DQPSK. Fig. 27 shows the effect of nonlinear phase noise on a 50%-duty-cycle RZ-DPSK signal at 42.7 Gb/s using a balanced receiver [237]. The signal distortion is measured by the required OSNR necessary to obtain a BER of 10^{-3}. The lower curve (circles) applies to a hypothetical system where noise is only added *at the RX*. Thus, only deterministic (intrachannel) signal–signal nonlinearities are present, but no nonlinear phase noise. When, again hypothetically, all the noise is added *at the TX* and copropagates with the signal over the entire transmission line, the receiver needs a higher OSNR to maintain BER $= 10^{-3}$ due to nonlinear phase noise (triangles). A realistic system, where noise is added at every OA along the transmission path (32 OAs in this case) is represented by squares in Fig. 27.

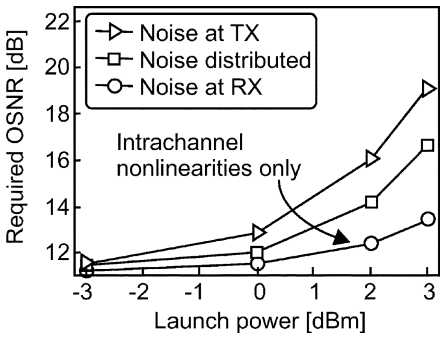

Fig. 27. *Effect of nonlinear phase noise on the required OSNR for single-channel transmission of a 42.7 Gb/s 50% RZ-DPSK signal. Fiber parameters are 32 spans of 80 km, D = 4.5 ps/(km-nm), S = 0.045 ps/(nm^2-km), α = 0.2 dB/km, n_2 = 2.5 x 10^{-20} m^2/W, and A_{eff} = 52.86 μm^2. The dispersion map is an SPDM with precompensation = −250 ps/nm, RDPS = 20 ps/nm, and NRD = 20 ps/nm.*

In addition to SPM, XPM can also mediate nonlinear phase noise [238]. The amplitude variations created by noise on channels can be transferred as phase distortions onto other channels through XPM. This phenomenon can become an important limitation for tight channel spacings ($\sim$ 50 GHz and below) at low bitrates (10 Gb/s) [238].

H. Nonlinearities and Modulation Formats

Even though a detailed understanding of the limitations from fiber nonlinearities for advanced modulation formats is still an active research topic, some numerical and experimental investigations suggest the types of nonlinear effects that are typically limiting transmission: intensity-modulated formats are limited by the effects discussed in the context of Fig. 21. For phase-modulated formats, at 2.5 and 10 Gb/s, the main limitations on nonlinear transmission generally come from nonlinear phase noise. At 40 Gb/s and above, intrachannel nonlinearities dominate, even though nonlinear phase noise can become a limitation at low OSNR (see Fig. 27).

Since fiber nonlinearity depends on a multitude of system parameters, the comparison of modulation formats with respect to their resilience to fiber nonlinearity is often somewhat subjective. For example, one commonly used way to quantify the resistance of a format to fiber nonlinearity is to find the optimum signal launch power by minimizing the BER for each format after a certain transmission distance. Two modulation formats are then said to have the same resistance to fiber nonlinearity if they achieve their respective minimum BER at the same signal launch power. Note that because of differences in receiver sensitivity by 5 dB and more (see Table 4), the minimum BER may differ substantially between two modulation

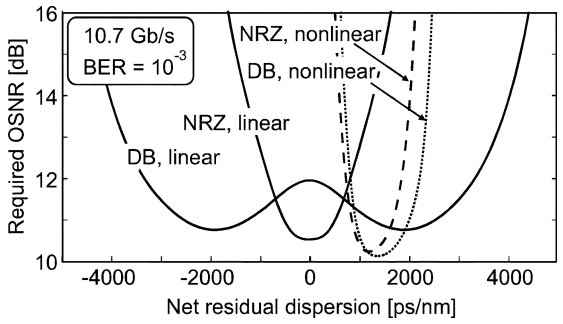

Fig. 28. *Reduction of the dispersion tolerance of DB with nonlinear transmission. NRZ results are shown for comparison. The large dispersion tolerance of DB relative to NRZ in linear transmission almost completely disappears after nonlinear transmission.*

formats even though they can have identical resistance to fiber nonlinearity (same optimum power levels). Modulation formats impacted by nonlinear phase noise can suffer further degradations at low delivered OSNR, resulting in a need to reassess the resistance to nonlinearity as the delivered OSNR changes for these formats. The remainder of this section focuses mostly on per-channel data rates of 40 Gb/s, since this is where advanced modulation formats start to become most beneficial. Additional comparisons of various advanced modulation formats for nonlinear transmission can be found in [239]–[241].

One of the first advanced modulation formats that was discussed in the context of optically amplified transmission systems was DB. At 10 Gb/s, the primary goal for using DB is to increase dispersion tolerance, while at 40 Gb/s, DB is mainly attractive for high spectral efficiency WDM systems. Despite its early implementation [103], [104], only a limited number of long-distance DB transmission demonstrations have been performed [241]–[248]. At 40 Gb/s, the resistance of DB to nonlinear transmission (with near-optimum dispersion mapping) does not differ substantially from similar duty cycle OOK [241], [246]. At 10 Gb/s, the first effect of fiber nonlinearity on DB is to reduce its dispersion tolerance [249]. Fig. 28 illustrates this phenomenon, showing the dispersion tolerance of 10-Gb/s DB and NRZ systems after linear (solid) and nonlinear (NRZ: dashed, DB: dotted) transmission. The transmission is over 16 spans of SSMF at 50-GHz WDM channel spacing and at +5 dBm/ch for both formats. In spite of the large dispersion of SSMF [$D = 17$ ps/(km nm)], the dominant nonlinearity is XPM due to the small channel spacing. Note that the large linear dispersion tolerance of DB ($\pm$4000 ps/nm at a 2-dB OSNR penalty) shrinks to become similar to the dispersion tolerance of NRZ after transmission (1500 ps/nm full width of the 2-dB dispersion window). This can be understood by realizing that XPM, as its name indicates, most importantly distorts the signal *phase*. Since the phase coding of DB is important for its dispersion tolerance, XPM rapidly destroys the dispersion tolerance of DB. However, a detailed assessment of the nonlinear transmission performance of DB in WDM systems at 10 Gb/s still remains to be performed.

Early studies of the effect of fiber nonlinearity on advanced modulation formats at per-channel data rates of 40 Gb/s used CSRZ [83], [250]. High powers over short reach showed that CSRZ is capable of suppressing IFWM due to the alternating phases from bit to bit [84], [251]. CSRZ was later used for longer reach experiments [252] and high spectral efficiencies of 0.8 b/s/Hz using strong optical filtering at the TX were achieved [253].

As mentioned in Section IV-G, narrow optical filtering can be applied at the transmitter or at the receiver to generate VSB formats [9], [42], [254], [255]. Experimental demonstrations [9], [121] suggest that, in the pseudolinear transmission regime, nonlinear transmission of VSB formats does not significantly differ from the transmission of the same signal without VSB filtering (double-sided formats).

Since IFWM depends on the relative phase between pulses [82], a variety of ways to encode an auxiliary optical phase modulation on the signal can be developed to suppress the specific effects of IFWM [55], [221], [256]–[261]. In a particularly interesting study [258], Randel showed that an optimum choice of relative phases between adjacent pulses to suppress IFWM in a set of four consecutive bits can be either $\{0, \pi/2, 0, \pi/2\}$ or $\{0, 0, \pi, \pi\}$. The mechanism for the reduction of IFWM using this coding schemes is by destructive interference of IFWM effects [258], [262]. This auxiliary phase encoding leads to modulation schemes with memory, either using pseudo-multilevel modulation or correlative coding (cf. Fig. 2).

Phase modulation (DPSK and DQPSK) has received considerable attention in recent years, mainly due to improved receiver sensitivity relative to OOK when balanced detection is employed (cf. Table 4). The nonlinear transmission of phase modulation formats is affected mainly by nonlinear phase noise [235], [238] (at 10 Gb/s) and by IFWM (at 40 Gb/s and higher). Because phase modulation is affected by nonlinear phase noise, transmission penalties are determined not only by the signal evolution but also by the level of copropagating noise, which should always be quoted in this context (cf. Fig. 27).

Propagation of 40-Gb/s DPSK over the most common fiber types (NZDF and SSMF) indicates that DPSK has a similar resistance to fiber nonlinearity as CSRZ when operated at an OSNR at the receiver that yields a BER of around 10^{-3}, suitable for FEC decoding. Even though DPSK and CSRZ may have similar resistance to fiber nonlinearity, the improved receiver sensitivity of DPSK generally results in better BER for DPSK relative to CSRZ, resulting in better system performance.

Many flavors of DPSK exists, including various RZ duty cycles ranging typically from 33% (RZ-DPSK) to 100% (NRZ-DPSK). In pseudolinear transmission, formats with lower duty cycles are generally more resistant to intrachannel nonlinearities for OOK formats [82]. For DSPK, the differences in nonlinear transmission between similar ranges of duty cycles are smaller than for OOK [263], [264].

Promising transmission results of DQPSK have also been reported [133], [136], [265]. However, a detailed comparison of the transmission performance of DQPSK to other modulation formats still remains to be performed.

At 10 Gb/s, the focus of advanced modulation formats is to improve transmission with little attention devoted to spectral efficiency, as spectral efficiencies in 10 Gb/s-based systems typically do not exceed 0.4 b/s/Hz. At bitrates near 10 Gb/s, the waveform disperses slowly during propagation; as a result, 10 Gb/s per channel systems suffer more from nonlinear phase noise than higher bitrate systems [235]. Experimental demonstrations using DPSK at 10 Gb/s in submarine systems [266] suggest an improvement in BER relative to OOK. However, the improvement in BER is less than the difference of receiver sensitivity between DPSK and OOK, indicating that DPSK is less resistant to fiber nonlinearity than OOK at 10 Gb/s in ultralong-haul systems due to nonlinear phase noise.

Finally, future optically routed networks will incorporate OADMs and the *simultaneous* resistance to the effects of optical filtering from OADMs on the one hand, and fiber nonlinearity on the other hand is required. A study [161] of long-haul propagation of different binary formats at 42.7 Gb/s in a transmission line that incorporate OADMs shows that nonlinear transmission can be strongly altered after tight optical filtering. Such findings emphasize how severely the nonlinearity performance of advanced modulation formats depends on the particular network specifications.

VII. CONCLUSION

High per-fiber capacities at an attractive cost per transported information bit are enabled by spectrally efficient WDM transport on flexible, optically routed networks. Advanced modulation formats play an important role in the design of such networks. We have discussed the generation and detection of the most important optical modulation formats for multigigabit/s per-channel data rates, where limits of available RF technology place important restrictions in the implementation of transponders. We have compared intensity and phase modulation formats with respect to their back-to-back receiver performance as well as their resilience to MPI and coherent crosstalk. We have discussed the robustness of optical modulation formats to signal distortions induced by CD, PMD, narrowband optical filtering, and fiber Kerr nonlinearity. ■

Acknowledgment

The authors acknowledge very valuable discussions with S. Chandrasekhar, A. H. Gnauck, G. Raybon, A. R. Chraplyvy, H. Kogelnik, R. Griffin, Y. Miyamoto, J. G. Proakis, and M. Nissov. The authors also thank E. Burrows, E. Wang, and M. Rübsamen for help with computations.

REFERENCES

[1] H. Kogelnik, "High-capacity optical communications: Personal recollections," *IEEE J. Sel. Topics Quantum Electron.*, vol. 6, no. 6, pp. 1279–1286, Nov./Dec. 2000.

[2] ——, "On optical communication: Reflections and perspectives," in *Proc. Eur. Conf. Optical Communication (ECOC)*, 2004, Paper Mo1.1.1.

[3] K. Fukuchi, T. Kasamatsu, M. Morie, R. Ohhira, T. Ito, K. Sekiya, D. Ogasahara, and T. Ono, "10.92-Tb/s (273 × 40-Gb/s) triple-band/ultra-dense WDM optical-repeatered transmission experiment," in *Proc. Optical Fiber Communication Conf. (OFC)*, 2001, Paper PD24.

[4] Y. Frignac, G. Charlet, W. Idler, R. Dischler, P. Tran, S. B. S. Lanne, C. Martinelli, G. Veith, A. Jourdan, J.-P. Hamaide, and S. Bigo, "Transmission of 256 wavelength-division and polarization-division-multiplexed channels at 42.7 Gb/s (10.2 Tb/s capacity) over 3 × 100 km of TeraLight fiber," in *Proc. Optical Fiber Communication Conf. (OFC)*, 2002, Paper FC5.

[5] G. Charlet, E. Corbel, J. Lazaro, A. Klekamp, R. Dischler, P. Tran, W. Idler, H. Mardoyan, A. Konczykowska, F. Jorge, and S. Bigo, "WDM transmission at 6 Tbit/s capacity over transatlantic distance and using 42.7 Gb/s differential phase-shift keying without pulse carver," in *Proc. Optical Fiber Communication Conf. (OFC)*, 2004, Paper PDP36.

[6] A. H. Gnauck, G. Raybon, S. Chandrasekhar, J. Leuthold, L. S. C. Doerr, A. Agarwal, S. Banerjee, D. Grosz, S. Hunsche, A. M. A. Kung, D. Maywar, M. Movassaghi, X. Liu, C. Xu, X. Wei, and D. M. Gill, "2.5 Tb/s (64 × 42.7 Gb/s) transmission over 40 × 100 km NZDSF using RZ-DPSK format and all-Raman-amplified spans," in *Proc. Optical Fiber Communication Conf. (OFC)*, 2002, Paper FC2.

[7] C. Rasmussen, T. Fjelde, J. Bennike, F. Liu, S. Dey, P. M. B. Mikkelsen, P. Serbe, P. V. der Wagt, Y. Akasaka, D. Harris, D. Gapontsev, V. Ivshin, and P. Reeves-Hall, "DWDM 40 G transmission over transpacific distance (10,000 km) using CSRZ-DPSK and enhanced FEC and all-Raman amplified 100 km Ultrawave fiber spans," in *Proc. Optical Fiber Communication Conf. (OFC)*, 2001, Paper PD18.

[8] D. J. Costello, J. Hagenauer, H. Imai, and S. B. Wicker, "Applications of error-control coding," *IEEE Trans. Inf. Theory*, vol. 44, no. 6, pp. 2531–2560, 1998.

[9] S. Bigo, "Multiterabit DWDM terrestrial transmission with bandwidth-limiting optical filtering," *IEEE J. Sel. Topics Quantum Electron.*, vol. 10, no. 2, pp. 329–340, Mar./Apr. 2004.

[10] Spectral Grids for WDM Applications: DWDM Frequency Grid, Standard ITU-T G.694.1, 2002.

[11] M. Birk, L. Raddatz, D. Fishman, S. Woodward, and P. Magill, "Field trial of end-to-end OC-768 transmission using 9 WDM channels over 1000 km of installed fiber," in *Proc. Optical Fiber Communication Conf. (OFC)*, 2003, Paper TuS4.

[12] D. Y. Al-Salameh, S. K. Korotky, D. S. Levy, T. O. Murphy, S. H. Patel, G. W. Richards, and E. S. Tentarelli, "Optical switching in transport networks," in *Optical Fiber Telecommunications IV A*, I. Kaminov and T. Li, Eds. New York: Academic, 2002, ch. 7, pp. 295–373.

[13] T. Nielsen and S. Chandrasekhar, "OFC 2004 workshop on optical and electronic mitigation of impairments," *J. Lightw. Technol.*, vol. 23, no. 1, pp. 131–142, Jan. 2005.

[14] D. Castagnozzi, "Digital signal processing and electronic equalization (EE) of ISI," in *Proc. Optical Fiber Communication Conf. (OFC)*, 2004, Paper WM6.

[15] A. Färbert, S. Langenbach, N. Stojanovic, C. Dorschky, T. Kupfer, C. Schulien, J.-P. Elbers, H. Wernz, H. Griesser, and C. Glingener, "Performance of a 10.7-Gb/s receiver with digital equalizer using maximum likelihood sequence estimation,"

in *Proc. Eur. Conf. Optical Communication (ECOC)*, 2004, Paper Th4.1.5.

[16] T. Mizuochi, K. Kubo, H. Yoshida, H. Fujita, H. Tagami, M. Akita, and K. Motoshima, "Next generation FEC for optical transmission systems," in *Proc. Optical Fiber Communication Conf. (OFC)*, 2003, Paper ThN1.

[17] D. McGhan, C. Laperle, A. Savchenko, C. Li, G. Mak, and M. O'Sullivan, "5120 km RZ-DPSK transmission over G.652 fiber at 10 Gb/s with no optical dispersion compensation," in *Proc. Optical Fiber Communication Conf. (OFC)*, 2005, Paper PDP27.

[18] Y. Yamamoto, "Receiver performance evaluation of various digital optical modulation-demodulation systems in the 0.5–10 μm wavelength region," *IEEE J. Quantum Electron.*, vol. 16, no. 11, pp. 1251–1259, Nov. 1980.

[19] R. A. Linke and A. H. Gnauck, "High-capacity coherent lightwave systems," *J. Lightw. Technol.*, vol. LT-6, no. 11, pp. 1750–1769, Nov. 1988.

[20] G. Jacobsen, *Noise in Digital Optical Transmission Systems*. Norwood, MA: Artech House, 1994.

[21] O. K. Tonguz and R. E. Wagner, "Equivalence between preamplified direct detection and heterodyne receivers," *J. Lightw. Technol.*, vol. 3, no. 11, pp. 835–837, Sep. 1991.

[22] A. H. Gnauck, J. Sinsky, P. J. Winzer, and S. Chandrasekhar, "Linear microwave-domain dispersion compensation of 10-Gb/s signals using heterodyne detection," in *Proc. Optical Fiber Communication Conf. (OFC)*, 2005, Paper PDP31.

[23] S. Tsukamoto, D.-S. Ly-Gagnon, K. Katoh, and K. Kikuchi, "Coherent demodulation of 40-Gbit/s polarization-multiplexed QPSK signals with 16-GHz spacing after 200-km transmission," in *Proc. Optical Fiber Communication Conf. (OFC)*, 2005, Paper PDP29.

[24] Proc. IEEE/LEOS Workshop Advanced Modulation Formats, 2004.

[25] J. Conradi, "Bandwidth-efficient modulation formats for digital fiber transmission systems," in *Optical Fiber Telecommunications IV B*, I. Kaminow and T. Li, Eds. New York: Academic, 2002, pp. 862–901.

[26] P. J. Winzer, "Optical transmitters, receivers, and noise," in *Wiley Encyclopedia of Telecommunications*, J. G. Proakis, Ed. New York: Wiley, pp. 1824–1840. [Online]. Available: http://www.mrw.interscience.wiley.com/eot/eot_sample_fs.html

[27] A. H. Gnauck, "Advanced amplitude- and phase coded formats for 40-Gb/s fiber transmission," in *Proc. IEEE/LEOS Annu. Meeting*, 2004, Paper WR1.

[28] S. Bigo, G. Charlet, and E. Corbel, "What has hybrid Phase/Intensity encoding brought to 40 Gbit/s ultralong-haul systems," in *Proc. Eur. Conf. Optical Communication (ECOC)*, 2004, Paper Th2.5.1.

[29] A. Hirano and Y. Miyamoto, "Novel modulation formats in ultra-highspeed optical transmission systems and their applications," in *Proc. Optical Fiber Communication Conf. (OFC)*, 2004, Paper ThM1.

[30] P. J. Winzer and R.-J. Essiambre, "Advanced optical modulation formats," in *Proc. Eur. Conf. Optical Communication (ECOC)*, 2003, Paper Th2.6.1.

[31] ——, "System trade-offs and optical modulation formats," in *Proc. Optical Amplifiers and their Applications (OAA)*, 2004, Paper OTuC4.

[32] P. J. Winzer, R.-J. Essiambre, and S. Chandrasekhar, "Dispersion-tolerant optical communication systems," in *Proc. Eur. Conf. Optical Communication (ECOC)*, 2004, Paper We2.4.1.

[33] I. P. Kaminow and T. L. Koch, Eds., *Optical Fiber Telecommunications III A +B*. New York: Academic, 1997.

[34] I. Kaminow and T. Li, Eds., *Optical Fiber Telecommunications IV A +B*. New York: Academic, 2002.

[35] G. P. Agrawal, *Fiber-Optic Communication Systems*, 3rd ed., New York: Wiley, 2002.

[36] R. Ramaswami and K. Sivarajan, *Optical Networks: A Practical Perspective*. San Francisco, CA: Morgan Kaufmann, 2001.

[37] L. G. Kazovsky, S. Benedetto, and A. E. Willner, *Optical Fiber Communication Systems*. Norwood, MA: Artech House, 1996.

[38] K. Okamoto, *Fundamentals of Optical Waveguides*. New York: Academic, 2000.

[39] S. Betti, G. D. Marchis, and E. Iannone, "Polarization modulated direct detection optical transmission systems," *J. Lightw. Technol.*, vol. 10, no. 12, pp. 1985–1997, Dec. 1992.

[40] A. S. Siddiqui, S. G. Edirisinghe, J. J. Lepley, J. G. Ellison, and S. D. Walker, "Dispersion-tolerant transmission using a duobinary polarization-shift keying transmission scheme," *IEEE Photon. Technol. Lett.*, vol. 14, no. 2, pp. 158–160, Feb. 2002.

[41] J. J. Lepley, J. G. Ellison, S. G. Edirisinghe, A. S. Siddiqui, and S. D. Walker, "Excess penalty impairments of polarization shift keying transmission format in presence of polarization mode dispersion," *Electron. Lett.*, vol. 36, no. 8, pp. 736–737, 2000.

[42] A. Hodzic, B. Konrad, and K. Petermann, "Improvement of system performance in $N \times 40 - \mathrm{Gb/s}$ WDM transmission using alternate polarizations," *IEEE Photon. Technol. Lett.*, vol. 15, no. 1, pp. 153–155, Jan. 2003.

[43] C. Xie, I. Kang, A. H. Gnauck, L. Moller, L. F. Mollenauer, and A. R. Grant, "Suppression of intrachannel nonlinear effects with alternate-polarization formats," *J. Lightw. Technol.*, vol. 22, no. 3, pp. 806–812, Mar. 2004.

[44] L. E. Nelson and H. Kogelnik, "Coherent crosstalk impairments in polarization multiplexed transmission due to polarization mode dispersion," *Opt. Express*, vol. 7, no. 10, pp. 350–361, 2000.

[45] J. G. Proakis, *Digital Communications*, 4th ed. New York: Mc Graw-Hill, 2001.

[46] R. Gitlin, J. F. Hayes, and S. B. Weinstein, *Data Communications Principles*. New York: Plenum, 1992.

[47] G. Kramer, A. Ashikhmin, A. J. V. Wijngaarden, and X. Wei, "Spectral efficiency of coded phase-shift keying for fiber-optic communication," *J. Lightw. Technol.*, vol. 21, no. 10, pp. 2438–2445, Oct. 2003.

[48] S. Walklin and J. Conradi, "Multilevel signaling for increasing the reach of 10-Gb/s lightwave systems," *J. Lightw. Technol.*, vol. 17, no. 11, pp. 2235–2248, Nov. 1999.

[49] R. A. Griffin and A. C. Carter, "Optical differential quadrature phase shift key (oDQPSK) for high-capacity optical transmission," in *Proc. Optical Fiber Communication Conf. (OFC)*, 2002, Paper WX6.

[50] R. A. Griffin, R. I. Johnstone, R. G. Walker, J. Hall, S. D. Wadsworth, K. Berry, A. C. Carter, M. J. Wale, J. Hughes, P. A. Jerram, and N. J. Parsons, "10 Gb/s optical differential quadrature phase shift key (DQPSK) transmission using GaAs/AlGaAs integration," in *Proc. Optical Fiber Communication Conf. (OFC)*, 2002, Paper FD6.

[51] M. Ohm, "Optical 8-DPSK and receiver with direct detection and multilevel electrical signals," in *IEEE/LEOS Workshop Advanced Modulation Formats*, 2004, pp. 45–46.

[52] M. Ohm and J. Speidel, "Quaternary optical ASK-DPSK and receivers with direct detection," *IEEE Photon. Technol. Lett.*, vol. 15, no. 1, pp. 159–161, Jan. 2003.

[53] S. Hayase, N. Kikuchi, K. Sekine, and S. Sasaki, "Proposal of 8-state per symbol (binary ASK and QPSK) 30-Gbit/s optical modulation/demodulation scheme," in *Proc. Eur. Conf. Optical Communication (ECOC)*, 2003, Paper Th2.6.4.

[54] E. Forestieri and G. Prati, "Novel optical line codes tolerant to fiber chromatic dispersion," *J. Lightw. Technol.*, vol. 19, no. 11, pp. 1675–1684, Nov. 2001.

[55] B. Vasic, V. S. Rao, I. B. Djordjevic, R. K. Kostuk, and I. Gabitov, "Ghost-pulse reduction in 40-Gb/s systems using line coding," *IEEE Photon. Technol. Lett.*, vol. 16, no. 7, pp. 1784–1786, Jul. 2004.

[56] D. Penninckx, M. Chbat, L. Pierre, and J.-P. Thiery, "The phase-shaped binary transmission (PSBT): A new technique to transmit far beyond the chromatic dispersion limit," *IEEE Photon. Technol. Lett.*, vol. 9, no. 2, pp. 259–261, Feb. 1997.

[57] J. B. Stark, J. E. Mazo, and R. Laroia, "Phased amplitude-shift signaling (PASS) codes: Increasing the spectral efficiency of DWDM transmission," in *Proc. Eur. Conf. Optical Communication (ECOC)*, 1998, pp. 373–374.

[58] L. Boivin and G. J. Pendock, "Receiver sensitivity for optically amplified RZ signals with arbitrary duty cycle," in *Proc. Optical Amplifiers and Their Applications (OAA)*, 1999, Paper ThB4.

[59] P. J. Winzer and A. Kalmar, "Sensitivity enhancement of optical receivers by impulsive coding," *J. Lightw. Technol.*, vol. 17, no. 2, pp. 171–177, Feb. 1999.

[60] P. J. Winzer, M. Pfennigbauer, M. M. Strasser, and W. R. Leeb, "Optimum filter bandwidths for optically preamplified RZ and NRZ receivers," *J. Lightw. Technol.*, vol. 19, no. 9, pp. 1263–1273, Sep. 2001.

[61] W. Idler, A. Klekamp, R. Dischler, J. Lazaro, and A. Konczykowska, "System performance and tolerances of 43 Gb/s ASK and DPSK modulation formats," in *Proc. Eur. Conf. Optical Communication (ECOC)*, 2003, Paper Th2.6.3.

[62] T. L. Koch, "Laser sources for amplified and WDM lightwave systems," in *Optical Fiber Telecommunications III*, I. P. Kaminow and T. L. Koch, Eds. New York: Academic, 1997, pp. 115–162.

[63] D. A. Ackermann, J. E. Johnson, L. J. P. Ketelsen, L. E. Eng, P. A. Kiely, and T. G. B. Mason, "Telecommunication lasers," in *Optical Fiber Telecommunications IV*, I. Kaminow and T. Li, Eds. New York: Academic, 2002, pp. 587–665.

[64] K. Sato, S. Kuwahara, Y. Miyamoto, and N. Shimizu, "40 gb/s direct modulation of

distributed feedback laser for very-short-reach optical links," *Electron. Lett.*, vol. 38, no. 15, pp. 816–817, 2002.

[65] B. Wedding, W. Pohlmann, H. Gross, and O. Thalau, "43 Gbit/s transmission over 210 km SMF with a directly modulated laser diode," in *Proc. Eur. Conf. Optical Communication (ECOC)*, 2003, Paper Mo4.3.7.

[66] Y. Yu, R. Lewen, S. Irmscher, U. Westergren, and L. Thylen, "80 Gb/s ETDM transmitter with a traveling-wave electroabsorption modulator," in *Proc. Eur. Conf. Optical Communication (ECOC)*, 2005, Paper OWE1.

[67] A. Ougazzaden, C. W. Lentz, T. G. B. Mason, K. G. Glogovsky, C. L. Reynolds, G. J. Przybylek, R. E. Leibenguth, T. L. Kercher, J. W. Boardman, M. T. Rader, J. M. Geary, F. S. Walters, J. M. F. L. J. Peticolas, S. N. G. Chu, A. Sirenka, R. J. Jurchenko, M. S. Hybertsen, L. J. P. Ketelsen, and G. Raybon, "40 Gb/s tandem electroabsorption modulator," in *Proc. Optical Fiber Communication Conf. (OFC)*, 2001, Paper PD14.

[68] A. H. Gnauck, S. K. Korotky, J. J. Veselka, J. Nagel, C. T. Kemmerer, W. J. Minford, and D. T. Moser, "Dispersion penalty reduction using an optical modulator with adjustable chirp," *IEEE Photon. Technol. Lett.*, vol. 3, no. 10, pp. 916–918, Oct. 1991.

[69] H. Kim and A. H. Gnauck, "Chirp characteristics of dual-drive Mach–Zehnder modulator with a finite DC extinction ratio," *IEEE Photon. Technol. Lett.*, vol. 14, no. 3, pp. 298–300, Mar. 2002.

[70] P. J. Winzer, C. Dorrer, R.-J. Essiambre, and I. Kang, "Chirped return-to-zero modulation by imbalanced pulse carver driving signals," *IEEE Photon. Technol. Lett.*, vol. 16, no. 5, pp. 1379–1381, May 2004.

[71] F. Heismann, S. K. Korotky, and J. J. Veselka, "Lithium niobate integrated optics: Selected contemporary devices and system applications," in *Optical Fiber Telecommunications III*, I. P. Kaminow and T. L. Koch, Eds. New York: Academic, 1997, pp. 377–462.

[72] A. Mahapatra and E. J. Murphy, "Electrooptic modulators," in *Optical Fiber Telecommunications IV*, I. Kaminow and T. Li, Eds. New York: Academic, 2002, pp. 258–294.

[73] R. A. Griffin, R. G. Walker, and R. I. Johnstone, "Integrated devices for advanced modulation formats," in *IEEE/LEOS Workshop Advanced Modulation Formats*, 2004, pp. 39–40.

[74] M. Erman, P. Jarry, R. Gamonal, P. Autier, J.-P. Chane, and P. Frijlink, "Mach–Zehnder modulators and optical switches on III-v semiconductors," *J. Lightw. Technol.*, vol. 6, no. 6, pp. 837–846, Jun. 1988.

[75] S. Akiyama, H. Itoh, T. Takeuchi, A. Kuramata, and T. Yamamoto, "Mach–Zehnder modulator driven by 1.2 v single electrical signal," *Electron. Lett.*, vol. 41, no. 1, pp. 40–41, 2005.

[76] R. A. Griffin, B. Pugh, J. Fraser, I. B. Betty, K. Anderson, G. Busico, C. Edge, and T. Simmons, "Compact, high power, MQW InP machzehnder transmitters with fullband tunability for 10 Gb/s DWDM," in *Proc. Eur. Conf. Optical Communication (ECOC)*, 2005, Paper Th2.6.2.

[77] K. Tsuzuki, H. Kikuchi, E. Yamada, H. Yasaka, and T. Ishibashi, "1.3-Vpp push–pull drive InP mach-zehnder modulator module for 40 Gbit/s operation," in *Proc. Eur. Conf. Optical Communication (ECOC)*, 2005, Paper Th2.6.3.

[78] N. M. Froberg, G. Raybon, U. Koren, B. I. Miller, M. G. Young, M. Chien, G. T. Harvey, A. H. Gnauck, and A. M. Johnson, "Generation of 2.5 Gbit/s soliton data stream with an integrated laser-modulator transmitter," *Electron. Lett.*, vol. 30, no. 22, pp. 1880–1881, 1994.

[79] Y. Kao, A. Leven, Y. Baeyens, Y. Chen, D. Grosz, F. Bannon, W. Fang, A. Kung, D. Maywar, T. Lakoba, A. Agarwal, S. Banerjee, and T. Wood, "10 Gb/s soliton generation for ULH transmission using a wideband GaAs pHemt amplifier," in *Proc. Optical Fiber Communication Conf. (OFC)*, 2003, Paper FF6.

[80] X. Liu and Y.-H. Kao, "Generation of RZ-DPSK using a single Mach–Zehnder modulator and novel driver electronics," in *Proc. Eur. Conf. Optical Communication (ECOC)*, 2004, Paper We3.4.2.

[81] M. Suzuki, H. Tanaka, K. Utaka, N. Edagawa, and Y. Matsushima, "Transform-limited 14 ps optical pulse generation with 15 GHz repetition rate by InGaAsP electroabsorption modulator," *Electron. Lett.*, vol. 28, no. 11, pp. 1007–1008, 1992.

[82] R.-J. Essiambre, G. Raybon, and B. Mikkelsen, *Pseudo-linear transmission of high-speed TDM signals: 40 and 160 Gb/s*, I. Kaminow and T. Li, Eds. New York: Academic, 2002, pp. 232–304.

[83] Y. Miyamoto, A. Hirano, K. Yonenaga, A. Sano, H. Toba, K. Murata, and O. Mitomi, "320-Gbit/s (8 × 40 Gbit/s) WDM transmission over 367-km with 120-km repeater spacing using carrier-suppressed return-to-zero format," *Electron. Lett.*, vol. 35, no. 23, pp. 2041–2042, 1999.

[84] A. Hirano, Y. Miyamoto, K. Yonenaga, A. Sano, and H. Toba, "40 Gbit/s l-band transmission experiment using SPM-tolerant carrier-suppressed RZ format," *Electron. Lett.*, vol. 35, no. 25, pp. 2213–2215, 1999.

[85] N. S. Bergano, "Undersea communication systems," in *Optical Fiber Telecommunication IV*, I. Kaminow and T. Li, Eds. New York: Academic, 2002, pp. 154–197.

[86] C. R. Menyuk, G. M. Carter, W. L. Kath, and R.-M. Mu, "Dispersion-managed solitons and chirped return to zero: What is the difference," in *Optical Fiber Telecommunications IV*, I. Kaminov and T. Li, Eds. New York: Academic, 2002, pp. 305–328.

[87] R. Ohhira, D. Ogasahara, and T. Ono, "Novel RZ signal format with alternate-chirp for suppression of nonlinear degradation in 40 Gb/s based WDM," in *Proc. Optical Fiber Communication Conf. (OFC)*, 2001, Paper WM2.

[88] E. A. Golovchenko, N. S. Bergano, C. R. Davidson, and A. N. Pilipetskii, "Modeling versus experiments of 1610 Gbit/s WDM chirped RZ pulse transmission over 7500 km," in *Proc. Optical Fiber Communication Conf. (OFC)*, 1999, Paper ThQ3.

[89] B. Bakhshi, M. Vaa, E. A. Golovchenko, W. W. Patterson, R. L. Maybach, and N. S. Bergano, "Comparison of CRZ, RZ and NRZ modulation formats in a 64 × 12.3 Gb/s WDM transmission experiment over 9000 km," in *Proc. Optical Fiber Communication Conf. (OFC)*, 2001, Paper WF4.

[90] R. A. Griffin, R. G. Walker, R. I. Johnstone, R. Harris, N. M. B. Perney, N. D. Whitbread, T. Widdowson, and P. Harper, "Integrated 10 Gb/s chirped return-to-zero transmitter using GaAs-AlGaAs modulators," in *Proc. Optical Fiber Communication Conf. (OFC)*, 2001, Paper PD15.

[91] G. P. Agrawal, *Nonlinear Fiber Optics*. New York: Academic, 2001.

[92] A. H. Gnauck and R. M. Jopson, "Dispersion compensation for optical fiber systems," in *Optical Fiber Telecommunications III*, I. P. Kaminov and T. L. Koch, Eds. New York: Academic, 1997, pp. 162–195.

[93] S. Chandrasekhar, C. R. Doerr, L. L. Buhl, D. Mahgerefteh, Y. Matsui, B. Johnson, C. Liao, X. Zheng, K. McCallion, Z. Fanand, and P. Tayebati, "Flexible transport at 10 Gb/s from 0 to 675 km (11,500 ps/nm) using a chirp-managed laser and no DCF and a dynamically adjustable dispersion-compensating receiver," in *Proc. Optical Fiber Communication Conf. (OFC)*, 2005, Paper PDP30.

[94] B. Wedding, "New method for optical transmission beyond dispersion limit," *Electron. Lett.*, vol. 28, no. 142, pp. 1298–1300, 1992.

[95] B. Wedding, B. Franz, and B. Junginger, "10-Gb/s optical transmission up to 253 km via standard single-mode fiber using the method of dispersion-supported transmission," *J. Lightw. Technol.*, vol. 12, no. 10, pp. 1720–1727, Oct. 1994.

[96] M. M. E. Said, J. Sitch, and M. I. Elmasry, "An electrically pre-equalized 10-Gb/s duobinary transmission system," *J. Lightw. Technol.*, vol. 23, no. 1, pp. 388–400, Jan. 2005.

[97] K. Roberts, "Making lightpaths independent of optical physics," in *Proc. IEEE/LEOS 16th Annu. Workshop Interconnections Within High Speed Digital Systems*, 2005, Paper MB3.

[98] P. J. Winzer and R. J. Essiambre, "Electronic pre-distortion for advanced modulation formats," in *Proc. Eur. Conf. Optical Communication (ECOC)*, 2005, Paper Tu4.2.2.

[99] R.-J. Essiambre and P. J. Winzer, "Fiber nonlinearities in electronicaly pre-distorted transmission," in *Proc. Eur. Conf. Optical Communication (ECOC)*, 2005, Paper Tu3.2.2.

[100] A. Lender, "The duobinary technique for high-speed data transmission," *IEEE Trans. Commun. Electron.*, vol. 82, pp. 214–218, May 1963.

[101] ——, "Correlative digital communication techniques," *IEEE Trans. Commun.*, vol. COM-12, no. 4, pp. 128–135, Dec. 1964.

[102] P. Kabal and S. Pasupathy, "Partial-response signaling," *IEEE Trans. Commun.*, vol. 23, no. 9, pp. 921–934, Sep. 1975.

[103] A. J. Price and N. LeMercier, "Reduced bandwidth optical digital intensity modulation with improved chromatic dispersion tolerance," *Electron. Lett.*, vol. 31, no. 1, pp. 58–59, 1995.

[104] K. Yonenaga, S. Kuwano, S. Norimatsu, and N. Shibata, "Optical duobinary transmission system with no receiver sensitivity degradation," *Electron. Lett.*, vol. 31, no. 4, pp. 302–304, 1995.

[105] D. Penninckx, L. Pierre, J.-P. Thiery, B. Clesca, M. Chbat, and J. L. Beylat, "Relation between spectrum bandwidth and the effects of chromatic dispersion

in optical transmissions," *Electron. Lett.*, vol. 32, no. 11, pp. 1023–1024, 1996.

[106] S. Walklin and J. Conradi, "On the relationship between chromatic dispersion and transmitter filter response in duobinary optical communication systems," *IEEE Photon. Technol. Lett.*, vol. 9, no. 7, pp. 1005–1007, Jul. 1997, see also: Comments by D. Penninckx, pp. 902–903, 1998.

[107] T. Ono, Y. Yano, K. Fukuchi, T. Ito, H. Yamazaki, M. Yamaguchi, and K. Emura, "Characteristics of optical duobinary signals in Terabit/s capacity, high-spectral efficiency WDM systems," *J. Lightw. Technol.*, vol. 16, no. 5, pp. 788–797, May 1998.

[108] H. Kim, G. Lee, H. Lee, S. K. Kim, I. Kang, S. Hwang, and Y. Oh, "On the use of 2.5-Gb/s Mach–Zehnder modulators to generate 10-Gb/s optical duobinary signals," *IEEE Photon. Technol. Lett.*, vol. 16, no. 11, pp. 2577–2579, Nov. 2004.

[109] D. M. Gill, A. H. Gnauck, X. Liu, X. Wei, D. S. Levy, S. Chandrasekhar, and C. R. Doerr, "42.7-Gb/s cost-effective duobinary optical transmitter using a commercial 10-Gb/s Mach–Zehnder modulator with optical filtering," *IEEE Photon. Technol. Lett.*, vol. 17, no. 4, pp. 917–919, Apr. 2005.

[110] P. J. Winzer, G. Raybon, and M. Duelk, "107-Gb/s optical ETDM transmitter for 100 G Ethernet transport," in *Proc. Eur. Conf. Optical Communication (ECOC)*, 2005, Paper Th4.1.1.

[111] D. Penninckx, H. Bissessur, P. Brindel, E. Gohin, and F. Bakhti, "Optical differential phase shift keying (DPSK) direct detection considered as a duobinary signal," in *Proc. Eur. Conf. Optical Communication (ECOC)*, 2001, Paper We.P.40.

[112] P. J. Winzer and J. Leuthold, "Return-to-zero modulator using a single NRZ drive signal and an optical delay interferometer," *IEEE Photon. Technol. Lett.*, vol. 13, no. 12, pp. 1298–1300, Dec. 2001.

[113] Y. Miyamoto, A. Hirano, S. Kuwahara, Y. Tada, H. Masuda, S. Aozasa, K. Murata, and H. Miyazawa, "S-band 3 × 120-km DSF transmission of 8 × 42.7-Gbit/s DWDM duobinary-carrier-suppressed RZ signals generated by novel wideband PM/AM conversion," in *Proc. Optical Amplifiers and Their Applications (OAA)*, 2001, Paper PD6.

[114] P. J. Winzer, A. H. Gnauck, G. Raybon, S. Chandrasekhar, Y. Suand, and J. Leuthold, "40-Gb/s alternate-mark-inversion return-to-zero (RZAMI) transmission over 2,000 km," *IEEE Photon. Technol. Lett.*, vol. 15, no. 5, pp. 766–768, May 2003.

[115] Y. Miyamoto, K. Yonenaga, A. Hirano, H. Toba, K. Murata, and H. Miyazawa, "Duobinary carrier-suppressed return-to-zero format and its application to 100-GHz spaced 8 × 43-Gb/s DWDM unrepeatered transmission over 163 km," in *Proc. Optical Fiber Communication Conf. (OFC)*, 2001, Paper TuU4.

[116] A. Matsuura, K. Yonenaga, Y. Miyamoto, and H. Toba, "Highspeed transmission based on optical modified duobinary signals," *Electron. Lett.*, vol. 35, no. 9, pp. 736–737, 1999.

[117] S. Shimotsu, S. Oikawa, T. Saitou, N. Mitsugi, K. Kubodera, T. Kawanishi, and M. Izutsu, "Single side-band modulation performance of a $LiNbO_3$ integrated modulator consisting of four-phase modulator waveguides," *IEEE Photon. Technol. Lett.*, vol. 13, no. 4, pp. 364–366, Apr. 2001.

[118] P. M. Watts, V. Mikhailov, M. Glick, P. Bayvel, and R. I. Killey, "Single sideband optical signal generation and chromatic dispersion compensation using digital filters," *Electron. Lett.*, vol. 40, no. 15, pp. 958–960, 2004.

[119] W. Idler, S. Bigo, Y. Frignac, B. Franz, and D. Veith, "Vestigial side band demultiplexing for ultra high capacity (0.64 bit/s/Hz) transmission of 128 × 40 Gb/s channels," in *Proc. Optical Fiber Communication Conf. (OFC)*, 2001, Paper MM3.

[120] S. Bigo, Y. Frignac, G. Charlet, W. Idler, S. Borne, H. Gross, R. Dischler, W. Poehlmann, P. Tran, C. Simonneau, D. Bayart, A. J. G. Veith, and J.-P. Hamaide, "10.2 Tbit/s (256 × 42.7 Gbit/s PDM/WDM) transmission over 100 km Teralight fiber with 1.28 bit/s/Hz spectral efficiency," in *Proc. Optical Fiber Communication Conf. (OFC)*, 2001, Paper PD25.

[121] T. Tsuritani, A. Agata, I. Morita, K. Tanaka, and N. Edagawa, "Performance comparison between DSB and VSB signals in 20 Gb/s based ultra-long-haul WDM systems," in *Proc. Optical Fiber Communication Conf. (OFC)*, 2001, Paper MM5.

[122] P. Mamyshev, B. Mikkelsen, F. Liu, S. Dey, J. Bennike, and C. Rasmussen, "Spectrally efficient pseudo duo-binary modulation formats for high-speed optical data transmission," presented at the *Conf. Lasers and Electro-optics 2002*, Long Beach, CA.

[123] A. Agarwal, S. Chandrasekhar, and R.-J. Essiambre, "42.7 Gb/s CSRZVSB for spectrally efficient meshed networks," in *Proc. Eur. Conf. Optical Communication (ECOC)*, 2004, Paper We3.4.4.

[124] A. H. Gnauck and P. J. Winzer, "Optical phase-shift-keyed transmission," *J. Lightw. Technol.*, vol. 23, no. 1, pp. 115–130, Jan. 2005.

[125] P. A. Humblet and M. Azizoglu, "On the bit error rate of lightwave systems with optical amplifiers," *J. Lightw. Technol.*, vol. 9, no. 11, pp. 1576–1582, Nov. 1991.

[126] T. Chikama, S. Watanabe, T. Naito, H. Onaka, T. Kiyonaga, Y. Onoda, H. Miyata, M. Suyama, M. Seino, and H. Kuwahara, "Modulation and demodulation techniques in optical heterodyne PSK transmission systems," *J. Lightw. Technol.*, vol. 8, no. 3, pp. 309–321, Mar. 1990.

[127] P. J. Winzer and H. Kim, "Degradations in balanced DPSK receivers," *IEEE Photon. Technol. Lett.*, vol. 15, no. 9, pp. 1282–1284, Sep. 2003.

[128] P. J. Winzer, S. Chandrasekhar, and H. Kim, "Impact of filtering on RZ-DPSK reception," *IEEE Photon. Technol. Lett.*, vol. 15, no. 6, pp. 840–842, Jun. 2003.

[129] H. Kim and P. J. Winzer, "Nonlinear phase noise in phase-coded transmission," in *Proc. Optical Fiber Communication Conf. (OFC)*, 2005, Paper OThO3.

[130] X. Gu and L. C. Blank, "10 gbit/s unrepeated three-level optical transmission over 100 km of standard fiber," *Electron. Lett.*, vol. 29, pp. 2209–2211, 1993.

[131] G. May, A. Solheim, and J. Conradi, "Extended 10 Gb/s fiber transmission distance at 1538 nm using a duobinary receiver," *IEEE Photon. Technol. Lett.*, vol. 6, no. 5, pp. 648–650, May 1994.

[132] J. H. Sinsky, M. Duelk, and A. Adamiecki, "High-speed electrical backplane transmission using duobinary signaling," *IEEE Trans. Microw. Theory Tech.*, vol. 53, no. 1, pp. 152–160, Jan. 2005.

[133] H. Kim and R.-J. Essiambre, "Transmission of 8 × 20 Gb/s DQPSK signals over 310-km SMF with 0.8-b/s/Hz spectral efficiency," *IEEE Photon. Technol. Lett.*, vol. 15, no. 5, pp. 769–771, May 2003.

[134] T. Tokle, C. R. Davidson, M. Nissov, J.-X. Cai, D. Foursa, and A. Pilipetskii, "6500 km transmission of RZ-DQPSK WDM signals," *Electron. Lett.*, vol. 40, no. 7, pp. 444–445, 2004.

[135] M. Ohm and T. Freckmann, "Comparison of different DQPSK transmitters with NRZ and RZ impulse shaping," in *IEEE/LEOS Workshop Advanced Modulation Formats*, 2004, pp. 7–8.

[136] A. H. Gnauck, P. J. Winzer, S. Chandrasekhar, and C. Dorrer, "Spectrally efficient (0.8 b/s/Hz) 1-Tb/s (25 × 42.7 Gb/s) RZ-DQPSK transmission over 28 100-km SSMF spans with 7 optical add/drops," in *Proc. Optical Fiber Communication Conf. (OFC)*, 2004, Paper Th4.4.1.

[137] M. Cavallari, C. R. S. Fludger, and P. J. Anslow, "Electronic signal processing for differential phase modulation formats," in *Proc. Optical Fiber Communication Conf. (OFC)*, 2004, Paper TuG2.

[138] N. Yoshikane and I. Morita, "1.14 b/s/Hz spectrally efficient 50 × 85.4-Gb/s transmission over 300 km using copolarized RZ-DQPSK signals," *J. Lightw. Technol.*, vol. 23, no. 1, pp. 108–114, Jan. 2005.

[139] J. Wang and J. M. Kahn, "Impact of chromatic and polarization-mode dispersions on DPSK systems using interferometric demodulation and direct detection," *J. Lightw. Technol.*, vol. 22, no. 2, pp. 362–371, Feb. 2004.

[140] H. Kim and P. J. Winzer, "Robustness to laser frequency offset in direct-detection DPSK and DQPSK systems," *J. Lightw. Technol.*, vol. 21, no. 9, pp. 1887–1891, Sep. 2003.

[141] C. R. Doerr, D. M. Gill, A. H. Gnauck, L. L. Buhl, P. J. Winzer, M. A. Cappuzzo, A. Wong-Foy, E. Y. Chen, and L. T. Gomez, "Simultaneous reception of both quadratures of 40-Gb/s DQPSK using a simple monolithic demodulator," in *Proc. Optical Fiber Communication Conf. (OFC)*, 2005, Paper PDP12.

[142] B. E. A. Saleh and M. C. Teich, *Fundamentals of Photonics*. New York: Wiley, 1991.

[143] H. Wu, J. A. Tierno, P. Pepeljugoski, J. Schaub, S. Gowda, J. A. Kash, and A. Hajimiri, "Integrated transversal equalizers in high-speed fiberoptic systems," *J. Solid-State Circuits*, vol. 38, no. 12, pp. 2131–2137, 2003.

[144] P. C. Becker, N. A. Olsson, and J. R. Simpson, *Erbium-Doped Fiber Amplifiers, Fundamentals and Technology*. New York: Academic, 1999.

[145] E. Desurvire, D. Bayart, B. Desthieux, and S. Bigo, *Erbium-Doped Fiber Amplifiers and Device and System Developments*. New York: Wiley, 2002.

[146] K. Rottwitt and A. J. Stentz, Raman amplification in lightwave communication systems," in *Optical Fiber*

Telecommunications IV, I. Kaminow and T. Li, Eds. New York: Academic, 2002, pp. 213–257.

[147] M. N. Islam, Ed., *Raman Amplifiers for Telecommunications 1 + 2*. New York: Springer-Verlag, 2003.

[148] H. A. Haus, *Electromagnetic Noise and Quantum Optical Measurements*. New York: Springer-Verlag, 2000.

[149] N. A. Olsson, "Lightwave systems with optical amplifiers," *J. Lightw. Technol.*, vol. 7, no. 7, pp. 1071–1082, Jul. 1989.

[150] "Session T4.4: Submarine line terminal equipment technology," in *Proc. SubOptic 2001 Int. Convention*, 2001.

[151] Interfaces for the Optical Transport Network (OTN), Standard ITU-T G.709, 2003.

[152] M. Pauer and P. J. Winzer, "Impact of extinction ratio on RZ gain in optically preamplified receivers," *IEEE Photon. Technol. Lett.*, vol. 15, no. 6, pp. 879–881, Jun. 2003.

[153] X. Zheng, F. Liu, and P. Jeppesen, "Receiver optimization for 40-Gb/s optical duobinary signal," *IEEE Photon. Technol. Lett.*, vol. 13, no. 7, pp. 744–746, Jul. 2001.

[154] D. O. Caplan, B. S. Robinson, R. J. Murphy, and M. L. Stevens, "Demonstration of 2.5-Gslot/s optically-preamplified M-PPM with 4 photons/bit receiver sensitivity," in *Proc. Optical Fiber Communication Conf. (OFC)*, 2005, Paper PDP32.

[155] P. J. Winzer, M. Pfennigbauer, and R.-J. Essiambre, "Coherent crosstalk in ultra-dense WDM systems," *J. Lightw. Technol.*, vol. 23, no. 4, pp. 1734–1744, Apr. 2005.

[156] P. J. Winzer and R.-J. Essiambre, "Optical receiver design trade-offs," in *Proc. Optical Fiber Communication Conf. (OFC)*, 2003, pp. 468–470.

[157] A. Hodzic, M. Winter, B. Konrad, S. Randel, and K. Petermann, "Optimized filtering for 40-Gb/s/Ch-based DWDM transmission systems over standard single-mode fiber," *IEEE Photon. Technol. Lett.*, vol. 15, no. 7, pp. 1002–1004, Jul. 2003.

[158] S. Suzuki and Y. Kokubun, "Design rule of wavelength filter bandwidth and pulsewidth for ultimate spectral efficiency limited by crosstalk in DWDM systems," *IEEE Photon. Technol. Lett.*, vol. 15, no. 11, pp. 1645–1647, Nov. 2003.

[159] M. Pfennigbauer and P. J. Winzer, "Choice of MUX/DEMUX filter characteristics for NRZ, RZ, and CSRZ DWDM systems," *J. Lightw. Technol.*, 2005.

[160] H. Kim and C. X. Yu, "Optical duobinary transmission system featuring improved receiver sensitivity and reduced optical bandwidth," *IEEE Photon. Technol. Lett.*, vol. 14, no. 8, pp. 1205–1207, Aug. 2002.

[161] G. Raybon, S. Chandrasekhar, A. H. Gnauck, B. Zhu, and L. L. Buhl, "Experimental investigation of long-haul transport at 42.7 Gb/s through concatenated optical add/drop nodes," in *Proc. Opt. Fiber Communication Conf. (OFC)*, 2004, Paper ThE4.

[162] G. Raybon, S. Chandrasekhar, A. Agarwal, A. H. Gnauck, J. S. L. L. Buhl, and A. Adamiecki, "Limitations of optical add/drop filtering on 42.7-Gb/s transmission with 50-GHz channel spacing," in *Proc. Eur. Conf. Optical Communication (ECOC)*, 2004, Paper Mo4.5.1.

[163] G. Raybon, A. Agarwal, S. Chandrasekhar, and R.-J. Essiambre, "Transmission of 42.7-Gb/s VSB-CSRZ over 1600 km and four OADM nodes with a spectral efficiency of 0.8-bit/s/Hz," in *Proc. Eur. Conf. Optical Communication (ECOC)*, 2005, Paper Mo3.2.7.

[164] G. Raybon, "Performance of advanced modulation formats in optically-routed networks," in *Proc. Optical Fiber Communication Conf. (OFC)*, 2006, Paper OThR1.

[165] J. Bromage, P. J. Winzer, and R.-J. Essiambre, Multiple-path interference and its impact on system design," in *Raman Amplifiers and Oscillators in Telecommunications*, M. N. Islam, Ed. New York: Springer-Verlag, 2003.

[166] C. Rasmussen, F. Liu, R. J. S. Pedersen, and B. F. Jorgensen, "Theoretical and experimental studies of the influence of the number of crosstalk signals on the penalty caused by incoherent optical crosstalk," in *Proc. Optical Fiber Communication Conf. (OFC)*, 1999, Paper TuR5.

[167] S. Radic, N. Vukovic, S. Chandrasekhar, A. Velingker, and A. Srivastava, "Forward error correction performance in the presence of rayleigh-dominated transmission noise," *IEEE Photon. Technol. Lett.*, vol. 15, no. 2, pp. 326–328, Feb. 2003.

[168] J. Bromage, C. H. Kim, P. J. Winzer, L. E. Nelson, R.-J. Essiambre, and R. M. Jopson, "Relative impact of multiple-path interference and amplified spontaneous emission noise on optical receiver performance," in *Proc. Optical Fiber Communication Conf. (OFC)*, 2002, Paper TuR3.

[169] C. R. S. Fludger, Y. Zhu, V. Handerek, and R. J. Mears, "Impact of MPI and modulation format an transmission systems employing distributed raman amplification," *Electron. Lett.*, vol. 37, no. 15, pp. 970–972, 2001.

[170] L. Eskildsen and P. B. Hansen, "Interferometric noise in lightwave systems with optical preamplifiers," *IEEE Photon. Technol. Lett.*, vol. 9, no. 11, pp. 1538–1540, Nov. 1997.

[171] S. Chandrasekhar, L. L. Buhl, and B. Zhu, "Performance of forward error correction coding in the presence of in-band crosstalk," in *Proc. Optical Fiber Communication Conf. (OFC)*, 2002, Paper WP1.

[172] A. Yariv, H. Blauvelt, and S.-W. Wu, "A reduction of interferometric phase-to-intensity conversion noise in fiber links by large index phase modulation of the optical beam," *J. Lightw. Technol.*, vol. 10, pp. 978–981, Jul. 1992.

[173] P. K. Pepeljugoski and K. Y. Lau, "Interferometric noise reduction in fiber-optic links by superposition of high frequency modulation," *J. Lightw. Technol.*, vol. 10, no. 7, pp. 957–963, Jul. 1992.

[174] F. Forghieri, R. W. Tkach, and A. R. Chraplyvy, "Dispersion compensating fiber: Is there merit in the figure of merit?," *IEEE Photon. Technol. Lett.*, vol. 9, no. 7, pp. 970–972, Jul. 1997.

[175] S. Chandrasekhar, "Dispersion tolerant alternative 10-Gb/s transmitters and implications for WDM optical networking," in *Proc. Optical Fiber Communication Conf. (OFC)*, 2006.

[176] H. Kogelnik, R. M. Jopson, and L. E. Nelson, Polarization-mode dispersion," in *Optial Fiber Telecommunication*, I. Kaminow and T. Li, Eds. New York: Academic, 2002, pp. 725–861.

[177] R. M. Jopson, L. E. Nelson, G. J. Pendock, and A. H. Gnauck, "Polarization-mode dispersion impairment in return-to-zero and non return-to-zero systems," in *Proc. Optical Fiber Communication Conf. (OFC)*, 1999, Paper WE3.

[178] P. J. Winzer, H. Kogelnik, C. H. Kim, H. Kim, R. M. Jopson, L. E. Nelson, and K. Ramanan, "Receiver impact on first-order PMD outage," *IEEE Photon. Technol. Lett.*, vol. 15, no. 10, pp. 1482–1484, Oct. 2003.

[179] C. Xie, S. Shen, and L. Moller, "Effects of transmitter imperfection on polarization mode dispersion impairments," *IEEE Photon. Technol. Lett.*, vol. 15, no. 4, pp. 614–616, Apr. 2003.

[180] C. H. Kim, H. Kim, R. M. Jopson, and P. J. Winzer, "Dependence of PMD penalties on decision point and receiver bandwidth," in *Proc. Optical Fiber Communication Conf. (OFC)*, 2002, Paper TuI4.

[181] N. Kaneda, X. Liu, Z. Zheng, X. Wei, M. Tayahi, M. Movassaghi, and D. Levy, "Improved polarization-mode-dispersion tolerance in duobinary transmission," *IEEE Photon. Technol. Lett.*, vol. 15, no. 7, pp. 1005–1007, Jul. 2003.

[182] M. Boroditsky, M. Brodsky, N. J. Frigo, P. Magill, C. Antonelli, and A. Mecozzi, "Outage probabilities for fiber routes with finite number of degrees of freedom," *IEEE Photon. Technol. Lett.*, vol. 17, no. 2, pp. 345–347, Feb. 2005.

[183] C. R. Doerr, S. Chandrasekhar, P. J. Winzer, A. R. Chraplyvy, A. H. Gnauck, L. W. Stulz, R. Pafchek, and E. Burrows, "Simple multichannel optical equalizer mitigating intersymbol interference for 40-Gb/s non return-to-zero signals," *J. Lightw. Technol.*, vol. 22, no. 1, pp. 249–256, Jan. 2004.

[184] H. F. Haunstein, W. Sauer-Greff, A. Dittrich, K. Sticht, and R. Urbansky, "Principles for electronic equalization of polarization-mode dispersion," *J. Lightw. Technol.*, vol. 22, no. 4, pp. 1169–1182, Apr. 2004.

[185] F. Buchali and H. Bulow, "Adaptive PMD compensation by electrical and optical techniques," *J. Lightw. Technol.*, vol. 22, no. 4, pp. 1116–1126, Apr. 2004.

[186] P. G. Drazin and R. S. Johnson, *Solitons: An Introduction*. Cambridge, U.K.: Cambridge Univ. Press, 1989.

[187] G. P. Agrawal, *Applications of Nonlinear Fiber Optics*. New York: Academic, 2001.

[188] R.-J. Essiambre and G. P. Agrawal, Soliton communication systems," in *Progress in Optics*, vol. 33, E. Wolf, Ed. Amsterdam, The Netherlands: North-Holland, 1997.

[189] L. F. Mollenauer, J. P. Gordon, and P. V. Mamyshev, Solitons in high bit-rate, long-distance transmission," in *Optical Fiber Telecommunications III A*, I. P. Kaminov and T. L. Koch, Eds. New York: Academic, 1997, pp. 373–460.

[190] L. F. Mollenauer, R. H. Stolen, and J. P. Gordon, "Experimental observation of picosecond pulse narrowing and solitons in optical fibers," *Phys. Rev. Lett.*, vol. 45, pp. 1095–1098, 1980.

[191] L. F. Mollenauer, J. P. Gordon, and M. N. Islam, "Soliton propagation in long fibers with periodically compensated loss," *IEEE J. Quantum Electron.*, vol. QE-22, no. 1, pp. 157–173, Jan. 1986.

[192] H. Kubota and M. Nakazawa, "Long-distance optical soliton transmission with lumped amplifiers," *IEEE J. Quantum Electron.*, vol. 26, no. 4, pp. 692–700, Apr. 1990.

[193] B. Biotteau, J.-P. Hamaide, F. Pitel, O. Audouin, P. Nouchi, and P. Sansonetti, "Enhancement of soliton system performance by use of new large effective area fibers," *Electron. Lett.*, vol. 31, pp. 2026–2027, 1995.

[194] L. F. Mollenauer, P. V. Mamyshev, and M. J. Neubelt, "Demonstration of soliton WDM transmission at 6 and 7×10 gbit/s, error free over transoceanic distances," *Electron. Lett.*, vol. 32, pp. 471–473, 1996.

[195] A. Hasegawa and M. Matsumoto, *Optical Solitons in Fibers*. New York: Springer-Verlag, 2002.

[196] D. Marcuse, A. R. Chraplyvy, and R. W. Tkach, "Effect of fiber nonlinearity on long-distance transmission," *J. Lightw. Technol.*, vol. 9, no. 1, pp. 121–128, Jan. 1991.

[197] P. V. Mamyshev and L. F. Mollenauer, "Pseudo-phase-matched four-wave mixing in soliton wavelength-division multiplexing transmission," *Opt. Lett.*, pp. 396–398, 1996.

[198] M. Suzuki, I. Morita, N. Edagawa, S. Yamamoto, H. Taga, and S. Akiba, "Reduction of gordon-haus timing jitter by periodic dispersion compensation in soliton transmission," *Electron. Lett.*, vol. 31, pp. 2027–2029, 1995.

[199] N. J. Smith, W. Forysiak, and N. J. Doran, "Reduced GordonHaus jitter due to enhanced power solitons in strongly dispersion managed systems," *Electron. Lett.*, vol. 32, pp. 2085–2086, 1996.

[200] N. J. Smith, N. J. Doran, W. Forysiak, and F. M. Knox, "Soliton transmission using periodic dispersion compensation," *J. Lightw. Technol.*, vol. 15, no. 10, pp. 1808–1822, Oct. 1997.

[201] J. H. B. Nijhof, W. Forysiak, and N. J. Doran, "The averaging method for finding exactly periodic dispersion-managed solitons," *IEEE J. Sel. Topics Quantum Electron.*, vol. 6, no. 2, pp. 330–336, Mar./Apr. 2000.

[202] E. A. Golovchenko, J. M. Jacob, A. N. Pilipetskii, C. R. Menyuk, and G. M. Carter, "Dispersion-managed solitons in a fiber loop with in-line filtering," *Opt. Lett.*, vol. 22, pp. 289–291, 1997.

[203] H. Taga, K. Imai, N. Takeda, M. Suzuki, S. Yamamoto, and S. Akiba, "10 WDM 10 Gbit/s recirculating loop transmission experiments using dispersion slope compensator and nonsoliton RZ pulse," *Electron. Lett.*, vol. 33, pp. 2058–2059, 1997.

[204] L. F. Mollenauer and P. V. Mamyshev, "Massive wavelength-division multiplexing with solitons," *IEEE J. Quantum Electron.*, vol. 34, no. 11, pp. 2089–2102, Nov. 1998.

[205] I. Morita, M. Suzuki, N. Edagawa, K. Tanaka, and S. Yamamoto, "Long-haul soliton WDM transmission with periodic dispersion compensation and dispersion slope compensation," *J. Lightw. Technol.*, vol. 17, no. 1, pp. 80–85, Jan. 1999.

[206] F. Favre, D. L. Guen, and T. Georges, "Experimental evidence of pseudo-periodical soliton propagation in dispersion-managed links," *J. Lightw. Technol.*, vol. 17, no. 6, pp. 1032–1036, Jun. 1999.

[207] L. F. Mollenauer, P. V. Mamyshev, J. Gripp, M. J. Neubelt, N. Mamysheva, L. Grüner-Nielsen, and T. Veng, "Demonstration of massive wavelength-division multiplexing over transoceanic distances by use of dispersion-managed solitons," *Opt. Lett.*, vol. 25, pp. 704–706, 2000.

[208] R.-J. Essiambre, B. Mikkelsen, and G. Raybon, "Intra-channel cross-phase modulation and four-wave mixing in high-speed TDM systems," *Electron. Lett.*, vol. 35, pp. 1576–1578, 1999.

[209] P. V. Mamyshev and N. A. Mamysheva, "Pulse-overlapped dispersion-managed data transmission and intrachannel four-wave mixing," *Opt. Lett.*, vol. 24, pp. 1454–1456, 1999.

[210] B. Mikkelsen, G. Raybon, R.-J. Essiambre, A. J. Stentz, T. N. Nielsen, D. W. Peckham, L. Hsu, L. Grüner-Nielsen, K. Dreyer, and J. E. Johnson, "320-Gb/s single-channel pseudolinear transmission over 200 km of nonzero-dispersion fiber," *IEEE Photon. Technol. Lett.*, vol. 12, no. 10, pp. 1400–1402, Oct. 2000.

[211] A. Mecozzi, C. B. Clausen, and M. Shtaif, "Analysis of intrachannel nonlinear effects in highly dispersed optical pulse transmission," *IEEE Photon. Technol. Lett.*, vol. 12, no. 4, pp. 392–394, Apr. 2000.

[212] ——, "System impact of intra-channel nonlinear effects in highly dispersed optical pulse transmission," *IEEE Photon. Technol. Lett.*, vol. 12, no. 12, pp. 1633–1635, Dec. 2000.

[213] T. Inoue and A. Maruta, "Pre-spread RZ pulse transmission for reducing intra-channel nonlinear interactions," in *Proc. IEEE/LEOS Annu. Meeting*, 2000, Paper MJ3.

[214] M. J. Ablowitz and T. Hirooka, "Resonant nonlinear intrachannel interactions in strongly dispersion-managed transmission systems," *Opt. Lett.*, vol. 25, pp. 1750–1752, 2000.

[215] A. Mecozzi, C. B. Clausen, M. Shtaif, S.-G. Park, and A. H. Gnauck, "Cancellation of timing and amplitude jitter in symmetric links using highly dispersed pulses," *IEEE Photon. Technol. Lett.*, vol. 13, no. 5, pp. 445–447, May 2001.

[216] S. Kumar, J. C. Mauro, S. Raghavan, and D. Q. Chowdhury, "Intrachannel nonlinear penalties in dispersion-managed transmission systems," *IEEE J. Sel. Topics Quantum Electron.*, vol. 8, no. 3, pp. 626–631, May/Jun. 2002.

[217] V. K. Mezentsev, S. K. Turitsyn, and N. J. Doran, "System optimization of 80 gbit/s single channel transmission over 1000 km of standard fiber," *Electron. Lett.*, vol. 36, pp. 1949–1950, 2000.

[218] A. Cauvin, Y. Frignac, and S. Bigo, "Nonlinear impairments at various bit rates in single-channel dispersion-managed systems," *Electron. Lett.*, vol. 39, pp. 1670–1671, 2003.

[219] R. I. Killey, H. J. Thiele, V. Mikhailov, and P. Bayvel, "Reduction of intrachannel nonlinear distortion in 40-Gb/s-based WDM transmission over standard fiber," *IEEE Photon. Technol. Lett.*, vol. 12, no. 12, pp. 1624–1626, Dec. 2000.

[220] T. Inoue and A. Maruta, "Suppression of nonlinear intrachannel interactions between return-to-zero pulses in dispersion-managed optical transmission systems," *J. Opt. Soc. Amer. B*, vol. 19, pp. 440–447, 2002.

[221] J. Martensson, A. Berntson, and M. Westlund, "Intra-channel pulse interactions in 40 Gbit/s dispersion-managed RZ transmission system," *Electron. Lett.*, vol. 36, pp. 244–246, 2000.

[222] S. Banerjee, A. Agarwal, D. F. Grosz, A. Küng, and D. N. Maywar, "Doubly periodic dispersion maps for 10 and 40 Gbit/s ultra-long-haul transmission," *Electron. Lett.*, vol. 40, pp. 1287–1288, 2004.

[223] C. Xie, "A doubly periodic dispersion map for ultralong-haul 10- and 40-Gb/s hybrid DWDM optical mesh networks," *IEEE Photon. Technol. Lett.*, vol. 17, no. 5, pp. 1091–1093, May 2005.

[224] K. S. Kim and M. E. Lines, "Temperature dependence of chromatic dispersion in dispersion-shifted fibers: Experiment and analysis," *Appl. Phys. Lett.*, vol. 73, pp. 2069–2074, 1993.

[225] K. Yonenaga, A. Hirano, S. Kuwahara, Y. Miyamoto, H. Toba, K. Sato, and H. Miyazawa, "Temperature-independent 80 Gbit/s OTDM transmission experiment using zero-dispersion-flattened transmission line," *Electron. Lett.*, vol. 36, pp. 343–345, 2000.

[226] P. Pecci, S. Lanne, Y. Frignac, J.-C. Antona, G. Charlet, and S. Bigo, "Tolerance to dispersion compensation parameters of six modulation formats in systems operating at 43 Gbit/s," *Electron. Lett.*, vol. 39, pp. 1844–1846, 2003.

[227] M. Midrio, F. Matera, and M. Settembre, "Reduction of amplified spontaneous emission noise impact on optically amplified systems in normal dispersion region of fiber," *Electron. Lett.*, vol. 33, pp. 1066–1068, 1997.

[228] R. Hui, M. OSullivan, A. Robinson, and M. Taylor, "Modulation instability and its impact in multispan optical amplified IMDD systems: Theory and experiments," *J. Lightw. Technol.*, vol. 15, no. 7, pp. 1071–1082, Jul. 1997.

[229] G. P. Agrawal, "Modulation instability induced by cross-phase modulation," *Phys. Rev. Lett.*, vol. 59, pp. 880–883, 1987.

[230] C. J. McKinstrie and R. Bingham, "The modulational instability of coupled waves," *Phys. Fluids*, vol. 1, pp. 230–237, 1989.

[231] A. Bononi, P. Serena, J.-C. Antona, and S. Bigo, "Implications of nonlinear interaction of signal and noise in low-OSNR transmission systems with FEC," in *Proc. Optical Fiber Communication Conf. (OFC)*, 2005, Paper OThW5.

[232] H. A. Haus and Y. Lai, "Quantum theory of soliton squeezing: A linearized approach," *J. Opt. Soc. Am. B*, vol. 7, pp. 386–392, 1990.

[233] J. P. Gordon and H. A. Haus, "Random walk of coherently amplified solitons in optical fiber transmission," *Opt. Lett.*, vol. 11, pp. 665–667, 1986.

[234] J. P. Gordon and L. F. Mollenauer, "Phase noise in photonic communications systems using linear amplifiers," *Opt. Lett.*, vol. 15, no. 23, pp. 1351–1353, 1990.

[235] H. Kim and A. H. Gnauck, "Experimental investigation of the performance limitation of DPSK systems due to nonlinear phase noise," *IEEE Photon. Technol. Lett.*, vol. 15, no. 2, pp. 320–322, Feb. 2003.

[236] T. Mizuochi, K. Ishida, T. Kobayashi, J. Abe, K. Kinjo, K. Motoshima, and K. Kasahara, "A comparative study of DPSK and OOK WDM transmission over transoceanic distances and their performance degradations due to nonlinear phase noise," *J. Lightw. Technol.*, vol. 21, no. 9, pp. 1933–1943, Sep. 2003.

[237] M. Ohm, R.-J. Essiambre, and P. J. Winzer, "Nonlinear phase noise and distortion in 42.7-Gbit/s RZ-DPSK systems," in *Proc. Eur. Conf. Optical Communication (ECOC)*, 2005.

[238] H. Kim, "Cross-phase-modulation-induced nonlinear phase noise in WDM direct-detection DPSK systems," *J. Lightw. Technol.*, vol. 21, no. 8, pp. 1770–1774, Aug. 2003.

[239] D. Dahan and G. Eisenstein, "Numerical comparison between distributed and discrete amplification in a point-to-point 40-Gb/s 40-WDM based transmission system with three different modulation formats," *J. Lightw. Technol.*, vol. 20, no. 3, pp. 379–388, Mar. 2002.

[240] A. Hodžić, B. Konrad, and K. Petermann, "Alternative modulation formats in n 40 Gb/s WDM standard fiber RZ-transmission systems," *J. Lightw. Technol.*, vol. 20, no. 4, pp. 598–607, Apr. 2002.

[241] A. H. Gnauck, X. Liu, X. Wei, D. M. Gill, and E. C. Burrows, "Comparison of modulation formats for 42.7-Gb/s single-channel transmission through 1980 km of SSMF," *IEEE Photon. Technol. Lett.*, vol. 16, no. 3, pp. 909–911, Mar. 2004.

[242] W. H. Loh, R. I. Laming, A. D. Ellis, and D. Atkinson, "10 Gb/s transmission over 700 km of standard single-mode fiber with 10-cm chirped fiber grating compensator and duobinary transmitter," *IEEE Photon. Technol. Lett.*, vol. 8, no. 9, pp. 1258–1260, Sep. 1996.

[243] S. Aisawa, J. Kani, M. Fukui, T. Sakamoto, M. Jinno, S. Norimatsu, H. Ono, and K. Oguchi, "Dispersion-compensation-free 1610 gbit/s wdm transmission in 1580 nm band over 640 km of dispersion-shifted fiber by employing optical duobinary coding," *Electron. Lett.*, pp. 480–481, 1998.

[244] S. Aisawa, J.-I. Kani, M. Fukui, T. Sakamoto, M. Jinno, S. Norimatsu, M. Yamada, H. Ono, and K. Oguchi, "A 1580-nm band wdm transmission technology employing optical duobinary coding," *J. Lightw. Technol.*, vol. 17, no. 2, pp. 191–199, Feb. 1999.

[245] H. Bissessur, G. Charlet, W. Idler, C. Simonneau, S. Borne, L. Pierre, R. Dischler, C. D. Barros, and P. Tran, "3.2 Tbit/s (80 × 40 Gbit/s) phase-shaped binary transmission over 3 × 100 km with 0.8 bit/s/Hz efficiency," *Electron. Lett.*, vol. 38, pp. 377–379, 2002.

[246] G. Charlet, J.-C. Antona, S. Lanne, P. Tran, W. Idler, M. Gorlier, S. Borne, A. Klekamp, C. Simonneau, L. Pierre, Y. Frignac, M. Molina, F. Beaumont, J.-P. Hamaide, and S. Bigo, "6.4 Tb/s (159 × 42.7 Gb/s) capacity over 21 × 100 km using bandwidth-limited phase-shaped binary transmission," in *Proc. Eur. Conf. Optical Communication (ECOC)*, 2002, Paper PD4.1.

[247] G. Charlet, J.-C. Antona, S. Lanne, and S. Bigo, "From 2,100 km to 2,700 km distance using phase-shaped binary transmission at 6.3 Tbit/s capacity," in *Proc. Optical Fiber Communication Conf. (OFC)*, 2003, Paper WE3.

[248] G. Charlet, S. Lanne, L. Pierre, C. Simonneau, P. Tran, H. Mardoyan, P. Brindel, M. Gorlier, J.-C. Antona, M. Molina, P. Sillard, J. Godin, W. Idler, and S. Bigo, "Cost-optimized 6.3 Tbit/s-capacity terrestrial link over 17 × 100 km using phase-shaped binary transmission in a conventional all-EDFA SMF-based system," in *Proc. Optical Fiber Communication Conf. (OFC)*, 2003, Paper PD25.

[249] W. Kaiser, M. Wichers, T. Wuth, W. Rosenkranz, C. Scheerer, C. Glingener, A. Farbert, J.-P. Elbers, and G. Fischer, "SPM limit of duobinary transmission," in *Proc. Eur. Conf. Optical Communication (ECOC)*, 2000, Paper We7.2.2.

[250] K. Yonenaga, Y. Miyamoto, A. Hirano, A. Sano, S. Kuwahara, H. Kawakami, H. Toba, K. Murata, M. Fukutoku, Y. Yamane, K. Noguchi, T. Ishibashi, and K. Nakajima, "320 Gbit/s WDM field experiment using 40 Gbit/s ETDM channels over 176 km dispersion-shifted fiber with nonlinearity tolerant signal format," *Electron. Lett.*, vol. 36, pp. 153–155, 2000.

[251] A. Sano and Y. Miyamoto, "Performance evaluation of prechirped RZ and CS-RZ formats in high-speed transmission systems with dispersion management," *J. Lightw. Technol.*, vol. 19, no. 12, pp. 1864–1871, Dec. 2001.

[252] K. Sekiya, T. Ito, H. Sugahara, K. Fukuchi, R. Ohhira, and T. Ono, "Flexible 40 Gbit/s WDM transmission beyond 1000 km enabled by 195 μm^2 A_{eff} PSCF and AC-RZ signal format," *Electron. Lett.*, vol. 39, pp. 386–388, 2003.

[253] A. Agarwal, S. Banerjee, D. F. Grosz, A. P. Kung, D. N. Maywar, A. Gurevich, and T. H. Wood, "Ultra-high-capacity long-haul 40-Gb/s WDM transmission with 0.8-b/s/Hz spectral efficiency by means of strong optical filtering," *IEEE Photon. Technol. Lett.*, vol. 15, no. 3, pp. 470–472, Mar. 2003.

[254] T. Tsuritani, A. Agata, K. Imai, I. Morita, K. Tanaka, T. Miyakawa, N. Edagawa, and M. Suzuki, "35 GHz spaced 20 gbps × 100 km WDM RZ transmission over 2700 km using SMF-based dispersion flattened fiber span," in *Proc. Eur. Conf. Optical Communication (ECOC)*, 2000, Paper PD1.5.

[255] T. Tsuritani, A. Agata, I. Morita, N. Edagawa, and S. Akiba, "Ultralong-haul 40-Gbit/s-based DWDM transmission using optically pre-filtered CS-RZ signals," *IEEE J. Sel. Topics Quantum Electron.*, vol. 10, no. 2, pp. 403–411, Mar./Apr. 2004.

[256] K. S. Cheng and J. Conradi, "Reduction of pulse-to-pulse interaction using alternative RZ formats in 40-Gb/s systems," *IEEE Photon. Technol. Lett.*, vol. 14, no. 1, pp. 98–100, Jan. 2002.

[257] P. Johannisson, D. Anderson, M. Marklund, A. Berntson, M. Forzati, and J. MÅrtensson, "Suppression of nonlinear effects by phase alternation in strongly dispersion-managed optical transmission," *Opt. Lett.*, vol. 27, pp. 1073–1075, 2002.

[258] S. Randel, B. Konrad, A. Hodžic, and K. Petermann, "Influence of bitwise phase changes on the performance of 160 Gbit/s transmission systems," in *Proc. Eur. Conf. Optical Communication (ECOC)*, 2002, Paper P3.31.

[259] M. Forzati, J. MÅrtensson, A. Berntson, A. Djupsjöbacka, and P. Johannisson, "Reduction of intrachannel four-wave mixing using the alternate-phase RZ modulation format," *IEEE Photon. Technol. Lett.*, vol. 14, no. 9, pp. 1285–1287, Sep. 2002.

[260] N. Alić and Y. Fainman, "Data-dependent phase coding for suppression of ghost pulses in optical fibers," *IEEE Photon. Technol. Lett.*, vol. 16, no. 4, pp. 1212–1214, Apr. 2004.

[261] M. Forzati, A. Berntson, and J. MÅrtensson, "IFWM suppression using APRZ with optimized phase-modulation parameters," *IEEE Photon. Technol. Lett.*, vol. 16, no. 10, pp. 2368–2370, Oct. 2004.

[262] D. M. Gill, A. H. Gnauck, X. Liu, X. Wei, and Y. Su, "$\pi/2$ alternate-phase on/off keyed 42.7 Gb/s long-haul transmission over 1980 km of standard single-mode fiber," *IEEE Photon. Technol. Lett.*, vol. 16, no. 3, pp. 906–908, Mar. 2004.

[263] Y. Zhu and A. Hadjifotiou, "Nonlinear tolerance benefit of modified-CSRZ DPSK modulation format," *Electron. Lett.*, vol. 40, pp. 903–904, 2004.

[264] G. Charlet, E. Corbel, J. Lazaro, A. Klekamp, R. Dischler, P. Tran, W. Idler, H. Mardoyan, A. Konczykowska, F. Jorge, and S. Bigo, "WDM transmission at 6-Tbit/s capacity over transatlantic distance, using 42.7-Gb/s differential phase-shift keying without pulse carver," *J. Lightw. Technol.*, vol. 23, no. 1, pp. 104–107, Jan. 2005.

[265] P. S. Cho, V. S. Grigoryan, Y. A. Godin, A. Salamon, and Y. Achiam, "Transmission of 25-Gb/s RZ-DQPSK signals with 25-GHz channel spacing over 1000 km of SMF-28 fiber," *IEEE Photon. Technol. Lett.*, vol. 15, no. 3, pp. 473–475, Mar. 2003.

[266] J.-X. Cai, D. G. Foursa, L. Liu, C. R. Davidson, Y. Cai, W. W. Patterson, A. J. Lucero, B. Bakhshi, G. Mohs, P. C. Corbett, V. Gupta, W. Anderson, M. Vaa, G. Domagala, M. Mazurczyk, H. Li, S. Jiang, M. Nissov, A. N. Pilipetskii, and N. S. Bergano, "RZ-DPSK field trial over 13 100 km of installed non-slope-matched submarine fibers," *J. Lightw. Technol.*, vol. 23, no. 1, pp. 95–103, Jan. 2005.

ABOUT THE AUTHORS

Peter J. Winzer (Senior Member, IEEE) received the M.S. and Ph.D. degrees in electrical engineering/communications engineering from the Vienna University of Technology, Austria, in 1996 and 1998, respectively.

His academic work, largely supported by the European Space Agency, was related to the analysis and modeling of space-borne Doppler wind lidar and highly sensitive free-space optical communication systems. In this context, he specialized on optical modulation formats and high-sensitivity receivers using coherent and direct detection. He continued to pursue this field of research after joining Bell Labs, Lucent Technologies, Holmdel, NJ, in 2000, where he focused on Raman amplification, optical modulation formats, advanced receiver concepts, and digital signal processing techniques for 10- and 40-Gb/s fiber-optic communication systems. He has authored and coauthered over 100 journal and conference papers and several book chapters, and has been teaching a short course on optical modulation formats and receiver concepts together with S. Chandrasekhar at ECOC and OFC conferences since 2003.

Dr. Winzer is a member of the Optical Society of America (OSA).

René-Jean Essiambre (Member, IEEE) received the B.S. and Ph.D. degrees in physics and optics from Universite Laval, Quebec City, QC, Canada. During his Ph.D. studies, he also spent one year at McGill University, Montreal, QC, Canada, working on solid-state physics.

From 1995 to 1997, he pursued postdoctoral studies with Prof. Agrawal at the Institute of Optics, University of Rochester, Rochester, NY. In September 1997, he joined Bell Labs, Lucent Technologies, Holmdel, NJ, where he is currenly a Distinguished Member of Technical Staff. He has authored and coauthored more than 75 scientific publications and several book chapters. He has worked in the field of optical switching, soliton communication systems, high-power fiber lasers, and mode-locked fiber lasers. Currently, his main areas of interest are high-speed transmission (40 and 160 Gb/s) and physical layer design of fiber-optic communication systems, including Raman amplification, Rayleigh backscattering, MPI, and particularly fiber nonlinearities. His current research focuses on network design, advanced modulation formats, optical phase conjugation and optical regeneration.

Dr. Essiambre is a member of the Optical Society of America (OSA). He is the recipient of the 2005 OSA Engineering Excellence Award.